

UNIVERSITÀ CATTOLICA SACRO CUORE

STATISTICAL AND ACTUARIAL SCIENCES

MJ: DATA BUSINESS ANALYTICS

RESTful Scraping API for Real Estate data, a Spatial Bayesian modeling perspective with INLA

Supervisor:

Dr. Marco DELLAVEDOVA

Author:

Niccolò SALVINI

Assistant Supervisor:

Dr. Vincenzo NARDELLI

AY 2019 / 2020



RESTful Scraping API for Real Estate data, a Spatial Bayesian modeling perspective with INLA

Niccolò Salvini¹

Lastest build: 18 gennaio, 2021

¹<https://niccolosalvini.netlify.app/>

Contents

1	Introduction	8
2	Web Scraping	10
2.1	A Gentle Introduction on Web Scraping	12
2.2	Anatomy of a url and reverse engineering	14
2.2.1	Scraping with <code>rvest</code>	18
2.3	Searching Technique for Scarping	21
2.4	Scraping Best Practices and Security provisions	23
2.5	HTTP overview	27
2.5.1	User Agent and further Identification Headers Spoofing	29
2.6	Dealing with failure	32
2.7	Parallel Scraping	33
2.7.1	Parallel <code>furrr</code> + <code>future</code>	36
2.7.2	Parallel <code>foreach</code> + <code>doFuture</code>	39
2.8	Open Challenges and Further Improvemements	41
2.9	Legal Profiles	43
3	API Technology Stack	45
3.1	RESTful API	47
3.1.1	Plumber HTTP API	50
3.1.2	Sanitization	52
3.1.3	Denial Of Service (DoS)	53
3.1.4	Logging	53
3.1.5	RESTful API docs	54
3.2	Docker	55
3.2.1	REST-API container	56

<i>CONTENTS</i>	2
3.3 NGINX reverse Proxy Server and Authorization	58
3.4 Docker-Compose	60
3.5 HTTPS(ecure) and SSL certificates	62
3.6 AWS EC2 instance	63
3.7 Software CI/CD Workflow	64
3.8 Further SF Integrations	65
4 INLA	67
4.1 The class of Latent Gaussian Models (LGM)	68
4.2 Gaussian Markov Random Field (GMRF)	72
4.3 INLA Laplace Approximations	74
4.4 R-INLA package	76
5 Point Referenced Data Modeling	81
5.1 Gaussian Process (GP)	84
5.2 The Stochastic Partial Differential Equation (SPDE) approach	89
5.3 Hedonic (rental) Price Models	91
5.4 Spatial Kriging{#kriging} 6.8	94
5.5 Model Criticism	95
5.6 Prior Specification	97
6 Exploratory Analysis	100
6.1 Data preparation	103
6.1.1 Maps and Geo-Visualisations	104
6.2 Counts and First Orientations	106
6.3 Text Mining in estate Review	112
6.4 Missing Assessement and Imputation	115
6.4.1 Missing assessement	115
6.4.2 Covariates Imputation	117
6.4.3 Shinyapp for mesh assessment	120
7 Model Selection & Fitting	121
8 Conclusions	123

<i>CONTENTS</i>	3
Appendix	124
8.1 Gaussian Process	124
8.2 SPDE and Triangularization (YT speech: Moraga (2020)) . .	129
8.3 Laplace Approximation	132

List of Tables

List of Figures

2.1	General url Anatomy, Doepud (2010) source	14
2.2	immobiliare url composed according to some filters, author's source	16
2.3	immobiliare.it website structure, author's source	17
2.4	pseudo code algorithm to reverse engineer url, author's source	19
2.5	rvest general flow chart, author's source	20
2.6	pseudo code algorithm for price search, author's source	23
2.7	pseudo code algorithm structure for fatstscrape, author's source	24
2.8	User-Server communication scheme via HTTP, source aut (2014)	28
2.9	proxy middle man,, source aut (2014)	32
2.10	pseudo code for a generic set of functions applied with possibly fail dealers , author's source	33
2.11	single threaded computing vs parallel computing, Barney (2020) source	34
2.12	futures reimaged as divide and conquer, author's source . . .	38
2.13	computational complexity analysis with Furr	39
2.14	local machine monitoring of cores during parallel scraping . .	40
2.15	computational complexity analysis with Furr	42
3.1	complete infrastructure, author's source	47
3.2	API general functioning, unknown source	48
3.3	Swagger UI in localhost on port 8000, author's source	55
3.4	Custom Dockerfile from salvini/api-immobiliare Docker Hub repository, author's source	57
3.5	NGINX gateway redirecting an incoming request, source Microsoft (2018)	60
3.6	Docker Compose YAML file orchestration for NGINX container and RESTful API, author's source	61

3.7	HTTPS encryption with SSL certificates, source aut (2014) . .	63
3.8	Software development CI/CD workflow, author's source	65
4.1	outputs for a <code>inla()</code> call, source: Krainski (2019)	77
4.2	SPDEtoy bubble plot, author's source	78
4.3	Linear predictor marginals, plot recoded in <code>ggplot2</code> , author's source	80
5.1	Point Referenced Data map plot (Leaflet Cheng et al. (2019)) of a RESTful API call on Milan Rental Real Estate 20-11-2019, Author's Source	82
5.2	Stockton data, Left: Spatial Lat and Long points pojected into the 3^{rd} dim $\log(Price)$, Right: spatial interpolation of points, source Marta Blangiardo (2015)	84
5.3	Left: isotropy concentric decaying contours, Right: anisotropy concentric decaying contours, source Blanchet-Scalliet et al. (2019)	86
5.4	Matérn function with 4 different values of ν (upper right legend), kept ϕ fixed, author's source	88
5.5	Left: monitoring stations in Piemonte region for PM10 pollution levels. Right: its triangulation using 123 vertices. Cameletti et al. (2012) source	90
5.6	Left: example of a spatial random field where $X(s) = \cos(s_1) + \sin(s_2)$, Right: $X(s)$ SPDE representation given a triangulation, Cameletti et al. (2012) source	91
5.7	Spatial prediction representation through DAG, source Marta Blangiardo (2015)	95
5.8	New prior (dashed) with parameters ($U = 0.968, \alpha = 0.01$), and the $\Gamma(shape = 1, rate = b)$ prior (solid).	99
6.1	Leaflet Map	105
6.2	Non Linear Spatial Relationship disclosed	105
6.3	Count plot for each housedolds category	106
6.4	Log Monthly Prices box-plots for the most common factor levels in Heating systems and Air Conditionings	108
6.5	Monthly Prices change wrt square meters footage in different n-roomed apt	110
6.6	Tie fighter coefficient plot for a log-linear model	112
6.7	Word Network Graph for 250 Estate Agencies Review	114

6.8	Missingness Heatmap plot	116
6.9	Missingness co-occurrence plot	118
8.1	Left panel: GP cloud of points fitted with a <i>circle</i> , Right panel: GP cloud of points fitted with a <i>ellipse</i> , source de Freitas (2013)	124
8.2	Triangulation weights and associated process value, Moraga (2020) source	130
8.3	Projection Matrix to map valjes from tringulation back to the GP, Moraga (2020) surce	131
8.4	Chisquared density function with parameter $k = 8$ (top) and $k = 16$ (down) solid line. The point line refers to the cor- responding Normal approximation obtained using the Laplace method	135

Chapter 1

Introduction

Trento:

- Argomento
- Problema
- Obiettivi
- Metodo
- Struttura della tesi

Main themes:

- Research Question
- Milan Real Estate Controversies in relation to research question
- why the API (perchè mi mancano i dati e perchè è il futuro)
- Open Data discussion personal hope of data sharing and benefits from open source
- Why a Bayesian approach
- Why INLA

According to Google research devoted to the analysis of USA real estate buyers' habits (National Association of Realtors, Google 2012), out of 10 % homebuyers use the Internet as one of the primary research tools, and 52 % of customers

start their search using the Internet. According to the information presented by Google, the number of real estate searches grows up yearly by 22 %. The main reason for customers is to find information which can reduce purchasing related risks (Peterson & Merino, 2003). In Latvia, 79.7 % of the population now goes online regularly (Latvijas Interneta Asociācija, 2015). Latvian Internet users have the same habits as the Internet users of the USA or developed Western countries. 7 out of 10 Internet users (70 %) look for information on web pages (CSP, 2015). Real estate buyers read general information about a real estate object and compare prices of various real estate objects

As a general discussion technologies implied can be thought as the distance between a service running locally on a laptop and something that it can actually be put into production, shared among company stakeholders, solving business related problems. When such technologies are applied data scientist and interlocutors gradually close the gap. Insights are better communicated, data is up-to-date and automation can save time. Nonetheless when the infrastructure is structured with vision then integrating or substituting existing technologies is not trivial. Anyway technologies can not be always embedded because they might be exclusively designed to work only on certain back ends, therefore some choices are not into discussion. With foresight RStudio by setting future-oriented guidelines has spent a lot of effort giving its users an easy, integrated and interconnected environment. By that it is meant that the RStudio community has tried to either integrate or open the possibility to a number of technologies that fill the blanks in their weaker parts. On top of many, an entire package has been dedicated to democratize REST APIs (Plumber (Trestle Technology, LLC, 2018)). As a further example developers in RStudio have created an entire new paradigm i.e. Shiny (Chang et al., 2020), a popular web app development package, that enforces the developer to have front-end and back-end technologies tied up in the same IDE. They also added performance monitoring and optimization packages that are fitted into shiny such as shinytest [metti tag] and shinyloadtest [metti tag] to simulate sessions and verify network traffic congestion.

Chapter 2

Web Scraping

The following chapter covers a modern technique and up-to-date libraries for web scraping in R and related challenges with a focus on the immobiliare.it case. The easiest way of collecting information from websites involves inspecting and manipulating URLs. While browsing web pages urls under the hood compose themselves in the navigation bar according to a certain encoded semantic, specifying domain, url paths and url parameters. As a matter of fact websites can be regarded as a complex system of nested folders where urls are the relative file path to access to the content desired. That implies if a function can mimic the url semantic by providing decoded, human-readable arguments, then any content in the website can be filtered and later accessed. Once urls are reproduced and stored into a variable, scraping function are called on these set of address. The major time improvement with respect to classical crawlers comes from retrieving a set of urls instead of gathering the entire website sitemap and then searching through keywords. This is made exploiting a scraping workflow library, namely `rvest` Wickham (2019), which takes inspiration from the scraping gold standard Python library Beautiful Soup Contributors (2004). A search algorithm strategy, calibrated on the specific scraping context, is nested inside scraping functions whose skeleton is reproduced for all the information demanded. The search strategy exploits different CSS queries that point to different data location within the web page, with the

aim to be sure to carry out a comprehensive exploration and to deliver data where available. Functions are then wrapped up around a “main” function that simplifies portability and enables parallelization. Both of the search logic flows are fronted presenting their pseudocode. HTTP protocol communication and related main concepts are introduced with the aim to familiarize with internet communication layers focusing on traffic from web server to web clients and viceversa and principal actors involved. By doing that some opinionated but highly diffused scraping best practices are incorporated into scraping taking inspiration by a further R library Polite Perepolkin (2019). Revised best practices try to balance scraping efficiency and *web etiquette*. As a result optimization happens both from the *web server* side; this is tackled by kindly asking for permission and sending delayed server requests rate based on Robotstxt file requirements. As well as from the *web client* by preventing scraping discontinuity caused by server blocks thanks to *User Agent* (HTTP request headers) pool *rotation* and *fail dealers*. *Parallel* computing is carried out due to data obsolescence, since the market on which scraping functions are called is vivid and responsive. At first concepts are introduced and then main centered on the specific R parallel ecosystem. Then a run time scraping benchmark is presented for two different modern parallel back end options future Bengtsson (2020b) and doParallel Corporation and Weston (2020), along with two parallel looping paradigms, *furrr* Vaughan and Dancho (2018) and *foreach* Microsoft and Weston (2020). Both of the two combinations have showed similar results, nevertheless the former offers a more *{Tidiverse}* coherence and a more comfortable debugging experience. Furthermore an overview of the still unlocked challenges is provided on the open source project and possible improvements, with the sincere hope that the effort put might be extended or integrated. In the end a heuristic overview on the main legal aspect is offered bringing also an orientation inspired by a “fair balance” trade off between web scraping practices and the most common claims. Then a court case study about a well known scraping litigation is brought demonstrating how law is not solid in this area and how scrapign market should find its own equilibrium.

2.1 A Gentle Introduction on Web Scraping

Definition 2.1 (Scraping). Web Scraping is a technique aimed at extracting unstructured data from static or dynamic internet web pages and collecting it in a structured way. Automated data collection, web extraction, web crawling, or web data mining are often used as synonyms to web scraping.

The World Wide Web (WWW or just the web”) data accessible today is calculated in zettabytes (Cisco, 2020) ($1 \text{ zettabyte} = 10^{21} \text{ bytes}$). This huge volume of data provides a wealth of resources for researchers and practitioners to obtain new insights in real time regarding individuals, organizations, or even macro-level socio-technical phenomena (Krotov and Tennyson, 2018). Unsurprisingly, researchers of Information Systems are increasingly turning to the internet for data that can address their research questions (2018). Taking advantage of the immense web data also requires a programmatic approach and a strong foundation in different web technologies. Besides the large amount of web access and data to be analyzed, there are three rather common problems related to big web data: variety, velocity, and veracity (Krotov and Silva, 2018), each of which exposes a singular aspect of scraping and constitutes some of the challenges fronted in later chapters. *Variety* mainly accounts the most commonly used mark-up languages on the web used for content creation and organization such as HTML (htm, 2020), CSS (css, 2020), XML (contributors, 2020j) and JSON (contributors, 2020g). Sometimes Javascript (contributors, 2020f) components are also embedded into websites. In this cases dedicated parsers are required which would add a further stumbling block. Starting from these points scraping requires at least to know the ropes of these technologies which are also assumed in this analysis. Indeed later a section will be partially dedicated to familiarize with the inner internet mechanism that manages the exchanges of information, such as HTTP protocols. *Velocity*: web data are in continuous flow status: it is created in real time, modified and changed continuously. This massively impacts the analysis that relies on those data which, as times passes, becomes obsolete. However it also

suggests the speed and pace at which data should be collected. From one hand data should be gathered as quicker as possible so that analysis or softwares are up-to-date, section 2.7. From the other this should happen in any case by constraining speed to common shared scraping best practices, which require occasional rests in requesting information. The latter issue is faced later in section 2.4. *Veracity*: Internet data quality and usability are still surrounded by confusion. A researcher can never entirely be sure if the data he wants are available on the internet and if the data are sufficiently accurate to be used in analysis. While for the former point data can be, from a theoretical perspective, accurately selected it can not be by any means predicted to exist. This is a crucial aspects of scraping, it should take care of dealing with the possibility to fail, in other words to be lost. The latter point that points to data quality is also crucial and it is assessed by a thoughtful market analysis that mostly assures the importance of immobiliare.it as a top player in italian real estate. As a consequence data coming from reliable source is also assumed to be reliable. Furthermore web scraping can be mainly applied in two common forms as in (Dogucu and Cetinkaya, 2020): the first is browser scraping, where extractions takes place through HTML/XML parser with regular expression matching from the website's source code. The second uses programming interfaces for applications, usually referred to APIs. The main goal of this chapter is to combine the two by shaping a HTML parser and make the code portable into an RESTful API whose software structure is found at ???. Regardless of how difficult it is the process of scraping, the circle introduced in aut (2014) and here revised with respect to the end goal, is almost always the same. Most scraping activities include the following sequence of tasks:

- Identification of data
- Algorithm search Strategy
- Data collection
- Data preprocess
- Data conversion

- Debugging and maintenance
- Portability

Scraping essentially is a clever combination and iteration of the previous tasks which should be heavily shaped on the target website or websites.

2.2 Anatomy of a url and reverse engineering

Uniform Resource Locators (URLs) (contributors, 2020h), also known as web addresses, determine the location of websites and other web contents and mechanism to retrieve it. Each URL begins with a scheme, purple in figure 2.2, specifying the protocol used to communicate client-application-server contact i.e. HTTPS. Other schemes, such as ftp (File transmission protocol) or mailto for email addresses correspond to SMTP (Simple Mail Transfer Protocol) standards.

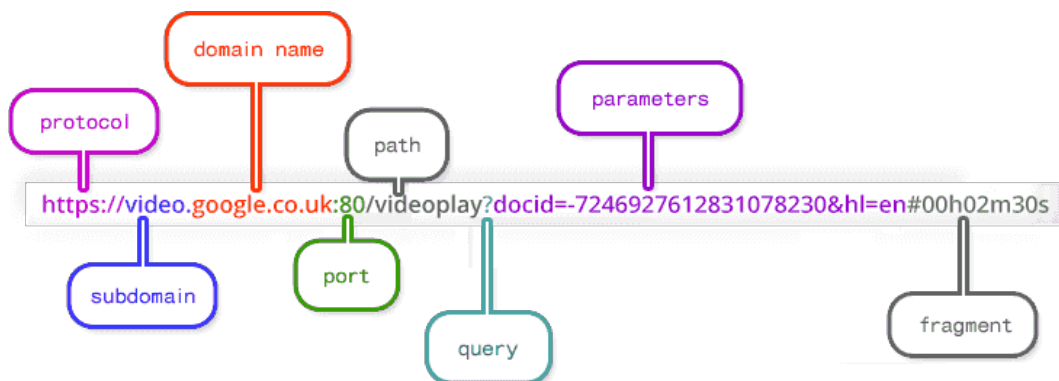


Figure 2.1: General url Anatomy, Doepud (2010) source

The *domain name* in red in figure 2.2, with a specific ID, indicates the server name where the interest resource is stored. The domain name is sometimes accompanied with the *port* whose main role is to point to the open door where data transportation happens. Default port for Transmission Control Protocol (*TCP*) is 80. In the following chapter ports will play a crucial role since a compose file will instruct containers (3.2) to open and route communication through these channels and then converge the whole traffic into a secured

one 3.3. Typically domain names are designed to be human friendly, indeed any domain name has its own proprietary IP and public IP (IPv4 and IPv6) address which is a complex number, e.g. local machine IP is 95.235.246.91. Here intervenes *DNS* whose function is to redirect domain name to IP and vice versa. The path specifies where the requested resource is located on the server and typically refers to a file or directory. Moving towards folders requires name path locations separated by slashes. In certain scenarios, URLs provide additional *path* information that allows the server to correctly process the request. The URL of a dynamic page (those of who are generated from a data base or user-generated web content) sometimes shows a *query* with one or more parameters followed by a question mark. *Parameters* follow a “field=value” scheme each of which is separated by a “&” character for every different parameter field, 6th character from the end in figure 2.2 parameter space. Each further parameter field added is appended at the end of the url string enabling complex and specific search queries. *Fragments* are an internal page reference often referred to as an anchor. They are typically at the end of a URL, starting with a hash (#) and pointing to specific part of a HTML document. Note that this is a full browser client-side operation and fragments are used to display only certain parts of already rendered website. The easiest way of collecting information from websites often involves inspecting and manipulating URLs which refer to the content requested. Therefore urls are the starting point for any scraper and they are also the only functional argument to be feeding to. Url parameters indeed help to route web clients to the requested information and this is done *under the hood* and unconsciously while the user is randomly browsing the web page. Let us assume to express the necessity to scrape only certain information from a generic website. Then if this data to be scraped can be circumscribed by properly setting url parameters, under those circumstances it is also demanded a way to consciously compose these urls. In other words a function (or a service) needs to mould urls by mimicking their mutations operated by browser while the user is navigating. As a matter of fact as filters (i.e. parameters) are applied to the initial search page for immo-

biare.it then parameters populate the navigation bar. For each of the filters specified a new parameter field and its own selected value are appended to the url string according to the website specific *semantic*. Each website has its own semantic. As an example are applied directly to the domain name `https://www.immobiliare.it/` the following filters (this is completely done in the dedicated panel):

- rental market (the alternative is selling)
- city is Milan
- bathrooms must be 2
- constrained zones search on “Cenisio” and “Fiera”

The resulting url is:

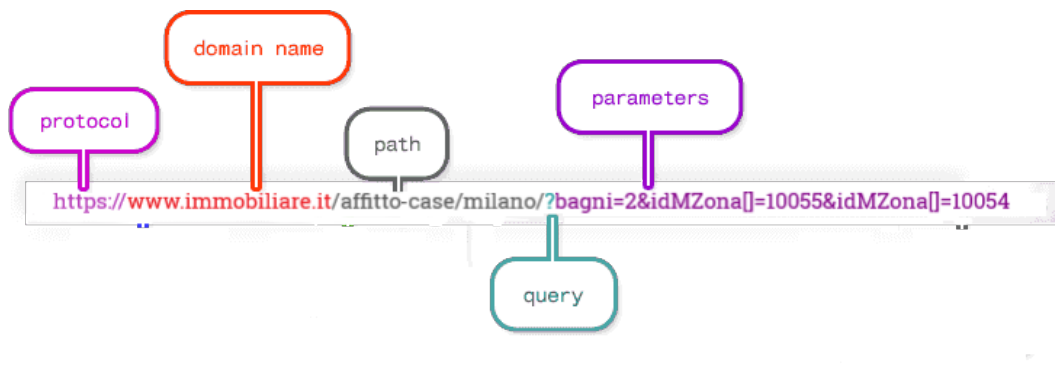


Figure 2.2: immobiliare url composed according to some filters, author’s source

At first glance immobiliare.it does not enact a *clean url* (contributors, 2020a) structure, which ultimately would simplify a lot the reverse semantic process. In truth parameters follows a chaotic semantic. While the filter city=“milano” is located in the url path the remaining are transferred to the url parameters. For some of them the logical trace back from the parameter field-value to their exact meaning is neat, i.e. `bagni=2` and can be said clean. Unfortunately for the others the semantic is not obvious and requires a further reverse layer to deal with. In addition to this fact the url in figure 2.2 reads to the very first page of the search meeting the filter requirements, which

groups the first 25 rental advertisements. The following set of 25 items can be reached by relocating the url address to: [https://www.immobiliare.it/affitto-case/milano/?bagni=2&idMZona\[\]=10055&idMZona\[\]=10054&pag=2](https://www.immobiliare.it/affitto-case/milano/?bagni=2&idMZona[]=10055&idMZona[]=10054&pag=2). The alteration regards the last part of the url and constitutes a further url parameter field to look for. Note that the first url does not contain “&pag=1”. For each page browsed by the user the resulting url happen to be the same plus the prefix “&pag=” glued with the correspondent n page number (from now on referred as *pagination*). This is carried on until pagination reaches either a stopping criteria argument or the last browsable web page (pagination sets as default option 10 pages, which returns a total of 250 rental advertisement). Therefore for each reversed semantic url are obtainable 25 different links, see figure 2.3 that is where actually are disclosed relevant data and the object of scraping. Links belonging to the 25 items set share the same anatomy: <https://www.immobiliare.it/annunci/84172630/> where the last *path* is associated to a unique ID, characteristic of the rental property. Unfortunately there is not any available solution to retrieve all the existing ID, therefore links needs to collected directly from “main” url in figure 2.2 as an obvious choice.

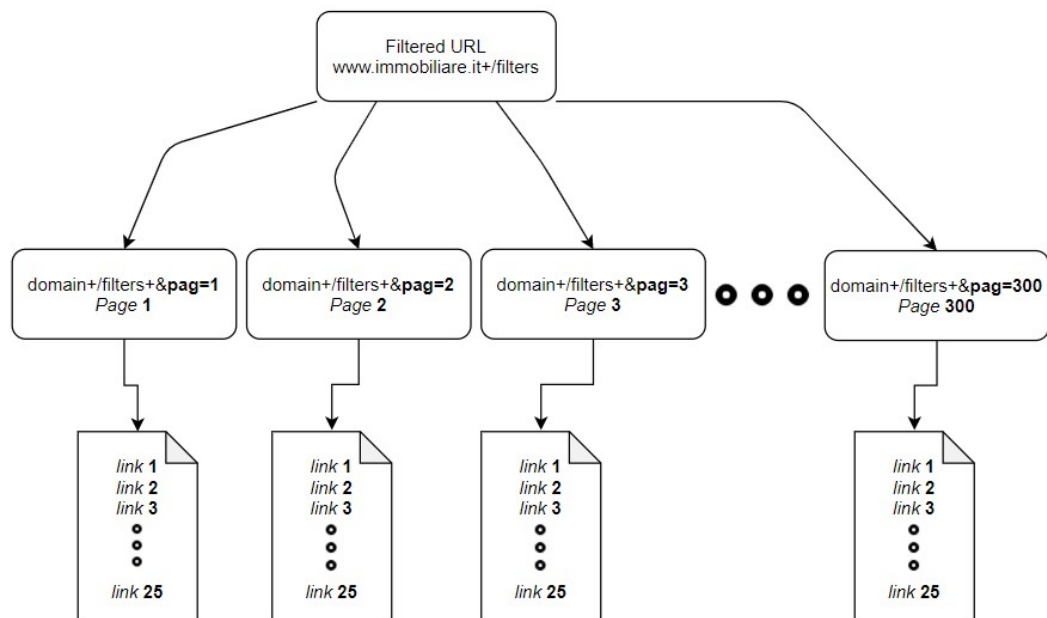


Figure 2.3: immobiliare.it website structure, author’s source

Therefore 4 steps are required to *reverse engineer* the url (2014) and to ultimately make the links access available:

1. Determine how the URL syntactic works for each parameter field
2. Build the url based on the reverse engineered sematic:
 - a. those ones who need an ID parameter value
 - b. clean ones who need to only explicit the parameter value
3. Pagination is applied to the url until stopping criteria are met
4. Obtain the links for each urls previously generated

Once identified the inner composition mechanism by an insistent trial and error then the url restoration could starts. Parameter values for those that requires an ID in figure 2.2 are encoded is a way that each number is associated to its respective zone ID e.g. as in figure 2.2 “Fiera” to 10055 or “Cenisio” to 10054. Therefore a decoding function should map the parameter value number back to the correspondent human understandable name e.g from 10055 to “Fiera” or 10054 to “Cenisio”, the exactly opposite logical operation. The decoding function exploits a JSON database file that matches for each ID its respective zone name exploiting suitable JSON properties. The JSON file is previously compounded by generating a number of random url queries and subsequently assigning the query names to their respective ID. As soon as the JSON file is populated the function can take advantage of that database and compose freely urls at need. Pagination generates a set of urls based on the number of pages requested. In the end for each urls belonging to the set of urls, links are collected by a dedicated function and stored into a vector. Furthermore if the user necessitate to directly supply a precomposed url the algorithm overrides the previous object and applies pagination on the provided url. The pseudocode in figure 2.4 paints the logic behind the reverse engineering process.

Input : npages(int), city(chr), macrozone(vec), type(chr),
url_fix(chr)

Output: npages_vec (vector of urls)

```

function get_link(args):
  if macrozone ≠ ∅ then
    idzone ← c()
    zone ← readJSON
    /* match macrozone with idzone */
    for i ∈ macrozone do
      if match macrozone[i] ∈ zone then
        return idzone[i]
      else
        stop:
        | error: zone i not recognized
      end
    end
    idzone ← glue_collapse(idzone)
    mzones ← glue(&idMZona[] = {idzone}) + &idMZona[] =)
  else
    dom ← "https://www.immobiliare.it/"
    stringa ← dom + type + "-case/" + city + mzones
    /* pagination */
    if regex checks if valid url then
      npages_vec ← glue({stringa}&pag = {2 : npages})
    else
      stop:
      | error:url seems not real
    end

    if url_fix ≠ ∅ then
      npages_vec ← glue({url_fix}&pag = {2 : npages})
    end
  end
end
return npages_vec

```

Figure 2.4: pseudo code algorithm to reverse engineer url, author's source

2.2.1 Scraping with `rvest`

Reverse engineered urls are then feeded to the scraper which arranges the process of scraping according to the flow chart imposed by `rvest` in figure 2.5. The sequential path followed is highlighted by the light blue wavy line and offers one solution among all the alternative ways to get to the final content. The left part with respect to the central dashed line of figure 2.5 takes care of setting up the session and parsing the response. As a consequence at first scraping in consistent way requires to open a session class object with `html_session`. Session arguments demands both the target url, as built in 2.4 and the request headers that the user may need to send to the web server. Data attached to the web server request will be further explored later in section 2.5.1, though they are mainly 4: User Agents, emails references, additional info and proxy servers. The session class objects contains a number of useful data regarding either the user log info and the target website such as: the url, the response, cookies, session times etc. Once the connection is established (response 200), functions that come after the opening rely on the object and its response. In other words while the session is happening the user will be authorized with the already provided headers data. As a result jumps from a link to the following within the same session are registered by in the object. Most importantly sessions contain the xml/html content response of the webpage, that is where data needs to be accessed.

Indeed at the right of dashed line in 2.5 are represented the last two steps configured into two `rvest` (Wickham, 2019) functions that locate the data within the HTML nodes and convert it into a human readable text, i.e. from HTML/XML to text. The most of the times can be crafty to find the exact HTML node or nodes set that contains the data wanted, especially when HTML trees are deep nested and dense. `html_node` function provides an argument that grants to specify a simple CSS/XPATH selector which may group a set of HTML/XML nodes or a single node. Help comes from an open source library and browser extension technology named SelectorGadget. Selector-

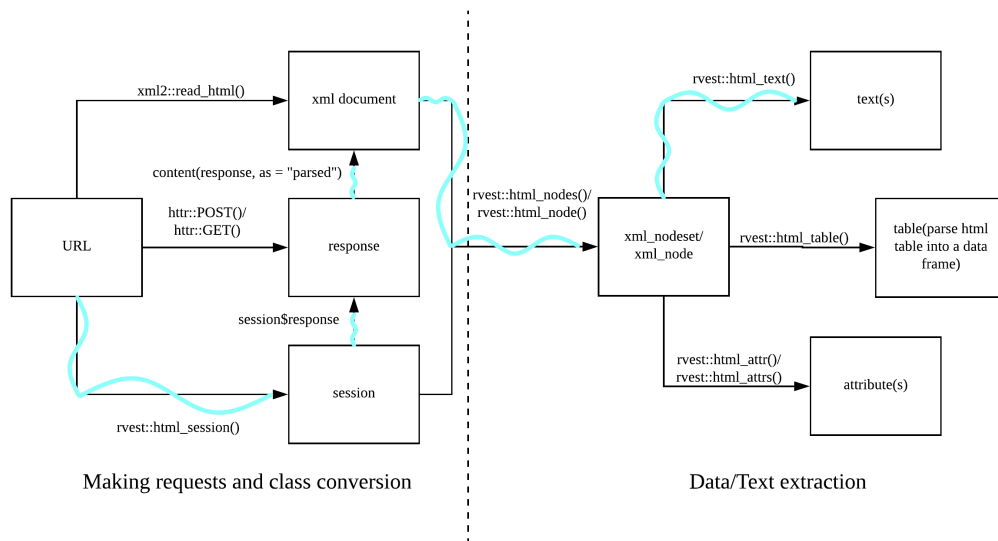


Figure 2.5: rvest general flow chart, author's source

Gadget (Cantino and Maxwell, 2013) which is a JavaScript bookmark that allows to interactively explore which CSS selector is needed to gather desired components from a webpage. Data can be repeated many times into webpages so the same information can be found at multiple CSS queries. This fact highlights one of the principles embodied in the following section 2.3 according to which searching methods gravitates. Once the CSS query points address to the desired content then data finally needs to be converted into text. This is what explicitly achieve `html_text`.

2.3 Searching Technique for Scarping

The present algorithm in figure 2.6 imposes a nested sequential search strategy and gravitates around the fact that data within the same webpage is repeated many times, so multiple CSS queries are available for the same information. Furthermore since data is repeated has also less probability to be missed. CSS sequential searches are calibrated from the highest probability of appearance in that CSS selector location to the lowest so that most visited locations are also the the most likely to grab data. A session object opensess, the one seen in

2.5), is initialized sending urls built in 2.4. The object `opensess` constitutes a check point obj because it is reused more than once along the algorithm flow. The object contains session data as well as HTML/XML content. Immediately after another object `price` parses the sessions and points to a CSS query through a set of HTML nodes. The CSS location `.im-mainFeatures__title` addresses a precise group of data which are found right below the main title. Expectations are that monthly price amount in that location is a single character vector string, containing price along with unnecessary non-UTF characters. Then the algorithm bumps into the first `if` statement. The logical condition checks whether the object `price` first CSS search went lost. If it does not the algorithm directly jumps to the end of the algorithm and returns a preprocessed single quantity. Indeed if it does it considers again the check point `opensess` and hits with a second css query `.im-features__value` , `.im-features__title`, pointing to a second data location. Note that the whole search is done within the same session (i.e. reusing the same session object), so no more additional request headers 2.5.1 has to be sent). Since the second CSS query points to data sequentially stored into a list object, the newly initialized `price2` is a type list object containing various information. Then the algorithm flows through a second `if` statement that checks whether "prezzo" is matched in the list, if it does the algorithm returns the +1 position index element with respect to the "prezzo" position. This happens because data in the list are stored by couples sequentially (as a flattened list), e.g. `list(title, "Appartamento Sempione", energy class, "G", "prezzo", 1200/al mese)`. Then in the end a third CSS query is called and a further nested `if` statement checks the emptiness of the latest CSS query. `price3` points to a hidden JSON object within the HTML content. If even the last search is lost then the algorithm escapes in the `else` statement by setting `NA_Character_`, ending with any CSS query is able to find price data. The search skeleton used for price scraping constitutes a standard reusable search method in the analysis for all the scraping functions. However for some of the information not all the CSS location points are available and the algorithm is forced to be rooted to only certain paths,

e.g. “condizionatore” can not be found under main title and so on.

```

Input : url
Output: price  $\vee$  price2  $\vee$  price3

opensess  $\leftarrow$  session(url) obj
price  $\leftarrow$  1st CSS query on opensess
if price =  $\emptyset$  then
  price2  $\leftarrow$  2nd CSS query on opensess
  if "prezzo"  $\in$  price2 then
    find index position
    pos = index position +1
    return price2[pos]
  else
    price3  $\leftarrow$  3rd CSS query on opensess
    if price3 =  $\emptyset$  then
      pluck JSON price element
      preprocess price3
      return price3
    else
      return NA
    end
  end
  preprocess price2
  return price2
else
  preprocess price
  return price
end

```

Figure 2.6: pseudo code algorithm for price search, author’s source

Once all the functions have been designed and optimized with respect to their scraping target they need to be grouped into a single “main” *fastscrape* function, figure 2.7. This is accomplished into the API function endpoint addressed in section 3.1.1, which also applies some sanitization, next chapter section 3.1.2, on users inputs and administers also some security API measures, as in 3.1.3 outside the main function. Moreover as it will be clear in section 2.7 the parallel back end will be registered outside the scraping function for unexplained inner functioning reasons.

pseudo code

```

Input : npages_vec
Output: result (dataframe)

function fastscrape(args):
    /* register start time */
    tic()
    /* call function inside dataframe columns */
    for url ∈ npages_vec do
        result ← {
            title ← scrapetitle(url)
            monthlyprice ← scrapeprice(url)
            nroom ← scrapenroom(url)
            sqmeter ← scrapesqmeter(url)
            href ← scrapehref(url)
            . . .
        }
    end
    /* register and print end time */
    toc()
    return (result)

```

Figure 2.7: pseudo code algorithm structure for fastscrape, author’s source

2.4 Scraping Best Practices and Security provisions

Web scraping have to naturally interact multiple times with both the *client* and *server side* and as a result many precautions must be seriously taken into consideration. From the server side a scraper can forward as many requests as it could (in the form of sessions opened) which might cause a traffic bottleneck (DOS attack contributors (2020b)) impacting the overall server capacity. As a further side effect it can confuse the nature of traffic due to fake user agents 2.5.1 and proxy servers, consequently analytics reports might be driven off track. Those are a small portion of the reasons why most of the servers have their dedicated Robots.txt files. Robots.txt Meissner (2020) are a way to kindly ask webbots, spiders, crawlers to access or not access certain parts of a webpage. The de facto “standard” never made it beyond a *informal* “Network Working Group INTERNET DRAFT”. Nonetheless, the use of robots.txt files

is widespread due to the vast number of web crawlers (e.g. Wikipedia robot¹, Google robot²). Bots from the own Google, Yahoo adhere to the rules defined in robots.txt files, although their *interpretation* might differ.

Robots.txt files (Meissner and Ren, 2020) essentially are plain text and always found at the root of a website’s domain. The syntax of the files follows a field-name value scheme with optional preceding user-agent. Blocks are separated by blank lines and the omission of a user-agent field (which directly corresponds to the HTTP user-agent field, cleared later in 2.5.1) is seen as referring to all bots. The whole set of possible field names are pinpointed in Google (2020), some important are: user-agent, disallow, allow, crawl-delay, sitemap and host. Some common standard interpretations are:

- Finding no robots.txt file at the server (e.g. HTTP status code 404) implies full permission.
- Sub-domains should have their own robots.txt file, if not it is assumed full permission.
- Redirects from subdomain www to the domain is considered no domain change - so whatever is found at the end of the redirect is considered to be the robots.txt file for the subdomain originally requested.

A comprehensive scraping library that observes a web etiquette is the polite (Perepolkin, 2019) package. Polite combines the effects of robotstxt, ratelimitr (2018) to limit sequential session requests together with the memoise (Wickham et al., 2017) for robotstxt response caching. Even though the solution meets the politeness requirements (from server and client side) ratelimitr is not designed to run in parallel as documented in the vignette (Shah, 2018). This is a strong limitation as a result the library is not applied. However the 3 simple but effective web etiquette principles around, which is the package wrapped up, describe what are the guidelines for a “polite” session:

¹<https://en.wikipedia.org/robots.txt>

²<https://www.google.com/robots.txt>

The three pillars of a polite session are seeking permission, taking slowly and never asking twice.

— Dmytro Perepolkin, polite author

The three pillars constituting the *Ethical* web scraping manifesto (Densmore, 2019) are considered as common shared *best practices* that are aimed to self regularize scrapers. In any case these guidelines have to be intended as eventual practices and by no means as required by the law. However many scrapers themselves, as website administrators or analyst, have been fighting for many and almost certainly coming years with bots, spiders and derivatives. As a matter of fact intensive scraping might fake out real client navigation logs and confuse digital footprint, which results in induced distorted analytics. On the other hand if data is not given and APIs are not available, then scraping is sadly no more an option. Therefore throughout this analysis the goal will be trying to find a well balanced trade-off between interests on the main actors involved. Newly balanced (with respect to the author thought) guidelines would try to implement at first an obedient check on the validity of the path to be scraped through a cached function. Secondly it will try to limit request rates to a more feasible time delay, by keeping into the equation also the client time constraints. In addition it should also guarantee the continuity in time of scraping not only from the possibility to fail section ??(possibly)), but also from servers “unfair” denial (in section 2.5.1). With that said a custom function caches the results of robotstxt into a variable i.e. `polite_permission`. Then paths allowed are evaluated prior any scraping function execution. Results should either negate or affirm the contingency to scrape the following url address.

```
## Memoised Function :
```

```
## [1] TRUE
```

`polite_permission` is then reused to check, if any, the server suggestion on crawl relay. In this particular context no delays are kindly advised. As a default

polite selection delay request rates are set equal to 2.5 seconds. Delayed are managed through the purrr stack. At first a rate object is initialized based on polite_permission results, as a consequence a rate_sleep delay is defined and iterated together with any request sent, as in Lionel Henry RStudio (2020b).

```
get_delay = function(memoised_robot, domain) {

  message(glue("Refreshing robots.txt data for %s ... "
    {domain}))

  temp = memoised_robot$crawl_delay

  if (length(temp) > 0 && !is.na(temp[1, ]$value)) {
    star = dplyr::filter(temp, useragent == "*")
    if (nrow(star) == 0)
      star = temp[1, ]
    as.numeric(star$value[1])
  } else {
    2.5
  }

}

get_delay(rbtxt_memoised, domain = dom)

## [1] 2.5
```

2.5 HTTP overview

URLs in browsers as in 2.1 are a way to access to web content whether this accounts for getting from one location to the following, or checking mails, listening to musics or downloading files. However Internet communication is a stratification of layers conceived to make the whole complex system working. In this context URLs are the layer responsible for *user interaction*. The rest

of the layers which involve techniques, standards and protocols, are called in ensemble Internet Protocols Suite (*IPS*) (2014). The TCP (Transmission Control Protocol) and IP (Internet Protocol) are two of the most important actors on the IP Suite and their role is to represent the *Internet layer* (IP) and the *transportation layer* (TCP). In addition they also guarantee trusted transmission of data. Inner properties and mechanism are beyond the scope of the analysis, luckily they are not required in this context. Resting on the transportation layer there are specialized message exchange protocols such as the HTTP (Hyper Text Transfer Protocol), FTP (File Transfer Protocol). In addition, there may be also e-mail exchange protocols for transmission, such as Post Office Protocol (POP) for Email Recovery and for storage and retrieval, IMAP (Internet Message Access Protocol). The aforementioned protocols describe default vocabulary and procedures to address particular tasks for both clients and servers and they can be ascribed to the transportation layer. HTTP is the most widespread, versatile enough to ask for almost any resource from a server and can also be used to transfer data to the server rather than to recover. In figure 2.8 is painted a schematized version of a User-Server general HTTP communication/session. If a website e.g. immobiliare.it³ is browsed from a web browser e.g. Chrome (the HTTP client) then the client is interrogating a Domain Name System (DNS) which IP address is associated with the domain part of the URL. When the browser has obtained the IP address as response from the DNS server then connection/session is established with HTTP server via TCP/IP. From a content perspective data is gathered piece-by-piece, if the content is not exclusively HTML then the browser client renders the content as soon as it receives data.

Furthermore HTTP should be borne in mind two essential facts.

- HTTP is not only a hypertext protocol, but it is used for all sorts of services (i.e. APIs)
- HTTP is a *stateless* protocol, which means that response and request

³<https://www.immobiliare.it/>

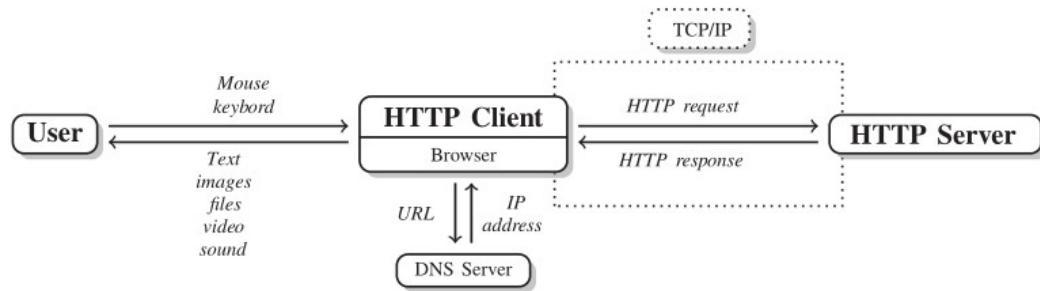


Figure 2.8: User-Server communication scheme via HTTP, source aut (2014)

and the the resulting interaction between client and server is managed by default as it were the first time they connected.

HTTP messages consist of three sections – start line, *headers* and body – whether client requests or server response messages. The start line of the server response begins with a declaration on the highest HTTP version. The header underneath the start line contains client and server meta data on the preferences for content displaying. Headers are arranged in a collection of name-value pairs. The body of an HTTP message contains the content of the response and can be either binary or plain text. Predominantly in the context of the analysis are headers which are the fields where lay the definition of the actions to take upon receiving a request or response. For what concerns the analysis the focus is on *identification headers* (both in request and response) whose role is to describe user preferences when sessions are opened i.e. default language, optimization of content display throughout devices. The exploited ones are:

(metti anche altra roba da altre fonti)

- *Authorization* (request): authentication field allows to insert personal credentials to access to dedicated content (log in to the immobiliare.it account). Credentials in requests are not really encrypted, rather they are encoded with Base64. Therefore they can be easily exposed to security breaches, which it does not happen when using HTTP (HTTP

Security) that applies encryption to basic authentication, extensively presented in 3.5.

- *Set-Cookie* (response): Cookies allow the server to keep user identity. They are a method to transform *stateless HTTP* communication (second point in previous) into a secure discussion in which potential answers rely on past talks.
- *User-Agent* (request), faced in next section 2.5.1.

2.5.1 User Agent and further Identification Headers Spoofing

Definition 2.2 (User Agents). The user Agent (from now on referred as UA) “retrieves, renders and facilitates end-user interaction with Web content” (User:Jallan, 2011).

In the HTTP identification headers the UA string is often considered as *content negotiator* (contributors, 2020i). On the basis of the UA, the web server can negotiate different CSS loadings, custom JavaScript delivery or it can automatically translate content on UA language preferences (WhoIsHostingThis.com, 2020). UA is a dense content string that includes many User details: the user application or software, the operating system (and versions), the web client, the web client’s version, as well as the web engine responsible for content displaying (e.g. AppleWebKit). When the request is sent from an application software as R (no web browser), the default UA is set as:

```
## [1] "libcurl/7.64.1 r-curl/4.3 http/1.4.2"
```

Indeed when a request comes from a web browser a full UA example and further components breakdown is (current machine):

Mozilla/5.0 (Windows NT 6.3; WOW64)AppleWebKit/537.36 (KHTML, like Gecko)Chrome/45.0.2454.85 Safari/537.36

- The browser application is Mozilla build version 5.0 (i.e. ‘Mozilla-compatible’).
- The Operating System is Windows NT 6.3; WOW64, running on Windows.
- The Web Kit provides a set of core classes to display web content in windows (UserAgentString.com, 1999), build version 537.36.
- The Web Browser is Chrome version 45.0.2454.85.
- The client is based on Safari, build 537.36.

The UA string is also one of the main responsible according to which Web crawlers and scrapers through a dedicated name field in robotstxt 2.4 may be ousted from accessing certain parts of a website. Since many requests are sent the web server may encounter insistently the same UA (since the device from which they are sent is the same) and as consequence it may block requests associated to the own UA. In order to avoid server block the scraping technique adopted in this analysis rotates a pool of UAs. That means each time requests are sent a different set of headers are drawn from the pool and then combined. The more the pool is populated the larger are the UA combinations. The solution proposed tries in addition to automatically and periodically resample the pool as soon as the website from which U agents ID are extracted updates newer UA strings.

```
set.seed(27)
url = "https://user-agents.net/"
agents = read_html(url) %>% html_nodes(css = ".agents_
  list_li") %>% html_text()

agents[sample(1)]

## [1] "Mozilla/5.0 (Linux; Android 10; LM-G710 Build/
  QKQ1.191222.002; wv) AppleWebKit/537.36 (KHTML, like
  Gecko) Version/4.0 Chrome/81.0.4044.138 Mobile
  Safari/537.36"
```

The same procedure has been applied to the From identification header attached to the request. E-mails, that are randomly generated from a website, are scraped and subsequently stored into a variable. A further way to imagine what this is considering low level API calls to dedicated servers nested into a more general higher level API. However UA field name technology has been recently sentenced as superseded in favor of a newer (2020) proactive content negotiator named *Hints* contributors (2020e).

An even more secure approach may be accomplished rotating proxy servers between the back and forth sending-receiving process.

Definition 2.3 (Proxy Server). A proxy server is a gateway between the web user and the web server.

While the user is exploiting a proxy server, internet traffic in the form of HTTP request, figure 2.9 flows through the proxy server on its way to the HTTP server requested. The request then comes back through that same proxy server and then the proxy server forwards the data received from the website back to the client. Form a user perspective benefits regards:

- anonymity on the Web
- overcome restriction access to IPs imposed to requests coming from certain locations

Many proxy servers are offered as paid version. In this particular case security barriers are not that high and this suggests to not apply them. As a further disclaimer many online services are providing free proxies server access, but this comes at a personal security cost due to a couple of reasons:



Figure 2.9: proxy middle man., source aut (2014)

- Free plan Proxies are shared among a number of different clients, so as long as someone has used them in the past for illegal purposes the client is indirectly inheriting their legal infringements.
- Very cheap proxies, for sure all of the ones free, have the activity redirected on their servers monitored, profiling in some cases a user privacy violation issue.

2.6 Dealing with failure

During scraping many difficulties coming from different source of problems are met. Some of them may come from the website’s layout changes (2.3), some of them may regard internet connection, some other may have been caused by security breaches (section 2.5.1). One of the most inefficient event it can happen is an unexpected error thrown while sending requests that causes all the data acquired and future coming going lost. In this particular context is even more worrying since scraping “main” functions is able to call 34 different functions each of which points to a different data location. Within a single function invocation, pagination contributes to initialize 10 pages. Each single page includes 25 different single links (??) leading to a number of 8500 single data pieces. Unfortunately the probability given 8500 associated to one piece being lost, unparsed is frankly high. For all the reasons said scraping functions needs to deal with the possibility to fail. This is carried out by the implementation of purrr vectorization function map (and its derivatives) and the adverb possibly Lionel Henry RStudio (2020a). *Possibly* takes as argument a function (map iteration over a list) and returns a modified version. In this case, the modified function returns an empty dataframe regardless of the error thrown. The approach is strongly encouraged when functions need to be mapped over large objects and time consuming processes as outlined in Hadley Wickham (2017) section 21.6. Moreover vecrotizaion is not only applied to a vector of urls, but also to a set of functions defined in the environemnt.

```

Input : urls: vector of crawled urls
Output: dataframe: scraped data
vectorized map iteration (in parallel)
for  $i \in \text{urls}$  do
  vectorized map iteration over scraping functions
  for  $f \in \text{functions}$  do
    possibly  $\text{fun} = f$ :
      sesh  $\leftarrow$  session( $i$  ,  $\text{agents}[\text{sample}(1)]$ , ...)
      f.results  $\leftarrow$  f(session)
      flatten f.results
    catch  $\text{error} \in \{\text{error1}, \text{error2}, \dots\}$ :
      | return NA
    end
  bind rows f.results
end
return f.results

```

Figure 2.10: pseudo code for a generic set of functions applied with possibly fail dealers , author's source

2.7 Parallel Scraping

Scraping run time is crucial when dealing with dynamic web pages. This assumption is stronger in Real Estate rental markets where time to market is a massive competitive advantage. From a run time perspective the dimension of the problem requires as many html session opened as single links crawled (refer to previous section 2.6). As a result computation needs to be *parallelized* in order to be feasible. The extraordinary amount of time taken in a non-parallel environment is caused by R executing scraping on a single processor *sequentially* url-by-url in a queue, left part of figure 2.11 (i.e. single threaded computing).

Definition 2.4 (parallel). *Parallel execution* is characterized as multiple operations taking place over overlapping time periods. (Eddelbuettel, 2020)

This requires multiple execution units and modern processors architecture provide multiple cores on a single processor and a way to redistribute computation (i.e. multi threaded computing). As a result tasks can be split into smaller chunks over processors and then multiple cores for each processor, right part of figure 2.11. Therefore Parallel scraping (sometimes improperly called asynchronous⁴) functions are proposed, so that computation do not employ vast

⁴<https://medium.com/@cumplingsi1993/the-difference-between-asynchronous-and-parallel-6400729fa897>

cpu time (i.e. cpu-bound) and space.

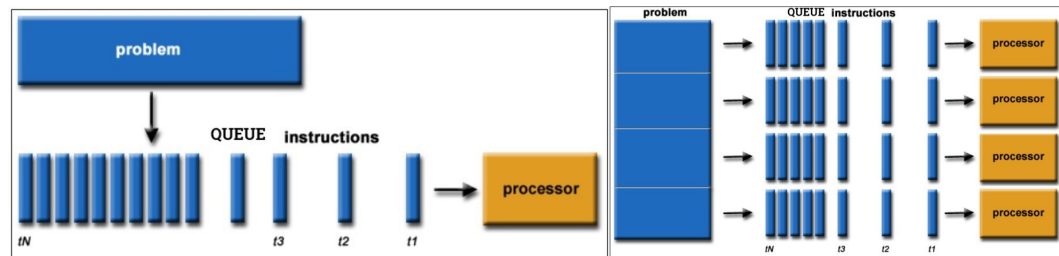


Figure 2.11: single threaded computing vs parallel computing, Barney (2020) source

Parallel execution heavily depends on hardware and software choice. Linux environments offers multi-core computation through *forking* (contributors, 2020c) (only on Linux) so that global variables are directly inherited by child processes. As a matter of fact when computation are split over cores they need to import whatever it takes to be carried out, such as libraries, variables, functions. From a certain angle they need to be treated as a containerized stand-alone environments. This can not happen in Windows (local machine) since it does not support multicore.

```
future::supportsMulticore()
```

```
## [1] FALSE
```

Cluster processing is an alternative to multi-core processing, where parallelization takes place through a collection of separate processes running in the background. The parent R session instructs the dependencies that needs to be sent to the children sessions. This is done by registering the parallel back end. Arguments to be supplied mainly regards the strategy (i.e. multi-core cluster, also said multisession) and the *working group*. The working group is a software concept (par, 2020), that points out the number of processes and their relative computing power/memory allocation according to which the task is going to be split. Moreover from a strictly theoretic perspective the *workers* (i.e. working group single units) can be greater than the number of physical cores detected. Although parallel libraries as a default choice (and choice for this analysis) ini-

tializes *as many workers as* physical HT (i.e. Hyper Threaded) *cores*. Parallel looping constructor libraries generally pops up as a direct cause of new parallel packages. The latest research activity by Bengtsson Bengtsson (2020c) indeed tries to unify all the previous back ends under the same umbrella of `doFuture`. The latter library allows to register many back ends for the most popular parallel looping options solving both the dependency inheritance problem and the OS agnostic challenge. The two alternatives proposed for going parallel are `Future` Bengtsson (2020b) with `furrr` Vaughan and Dancho (2018) and `doFuture` (2020c) along with the `foreach` Microsoft and Weston (2020) loop constructor. The former is a generic, low-level API for parallel processing as in Bengtsson (2020d). The latter takes inspiration by the previous work and it provides a back-end agnostic version of `doParallel` Corporation and Weston (2020). Further concepts on parallel computing are beyond the scope of the analysis. However they can be explored in Barney (2020), which may offers a comprehensive perspective on Parallel theory both on hardware and software. Indeed for a full reference on the R parallel ecosystem, run time simulations and advanced algorithm back end design strategies, the authorities are `par` (2020). If the interest is to cut short theory and directly put existing R code into parallel, a valuable resource is covered in `blog`⁵, which also investigate the main debugging aspects.

2.7.1 Parallel `furrr`+`future`

cerca di centrare di più su scraping

Simulations are conducted on a not-rate-delayed (section 2.4) and restricted set of functions which may be considered as a “lightweight” version of the final API scraping endpoint. As a disclaimer run time simulations may not be really representative to the problem since they are performed on a windows 10, Intel(R) Core(TM) i7-8750H 12 cores RAM 16.0 GB local machine. Indeed

⁵<https://nceas.github.io/oss-lessons/parallel-computing-in-r/parallel-computing-in-r.html>

the API is served on a Linux Ubuntu distro t3.micro 2 cores RAM 1.0 GB server which may adopt forking. Simulations for the reasons said can only offer a run time performance approximation for both of the parallel + looping constructor combinations.

The first simulation considers `furrr` which enables mapping (i.e. vectorization with `map`) through a list of urls with `purrr` and parallelization with `Future`. `Future` gravitates around a programming concept called “future”, initially introduced in late 70’s by Baker (Baker and Hewitt, 1977). Futures are abstractions for values that may be available at a certain time point later (2020b). These values are result of an evaluated expression, this allows to actually divide the assignment operation from the proper result computation. Futures have two stages *unresolved* or *resolved*. If the value is queried while the future is still unresolved, the current process is blocked until the stage is resolved. The time and the way futures are resolved massively relies on which strategy is used to evaluate them. For instance, a future can be resolved using a *sequential* strategy, which means it is resolved in the current R session. Other strategies registered with `plan()`, such as *multi-core* (on Linux) and *multisession*, may resolve futures in parallel, as already pointed out, by evaluating expressions on the current machine in forked processes or concurrently on a cluster of R background sessions. With parallel futures the current/main R process does not get “bottlenecked”, which means it is available for further processing while the futures are being resolved in separate processes running in the background. Therefore with a “multisession” plan are opened as many R background sessions as workers/cores on which chunks of futures (urls) are split and resolved in parallel. From an algorithmic point of view It can be compared to a *divide and conquer* strategy where the target urls are at first redistributed among workers/cores (unresolved) through background sessions and then are scraped in equally distributed chunks (resolved). Furthermore `furrr` has also a convenient tuning option which can interfere with the redistribution scheduling of urls’ chunks over workers. The argument `scheduling` can adjust the average number of chunks per worker. Setting it equal to 2 brings *dinamicity* (2018)

to the scheduling so that if at some point a worker is busier then chunks are sent to the more free ones.

(migliore rappresentazione)

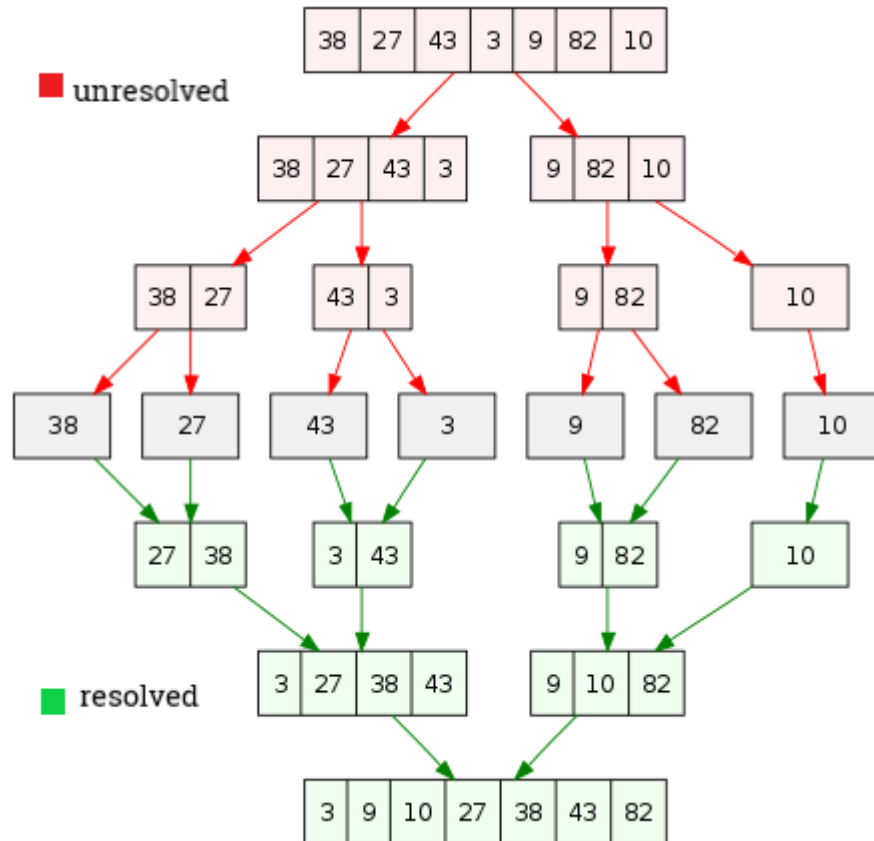


Figure 2.12: futures reimaged as divide and conquer, author's source

The upper plot in figure 2.13 are 20 simulations of 100 url (2500 data points) performed by the lightweight scraping. On the x-axis are plotted the 20 simulations and on the y-axis are represented the respective elapsed times. One major point to breakdown is the first simulation run time measurement which is considerably higher with respect to the others i.e. 15 sec vs mean 7.72 sec. Empirical demonstrations traces this behavior back to the opening time for all the background sessions. As a result the more are the back ground sessions/workers, the more it would be the time occupied to pop up all the sessions. As opposite whence many sessions are opened the mean execution time for each simulation is slightly less. The lower plot in in figure 2.13 tries to capture the run time slope behavior of the scraping function when urls (1 to 80) are cumu-

lated one by one. The first iteration scrapes 1 single url, the second iteration 2, the third 3 etc. Three replications of the experiment has been made, evidenced by three colours. The former urls are more time consuming confirming the hypothesis casted before. Variability within the first 40 urls for the three repetitions does not show diversion. However It slightly increases when the 40 threshold is trespassed. Two outliers in the yellow line are visible in the nearby of 50 and 60. It can be assumed that workers in that urls neighbor may be overloaded but no evidences are witnessed on cores activity as in plot 2.14. The measured computational complexity of scraping when n is number of urls seems to be much more less than linear $\mathcal{O}(0.06n)$.

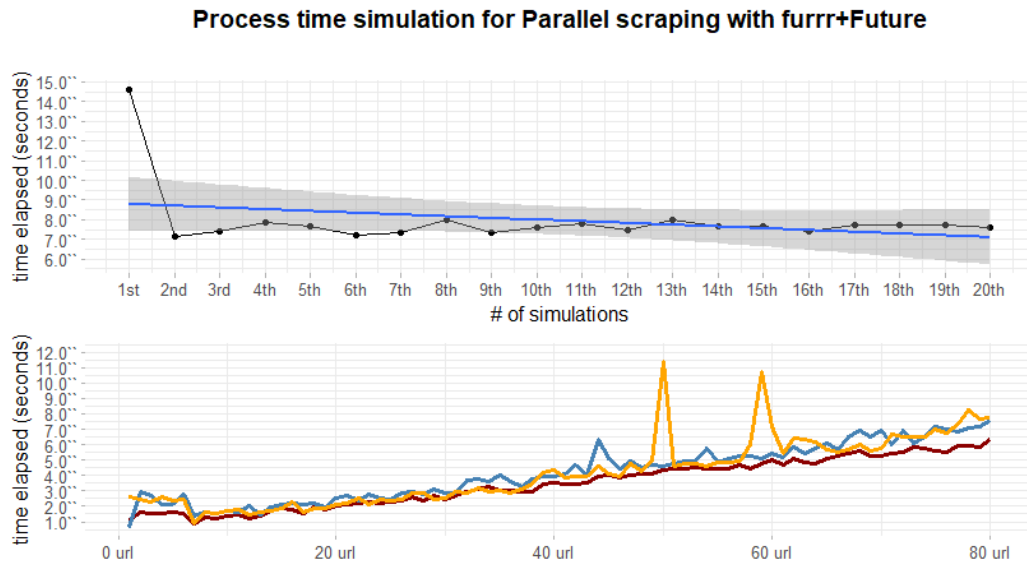


Figure 2.13: computational complexity analysis with Furr

2.7.2 Parallel foreach+doFuture

A second attempt tries to encapsulate foreach (Microsoft and Weston, 2020) originally developed by Microsoft R, being a very fast loop alternative, parallelized with doFuture. The package registered with older back ends required rigorous effort to specify exact dependencies for child process inside foreach arguments .export. From a certain angle the approach could led to an indirect

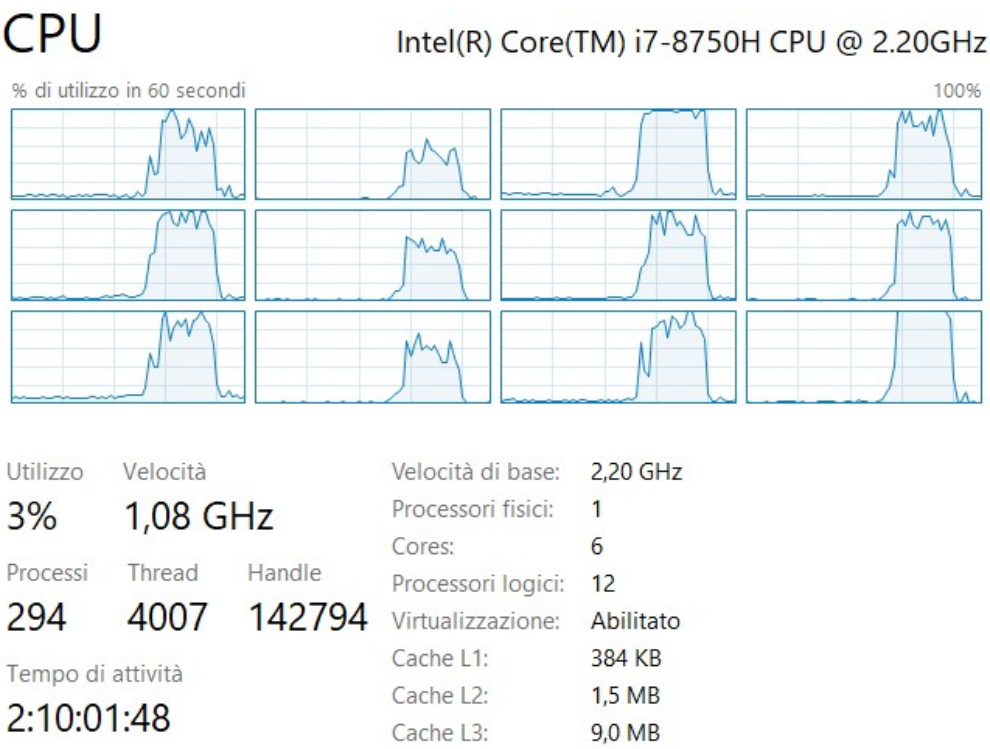


Figure 2.14: local machine monitoring of cores during parallel scraping

benefit from memory optimization. If global variables needs to be stated than the developer might be forced to focus on limiting packages exporting. Indeed since `doFuture` implements optimized auto dependency search this problem may be considered solved as in Bengtsson (2020c). Two major looping related speed improvements may come from `.inorder` and `.multicombine` arguments which both take advantage of parallel split disorder a subsequent recombination of results. In the context where data collection order matters this is extremely wrong, but since in this case order is defined through url composition based on criteria expressed inside nodes contents this can be totally applied. A drawback of enabling `.multicombine` is a worst debugging experience since errors are thrown at the end when results are reunited and no traceback of the error is given.

The upper part in 2.15 displays lower initialization lag from R sessions opening and parallel execution that also lead to a lower mean execution time of 6.42 seconds. No other interesting behavior are detected. The lower plot displays high similarities with the curves in 2.13 highlighting an outlier in the same proximities of 45/50 urls. The blue simulation repetition shows an uncommon pattern that is not seen in the other plot. Segmented variability from 40 to 80 suggests a higher value which may be addressed do instability. As a result the approach is discarded in favor of `furrr + future` which also offers both a comfortable `{Tidyverse}` oriented framework and offers an easy debugging experience.

2.8 Open Challenges and Further Improvements

Although results are quite encouraging still one of the main challenges remains unsolved. In fact optimization has involved each scraping layer but scraping function must be continuously kept up with the `immobiliare.it` changes, particularly the crawling part. Indeed the proper scraping part, with some further

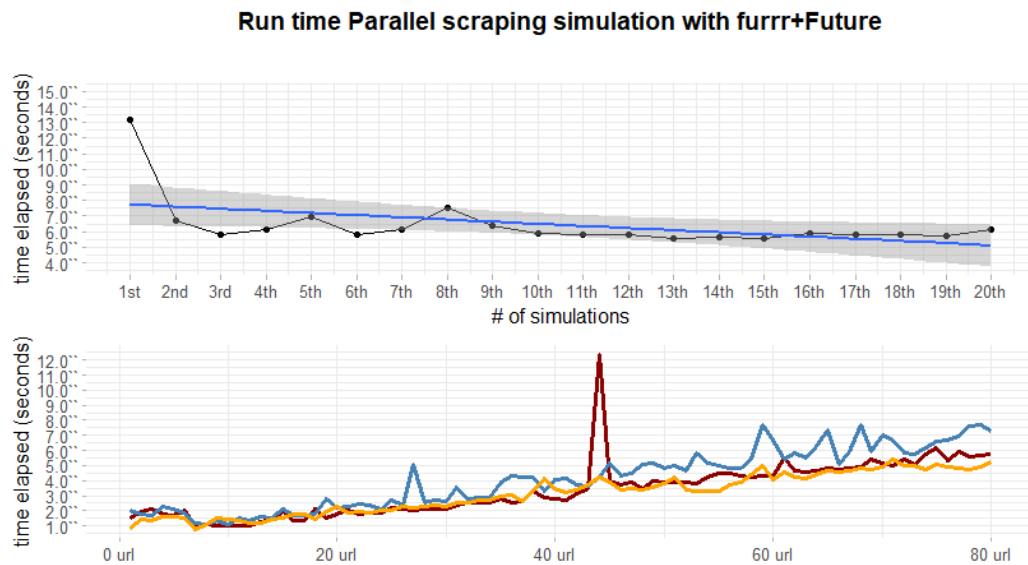


Figure 2.15: computational complexity analysis with Furrr

adjustments can take care of auto-search for exact information within the web page even if the design changes. This idea is massively applied in the package Rcrawler Khalil (2018), which doesn't apply segmentation in crawling, instead it downloads the entire website and then inspects targeted keywords. The major benefit relies in crawling HTML/XML that are agreed to be generally lightweight in this way the process does not weigh down the run time. Whence all files are saved locally the algorithm applies search methodologies within the HTML files. Run time performance with algorithm of this kind with respect to the amount of data gathered are very efficient, nevertheless results are not always effective due to keywords disambiguation. Afterall a way safer and time saving approach to general scraping may be including complex theme specific regular expressions on the HTML text which univocally identify CSS data location. With that said the idea would be an unsupervised algorithm that combines the traditional browser search + a selector gadget for CSS conversion. As a disclaimer Rcrawler is designed to be flexible to scrape a vast number of websites. As opposite the scraping functions here presented are exclusively built on top of immobiliare.it, even though they can be extended with a small

effort to other category related website ???. On the parallel computing side a further boosts might be added with parallel distributed processing through HPC (high-performance computing) clusters by `future.batchtools` Bengtsson (2020a). The package implements a generic future wrapper around `batchtools` with job scheduler like Torque, Slurm, Sge and many more. A higher level API built on top of the Future framework that exploits Google Cloud Engine Clusters⁶ i.e. `cloudyR` allows to distribute computation on Google machines.

2.9 Legal Profiles

There is a legitimate *gray* web scrapers area, not only creating possible new uses for the data collected, but also potentially damaging the host website (Media, 2017). Online platforms and the hunger for new data insights are increasingly seeking to defend their information from web scrapers. Online platforms are unfortunately not always successful distinguishing users between polite, impolite and criminals, risking new ones Valid competition and creativity. A minimal but effective self limitation can really be The courts have fought hard to achieve clear judgments Cases for web scraping. The crucial obstacle is a coherent verdicts to ascertain “Kitchen Sink” (MERRIAM-WEBSTER, 2018), the standard web claim discontroversy on scraping. Kitchen Sink main arguments are:

- Legal lawsuits under the Computer Fraud and Abuse Act (CFAA) allegation that the defendant “overtook” allowed access *miss lit*
- Copyright infringement charges under the Digital Millennium Act or federal copyright law Copyright laws *miss lit*
- “state trespass to chattels claims” *miss lit*
- Contract agreements terms violation claims

A second challenge to clear verdicts is that there are several purposes for which a business model operates in a continuum of social acceptability hiring web

⁶<https://cloudyr.github.io/googleComputeEngineR/articles/massive-parallel.html>

scrapers (Maheedharan, 2016). As an example Googlebot ranks, sorts and indexes search results for Google users, without which the search would not be optimized and business would not profit from this fact. A more coherent case is represented by the exploitation of scraping on online Real Estate advertiser whose importance is ascertained by the fact that they are the first house purchase media 52% (USA survey) and searches are expected to be growing by 22% per year (Peterson and Merino, 2003). On the other hand it is estimated that the 20% of crawlers are actually DoSsing scrapers (LaFrance, 2017) causing an economic damage, as in 3.1.3. Unfortunately the majority of web scraping services fall between these two extremes (2017). The most discussed and observed case regards LinkedIn Corp. “LinkedIn” vs hiQ Labs Inc. (“hiQ”) whose claim argues the exploitation of the former personal profile data to offer a series of HR services. The litigation started by accusing hiQ with “using processes to improperly, and without authorization, access and copy data from LinkedIn’s website” (Corporation, 2017). As reinforcement to their arguments they presented also a citation directly from their terms raising the point on copying, web scraping prohibition without their explicit consent. Furthermore LinkedIn noted that technical barriers were taken into existence to restrict the access of hiQ to the platform and warned of a breach of state and federal law by ignoring such barriers (2017). As a response HiQ submitted a temporary restraining order to prevent LinkedIn from denying the access to their platform, focusing on the aspect that the motivation was led by an anticompetitive intent. LinkedIn’s response brought into the litigation CFAA which actually pollutes argumentation since Court evidences that CFAA is ambiguous whether it is granting or restricting the access to public available website (Edward G. Black, 2017). In other words CFAA intent was to protect user data when they are authenticated with passwords, and in no case out of these borders. In the end the litigation moved to the Ninth Circuit where in 2019 it uphelds the preliminary injunction to prohibit LinkedIn from continuing to provide access to publicly accessible LinkedIn member profiles to the claimant hiQ Labs (contributors, 2020d). Immobiliare.it expressed similarly

to linkedin in their terms (immobiliare.it, 2020) the prohibition to reproduce any form of intellectual property in their web pages. This once again does not imply the inaccessibility to scraping their content and should not in any case prevent the usage of an open sourced tool inspired by research grounds and efficient market choices.

Chapter 3

API Technology Stack

The previous chapter has encapsulated the main concepts behind the design of consistent, secure, and fast scraping functions with R. In truth challenges not only regard scraping per se, but also the way and how many times the service has to interact with different clients. Indeed the fact that functions are compressed into scripts does not imply that are shareable and portable. As a consequence when they are executed they also need to be at first understood and secondly loaded into a dedicated R environment (higher and lower dependencies). Moreover results are actually computed, whether in parallel or not, with local machines resources that are limited in many sense. In the end exposing the service traffic to the public or internally to a network of servers requires authentication and precautions from both malicious attack and privacy dangers. Actually from a restricted personal usage perspective what has been done since now is totally feasible. But in a large-scale orientation where different stakeholders should gather massive amount of data, then a unsuitable service may cause an enormous waste of time. The following chapter tries to capture the essence and its specific context usage of each technology involved that address each aforementioned issues raised. In parallel it highlights the *fil rouge* that ties together the chronological order according to which the stack has been developed.

The recipe proposed serves a REST Plumber API (an R framework) with 2

endpoints each of which calls Parallel scraping functions accomodated in section 2. Precautions regards sanitization of user inputs, anti-Dossing strategies and log monitoring. The software enviroment is containerized in a Docker container and *Composed* with a further container housing NGINX proxy server. Orchestration is managed with docker compose. NGINX with SSL certificates bring HTTPS communication and authentication. An AWS free tier EC2 server hosts the orchestation of containers and the IP is made Elastic. Furthermore the software development is made automatic with a straightforward composition of cloud services that ignites sequential building when local changes are pushed to cloud repository.

Technology stack:

- GitHub version control and CI
- Plumber REST API, section 3.1.1
- Docker containers and compose, section 3.2
- NGINX reverse proxy, section 3.3
- HTTPS and SSL certificates 3.5
- AWS EC2 3.6

immagine infrastruttura da rivedere

As a further note each single part of this thesis is comprised according to the service inspiring criteria of portability and self containerization. RMarkdown (Allaire et al., 2020) documents (book's chapters) are knitted and then rendered as .html files extension through Bookdown (Xie, 2016). The resulting .html documents are instructed by a .yml file and then are rendered as Gitbook format. Gitbooks are interactive online documentation that are employed to build books, technical documentation as well as research papers. That makes thesis' graphs and codes interactive. Moreover Gitbooks enables custom buttons to directly create a push request on documents from source, which may be convenient for continous review. It is able to directly share documents on social media, as well as to change the the documents' style, such as fonts and

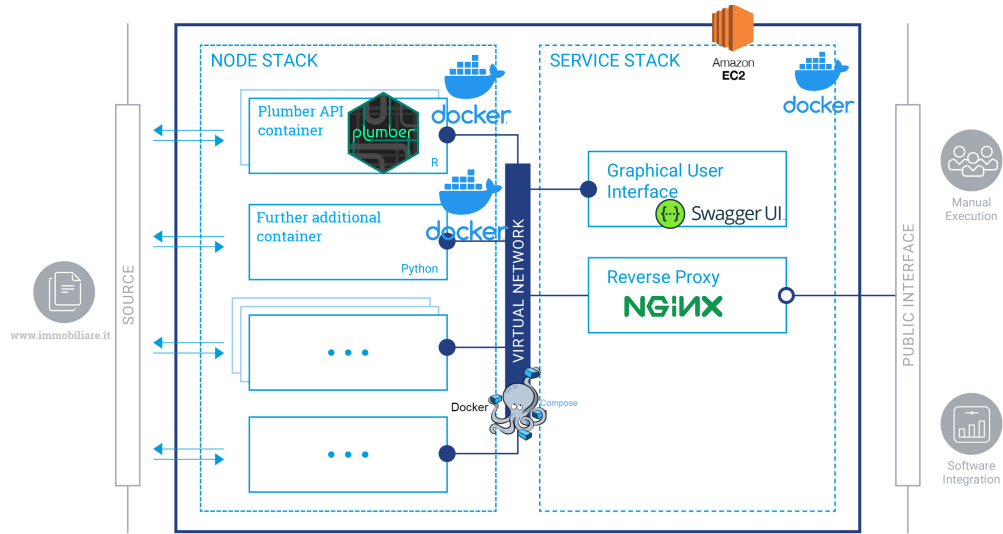


Figure 3.1: complete infrastructure, author's source

background color.

Files are ultimately pushed into a Github repository¹, that enables thesis version controlling. By a simple trick with GH pages a new branch is opened. .html files are displayed into a sub domain repository hosted at link², as a consequence thesis is also linked online. Moreover the Gitbook is able to produce also a .pdf version output through a Xelatex engine. Xelatex compiles .Rmd documents according to formatting rules contained in both a .tex template and a further .yml and produces the final .pdf paper output.

3.1 RESTful API

Definition 3.1 (API). API stands for application programming interface and it is a set of definitions and protocols for building and integrating application software. Most importantly APIs let a product or a service communicate with other products and services without having to know how they're implemented.

API may be considered as a mediator between users or clients sending a re-

¹<https://github.com/NiccoloSalvini/thesis>

²<https://niccolosalvini.github.io/thesis/>

quest, left part figure 3.2 and the web resource or services they want (returning back a response) middle part figure 3.2. It also acts as means of exchanging resources and knowledge with an entity, as databases left part figure 3.2 preserving protection, control and authentication, such as who gets access to what. There are many types of APIs that exploit different media and architectures to communicate with apps or services.

Definition 3.2 (REST). The specification REST stands for **RE**presentational **S**tate **T**ransfer and is a set of *architectural principles*.

If a client request is made using a REST API, a representation of the resource state is passed to a requestor or *endpoint* (wha, 2018). This information is returned in one of the formats of multiple formats using *HTTP*: JSON, HTML, XLT, Python, PHP or simple text. JSON is the most common programming language to use because it is language agnostic (2018) and easy to interpret both for people and machines. REST architecture depends upon HTTP, as a matter of fact REST API inherits from HTTP the stateless property, second pillar in 2.5. Calling a REST API (producing a request) demands composing a well defined URL lower part in figure 3.2, whose semantic is able to uniquely identify the resource or a group of resources (sending back a response) along with the most common HTTP methods, as GET, PUT, POST, DELETE.

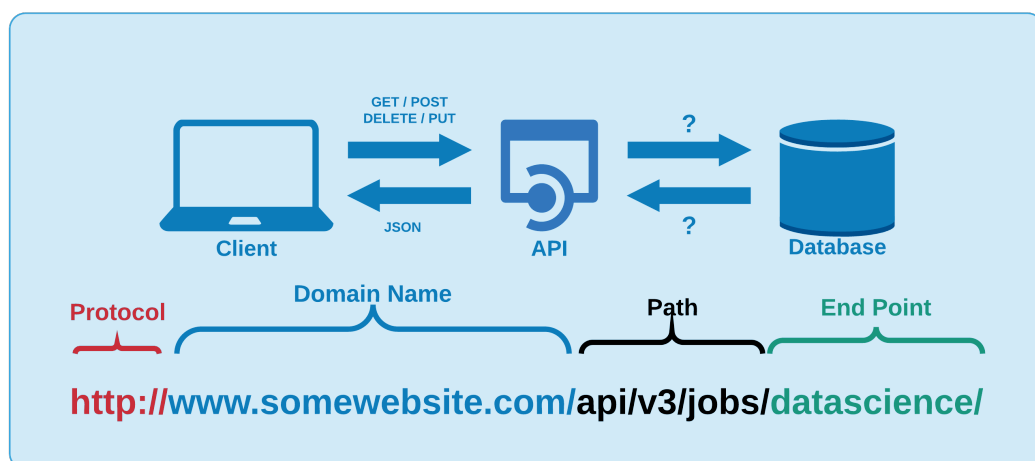


Figure 3.2: API general functioning, unknown source

When an API adheres to REST 3.2 principles is said RESTful. Principles are:

- A client-server architecture made up of clients, servers, and resources, with requests managed through HTTP method.
- Stateless client-server communication, meaning no client information is stored between requests and each request is separate and disconnected.
- Cacheable data that streamlines client-server interactions.
- A uniform interface between components so that information is transferred in a standard form. This requires that:
 - resources requested are identifiable and separate from the representations sent to the client.
 - resources can be manipulated by the client via the representation they receive because the representation contains enough information to do so.
 - self-descriptive messages returned to the client have enough information to describe how the client should process it.
- A layered system that organizes each type of server (those responsible for security, load-balancing, etc.) involved the retrieval of requested information into hierarchies, invisible to the client.

RESTful APIs receives HTTP request inputs and elaborates them through endpoints. Endpoints are the final step in the process of submitting an API request and they can interpreted as the responsables for generating a response (2018). Further documentation and differences between HTTP and REST API can be found to this reference³. Open and popular RESTful API examples are:

- BigQuery API: A data platform for customers to create, manage, share and query data.
- YouTube Data API v3: The YouTube Data API v3 is an API that provides access to YouTube data, such as videos, playlists, and channels.

³https://docs.aws.amazon.com/it_it/apigateway/latest/developerguide/http-api-vs-rest.html

- Skyscanner Flight Search API: The Skyscanner API lets you search for flights & get flight prices from Skyscanner's database of prices, as well as get live quotes directly from ticketing agencies.
- Openweathermap API: current weather data for any location on Earth including over 200,000 cities.

3.1.1 Plumber HTTP API

Plumber is a R framework (?), allowing users to construct HTTP APIs simply by adding decoration comment to the existing R code, in this context to scraping code. Decorations are a special type of comments that suggests to Plumber where and when the API specifications start. Below is reported a toy API with 3 endpoints inspired by the original documentation. Endpoints in the following code chunk are identifiable by the three distinguishing comment blocks, separated by the aforementioned decorations. http API specifications require the user to set the endpoint description (first comment), to specify the parameters role and input type (second), and the http method i.e. GET, POST followed by the endpoints invocation verb e.g. echo, plot, sum (third).

```
# plumber.R

## Echo back the input
## @param msg The message to echo
## @get /echo
function(msg="") {
  list(msg = paste0("The message is : ", msg, " "))
}

## Plot a histogram
## @param n the number of samples
## @serializer png
## @get /plot
```

```

function(n = 10) {
  rand = rnorm(n = n)
  hist(rand)
}

## Return the sum of two numbers
## @param a The first number to add
## @param b The second number to add
## @post /sum
function(a, b) {
  as.numeric(a) + as.numeric(b)
}

```

Once HTTP api calls are sent to machines belonging to a single server or a network of servers, whether it is public or private they converge through endpoints. Endpoints execute functions involving the parameters specified through the call and by default response is JSON type. The first endpoint “echo” invocation simply *echoes* back the text that it was sent. The second endpoints generates a histogram *plot* i.e. .png file based on a Normally distributed sample whose observation number are “n”. The third endpoint calculates the *sum* of a couple of number attached to the call. Scraping function are then implemented within the API framework and arguments becomes parameters for an incoming request. Many more options may induce plumber endpoints to respond in the preferred fashion, in any case are beyond the scope of the analysis. Exposing APIs on a private network or on a public server security is a major issue. Concerns and thought process therefore must adapt accordingly. There are several variables and consequent attacks that should be considered while creating Plumber APIs, but the focus will differ depending on the API audience. For example if APIs are offered without authentication on the Internet, potential vulnerabilities should seriously convince the api maintainer to properly account each of them. Three in the context of the analysis are

critical:

- Sanitization
- Denial Of Service (DoS)
- Logging

3.1.2 Sanitization

Whenever APIs accept input from a random user this is directly injected into functions through endpoints, therefore the worst case scenario should be prepared. In the context of the analysis users are required to specify to the endpoints arguments such as cities, zones, number of pages and many others. Chances are that users might either misspell inputs or use different encoding (accents) or rather use capital letters when functions are capital sensitive. Endpoints should take account of the behavior by sanitizing whatever it comes into the function. The process at first requires an intense and creative investigation on what it can be misused and how. Then Secondly new functional inputs are defined so that they take the user generated input and give back a sanitized version inside the function. In the code chunk below are shown a couple of examples of sanitization of inputs:

```
tipo = tolower(type) %>% str_trim()
citta = tolower(city) %>% iconv(to = "ASCII//TRANSLIT")
      %>% str_trim()
macrozone = tolower(macrozone) %>% iconv(to = "ASCII//
      TRANSLIT") %>% str_trim()
```

Inputs make their entrance into functions through arguments “type”, “city” and “macrozone” and are immediately preprocessed. They are in sequence converted to lower cases, then extra spaces are trimmed, in the end accents are flattened.

3.1.3 Denial Of Service (DoS)

Denial-of-service attacks (DoS) are used to temporarily shut down a server or service through traffic congestion. A DoS scenario could be triggered accidentally by a malicious user requesting the server for an infinite looping task. Other scenarios might depict a malicious hacker who uses a large number of machines to repeatedly make time consuming requests to occupy the server, this is the case of DDoS (Distributed Denial of Service). DoS or DDoS attacks may also induce anomalies and deprives system resources, which in the context of hosting services may result in astronomical fees charged. Dos attack as a consequence may also induce distorted website/API logs analytics, leading to distorted reports. A simple but effective approach tries to limit and stop the number of request sent:

```

if (npages > 300 & npages > 0){
    msg = "Don't DoS me!"
    res$status = 500 # code num:
        Bad request
    stop(list(error=jsonlite::unbox
        (msg)))
}

```

The code chunk above intercepts DoS attacks by limiting to 300 the number of pages to be server to the API. Furthermore it converts outputs error messages printed on console into JSON format and then pass them as output. This simplify distinguishing malicious attacks from a type errors. DDoS attacks are secured by SSL certificates and Authentication covered later in the chapter.

3.1.4 Logging

Plumber uses “filters” that can be resorted to describe a “pipeline” for processing incoming request. This enables API maintainers to separate complex logic into discrete, comprehensible steps. Usually, before trying to find an endpoint

that satisfies a request, Plumber passes the request through the *filters*. When APIs are called, requests pass through filters one at a time and Plumber forwards i.e. `forward()` the request to the next filter until the endpoints. Filters applications ranges from excluding client request based on request parameters or may offer also a thin layer of authentication. Filters might also be used as a logging for requests where logging, i.e. the act of keeping a log (?), is recording events in an operating system or running software from other users of communication software, or messages among different subjects. A request log filter might have this appearance:

```
##* Log information
##* @filter logging
function(req){
    cat(as.character(Sys.time() ), "—" ,
        req$HTTP_USER_AGENT, "@",
        req$REMOTE_ADDR, "\n",
        req$QUERY_STRING, "\n")
    plumber::forward()
}
```

The above filter parses the request through the default request argument `req`, then it prints out messages about the incoming User Agent (i.e. `HTTP_USER_AGENT`) (section 2.5.1), the `REMOTE_ADDR` which is the IP address of the client making the request (2018) and the `QUERY_STRING` that records the parameters directly sent the endpoint. This helps to traceback clients activity on the API as well as detecting misuse.

3.1.5 RESTful API docs

The service disposes of 2 endpoints `/fastscrape` , `/completescrape`. Parameters, aligned next to the endpoint name in figure 3.3, are the same for both of the endpoints since they rely on the same reverse engineering url algorithm 2.4, explained in section 2.1. Moreover Plumber APIs are natively wrapped

up around Swagger UI helping development team or end users to imagine and communicate with the resources of the API without any discharge logic (SMARTBEAR, 2019). The OpenAPI (formerly referred to as Swagger), with the visual documentation facilitates backend implementation and client side consumption, as well as being automatically created by the APIs specification (parameters, endpoints...). Some of the major assets in Swagger UI are: The user interface works in any environment, whether locally or web and it is suited for all main browsers. Rest API documentation can be reached to the API address in the `/__docs__` path, in the upper navigation bar of figure 3.3. A further parameter argument, namely `thesis` into both of the endpoint has been added in order to make the API calls reproducible by providing to the scraping function a pre-compiled url to scrape.

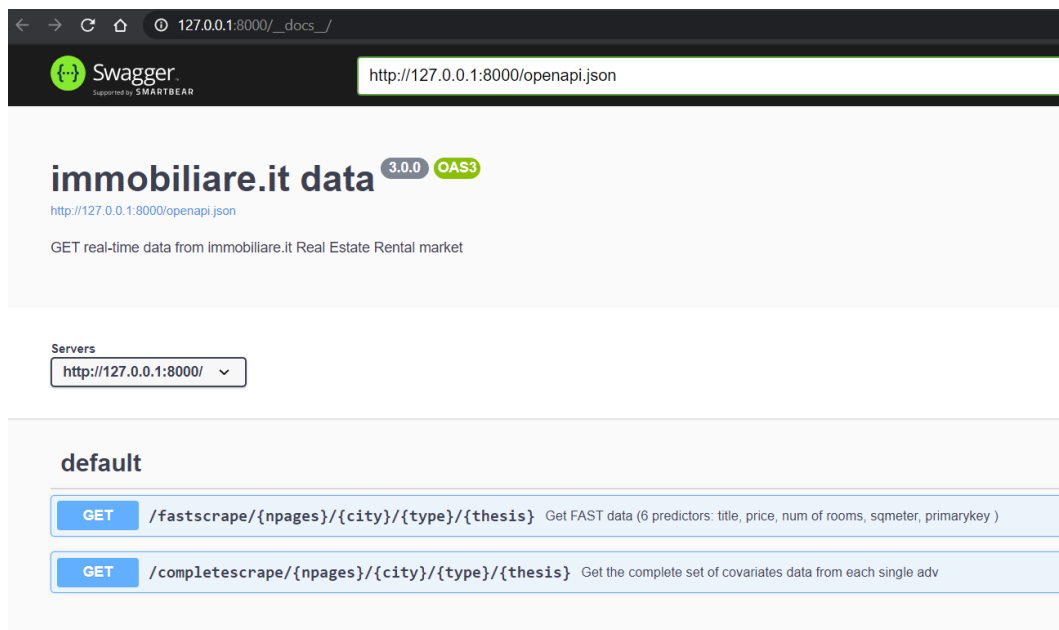


Figure 3.3: Swagger UI in localhost on port 8000, author's source

3.2 Docker

The API up to this point needs a dedicated lightweight software environment that minimizes dependencies both improving performances and enabling *cloud*

computing coverage. A fast growing technology known as *Docker* might extend these capabilities.

Definition 3.3 (Docker and Containers). *Docker* (Merkel, 2014) is a software technology to create and deploy applications using containers. *Docker containers* are a standard unit of software (i.e. software boxes) where everything needed for applications, such as libraries or dependencies can be run reliably and quickly. Containers are also portable, in the sense that they can be taken from one computing environment to the following without further adaptations.

Containers can be thought as a software abstraction that groups code and dependencies together. One critical advantage of containers is that multiple containers can run on the same machine with the same OS along with their specific dependencies (docker compose). Each container can run its own isolated process in the user space, so that each task/application is exhaustively and complementary to the other. The fact that containers are treated singularly enables a collaborative framework that it also simplifies bugs isolation.

Actually *Docker containers* are the build stage of *Docker Images*. Docker images therefore are the starting point to containerize a software environment. They are built up from a series of software layers each of which represents an instruction in the image's *Dockerfile* (2020a) . In addition images can be open sourced and reused through Docker Hub. *Docker Hub* is a web service provided by Docker for searching and sharing container images with other teams or developers in the community. Docker Hub can authorize third party applications as GitHub entailing an collaborative image version control, this would be critical for software development as disguised in section (3.7).

3.2.1 REST-API container

Docker can build containers from images by reading instructions from a Dockerfile. A Dockerfile is a text document that contains the commands/rules a generic user could call on the CLI to assemble an image. Executing the

command `docker build` from working directory the user can trigger the build. Building consists of executing sequentially several command-line instructions that specifies the software environment. As a matter of fact the concept of containers takes inspiration by the fact that many single software layers are stacked up over at the following. An open source project named `rocker`⁴ already disposes of a group of pre-set task-specific image configurations from which further custom `dockerfile` can be built on top of. Therefore images are overwritten with higher level dependencies i.e. package libraries, since lower levels Linux dependencies are already partially handled. Indeed as in 3.7 an automatic development workflow is proposed that triggers the building of the image when changes are pushed to github.

The custom `Dockerfile` in figure 3.4) is able to build the `rest-api` container:

```
2 FROM rocker/tidyverse:latest
3
4 MAINTAINER Niccolo Salvini "niccolo.salvini27@gmail.com"
5
6 RUN apt-get update && apt-get install -y \
7     libxml2-dev \
8     libudunits2-dev
9
10 # install R packages
11 RUN R -e "install.packages(c('plumber', 'rvest', 'stringi', 'here', 'tictoc',
12     'future', 'here', 'parallel', 'furrr', 'robotstxt' ), dependencies = TRUE)"
13 COPY /scraping
14
15 WORKDIR /scraping
16
17 # expose port
18 EXPOSE 8000
19
20 ENTRYPOINT ["Rscript", "main.R"]
```

Figure 3.4: Custom `Dockerfile` from `salvini/api-immobiliare` Docker Hub repository, author's source

Each line from the `Dockerfile` has its own specific role:

- `FROM rocker/tidyverse:latest` : The command imports from `rocker` project a pre set configuration containing the latest version of base-R along with the `tidyverse` (Wickham et al., 2019) R packages collection.

⁴<https://www.rocker-project.org/images/>

- MAINTAINER Niccolo Salvini "niccolo.salvini27@gmail.com" : The command tags the maintainer and its e-mail contact information.
- RUN apt-get update && apt-get install -y \ libxml2-dev \ libudunits2-dev : The command update and install remaining "lower" Linux dependencies required to run Plumber and rvest.
- RUN R -e "install.packages(c('tictoc ','here ','...', dependencies=TRUE))" : The command install all the further lower level libraries required to execute the files. Since some packages have inner dependencies the option dependencies=TRUE is necessary.
- COPY /scraping : The command tells Docker to copy into the container files in /scraping folder (where API specs are)
- WORKDIR /scraping : The command tells Docker to set /scraping as working directory
- EXPOSE 8000 : The commands instructs Docker engine that the container listens on the specified network ports 8000 at runtime. Default *transportation* layer is TCP.
- ENTRYPOINT ["Rscript", "main.R"] : the command tells docker engine to execute the file main.R where are contained the Plumber router options (i.e. host and port specifications).

3.3 NGINX reverse Proxy Server and Authorization

Proxy server in this context offers the opposite angle for the exact same security problem. As a matter of fact the downside is that they can be exploited for the same reason for which they have been criticized at the end of section (2.5.1). Reverse Proxy server are a special type of gateway 2.3 that is usually located behind a private network firewall to route client requests to the

corresponding backend server (NGINX, 2014). An reverse proxy offers an extra abstraction and control level to ensure that network traffic flows smoothly between clients and servers. NGINX as it can be inferred by its official documentation empowers traffic flows by:

- *Load balancing:* A reverse proxy server will stand guard in front of back end servers and redirect requests across a group of servers in a way that maximizes speed and capacity usage as well as not overloading the server. When a server crashes, the load balancer redirects traffic to the other online servers (note required since traffic is not expected to be enormous).
- *Web acceleration:* A reverse proxies can condense input and output data by caching frequently requested information. This assists traffic between clients and servers avoiding to request data more than once. They can also apply SSL encryption, which improves their performance by eliminating loads from web servers.
- *Security and anonymity:* A reverse proxy server protects identities and serves as an additional protection against security threats seen in subsections (3.1.2, ??) by intercepting requests before they reach end server.

When a user calls the API, NGINX acts as a gateway asking for credentials and registering log data (HTTP identification headers). If the request has already been asked then cached response is returned. If it does not then the request is routed to the endpoint, service A and B in figure 3.5. Endpoints elaborate the request into the response, which flows back at first to the gateway and then finally to the client. Logging data can be feeded to a dashboard monitoring traffic and API exposure.

Then without any further software installation, the developer can simply make use of the latest NGINX open sourced image to build the NGINX proxy server within the same image. A further configuration file should manage NGINX

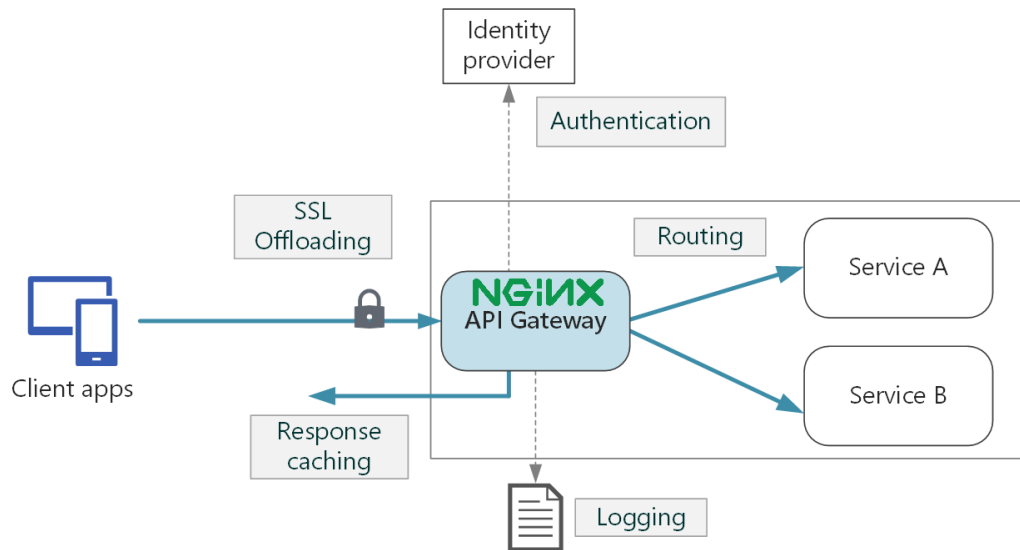


Figure 3.5: NGINX gateway redirecting an incoming request, source Microsoft (2018)

inner settings that links volumes, ports and IPs, but details are beyond the scope of the analysis.

3.4 Docker-Compose

Compose is a multi-container Docker framework to define and run complex application and services, that means isolated stand alone containers can communicate one to each other. The orchestration of containers is managed through a `.yaml` file `docker-compose.yml` that configures the whole set of facilities designed for the services. Services are then build with a single docker command `docker-compose up` on the basis of the instruction `yaml` file. Compose also enables *Volumes*, which are used in Docker for **data persistence** (Inc., 2020b). *Volumes* allows to keep data secured from docker stop or delete containers. Docker Volumes in a nutshell works as the linkage between a physical file system path (folders, directories) plugged/**mounted** into the virtual container file system path. The main properties for Composition as in documentation (Inc., 2020a) regards:

- *A central host in multiple isolated environments:* Compose provides a label for a project to distinguish environments. The default project name is the directory path.
- *Preserve data volumes (which are the preferred Docker mechanism to consume data generated and used by containers) when building containers:* Compose maintains all of the services' Volumes. When Docker-compose is running, it transfers the Volumes from the old container into the new container when it detects containers from previous runs. This method guarantees that no Volume data produced is lost.
- *Only recreate containers that have changed:* Compose caches the configuration and re-use the same containers when it reboot a service which hasn't changed. Re-use containers means it provides really fast improvements to the environment when developing complex services.
- *Variables and moving a composition between environments:* Compose supports file variables which might be used to adjust any composition to various environments or users.

The first line defines the versions according to which Compose orchestrates containers. Services are two, the rest-api and NGINX. The former whose name is restful-api builds the container starting from the Dockerfile contained into the rest_api path specified as in 3.2.1. The first service also mounts Volumes from shared_data to itself in the virtual container file path. Port 8000 opened (3.2.1) is linked to the 7000 one. Restarting set to "always" secures the latest container version. The latter service is NGINX 3.3 which proxies traffic from 80 and 443 based on .conf file whose specifications are beyond the scope of the analysis. Volumes makes sure that specifications are arranged in the default path choice. The option depends_on defines the chronological condition according to which containers should be run and then composed.


```
1 version: "3.6"
2
3 services:
4   rest-api:
5     container_name: restful-api
6     build:
7       context: ./rest_api # Docker image is rebuild from directory which contains Dockerfile
8     volumes:
9       - ./shared_data:/shared_data
10    ports:
11      - "7000:8000"
12    restart: always
13
14   nginx:
15     container_name: nginx-reverseproxy
16     image: nginx:1.9
17     ports:
18       - "80:80"
19       - "443:443"
20     volumes:
21       - ./nginx.conf:/etc/nginx/nginx.conf:ro
22     restart: always
23     depends_on:
24       - rest-api
25
26
27
```

Figure 3.6: Docker Compose YAML file orchestration for NGINX container and RESTful API, author's source

3.5 HTTPS(ecure) and SSL certificates

Communication even though properly secured and distributed with NGINX is still not encrypted so sensitive data are still being exposed. HTTP Secured (HTTPS) is a product of HTTP combined with SSL/TLS (Secure Sockets Layer/Transportation Security Layer) protocol rather than a protocol itself. HTTPS is strictly appropriate when transmitting sensitive data such as banking or on-line buying. Its importance is highlighted by the fact that nowadays is rather more common to find HTTPS than HTTP. The Secured method encrypts all contacts between the client and the server, figure 3.7. The HTTPS scheme in actual is "HTTPS" and its default port is 443 (that should be exposed too in the dockerfile). SSL runs as a sublayer of the *application* layer (a further internet layer, refer to section 2.5), this ensures that HTTP messages are encrypted prior being transmitted to the server (SSL Offloading box in figure 3.5) whether it is a proxy server or directly a web server.

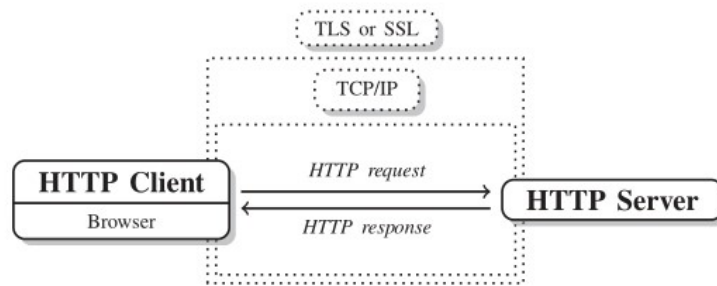


Figure 3.7: HTTPS encryption with SSL certificates, source aut (2014)

From a port communication point of view at first NGINX container listens to on port 80 and that it is where all requests should relay to IP_machine_address:8000. As a result the RESTful API is published on Port 80 instead of 8000. Secondly it listens on the SSL port 443 and points to the key and certificate files that have been created in the Dockerfile.

3.6 AWS EC2 instance

From henceforth the software container environment can be reproduced regardless of the mounted OS. Scalability and accessibility is worked out by exporting orchestrated containers on a web server. There are many hosting services options that varies primary on the budget and consequently on the API audience. A flexible cloud provider combined with NGINX load balancing *ceteris paribus* may offer a stable and reliable service for a reasonable price, even considering a bad-case scenario where requests are many and insistent.

Definition 3.4 (AWS EC2). Amazon Elastic Compute Cloud (EC2) is a web service that contributes to a secure, flexible computing capacity in the AWS cloud. EC2 allows to rent as many virtual servers as needed with customized capacity, security and storage.

AWS EC2 represents a popular hosting option, most importantly this path is already narrowed by many open source contributors. The selected target is

a AWS free tier t3.micro whose specifications are: 2 vCPU (Virtual CPU), 1 GB memory and a mounted Ubuntu distribution OS. Moreover T3 instances are known to provide device, memory, and network resource balance and have been developed for applications that experience transient spikes in use with modest CPU use. They are designed especially to serve low-latency interactive applications, small and medium databases, virtual desktops, development environments, code repositories, and business-critical applications, therefore they suit the needs. Prior any new instance initialization AWS offers to tune servers' set up options. Networking and VPC are chosen to be left as is since they can always be updated at need. Storage is increased to 30 GB which represents the free tier eligibility upper limit. Tags are not required. Indeed security at first needs to account for a SSH connection that allows communication with the server i.e. open port 22. Secondly it should account for port openings accordingly to NGINX configuration file and rest-api dockerfile (3.2.1), port 80 (default for TCP) and 443 (HTTPS default) are opened. Once the instance is running the server can be accessed through SSH (Putty or Bash depending on the OS) behind authentication.

3.7 Software CI/CD Workflow

Software changes can happen quite often due to the dynamic nature of the RESTful API's target website. This requires a modern stack of cloud technologies to update, revert and quickly deploy software versions, or even adapt software architecture. As a consequence the software CI/CD manages minor changes with local commits to the project, which are then directly pushed through git into a GitHub repository, upper left quadrant 3.8. The repository directly communicates with an open DockerHub repository that sequentially triggers the compose-up command of the compose.yml file, and through that the docker images whenever any changes are pushed, upper right quadrant 3.8. Images are tagged and cached so that versions are controlled and Software build avoids to rerun containers that have not suffered any change. Debugging

stage is constrained by logs generated by docker engine. Furthermore the build stage in R since 2019 required long time due to package compiling, but since the appearance of Rstudio package manager⁵ which includes beta support for pre-compiled R packages they can be installed 3 times faster (Nolis, 2020). When newer images are available they can be pulled from the EC2 server and rerun in detached mode. Massive software changes are managed through GitHub branches, even though it must be kept in mind to switch lautomatic building brench. The Ec2 server is associated to an Elastic IPs address allowing to reuse the address for external databases connections and DNS services as Cloudflare (for SSL certificates). Moreover elastic IPs are effective when the EC2 server stands in need of upgrading or downgrading or when the server may fail, thus restoring and apply the IP address for a new server.

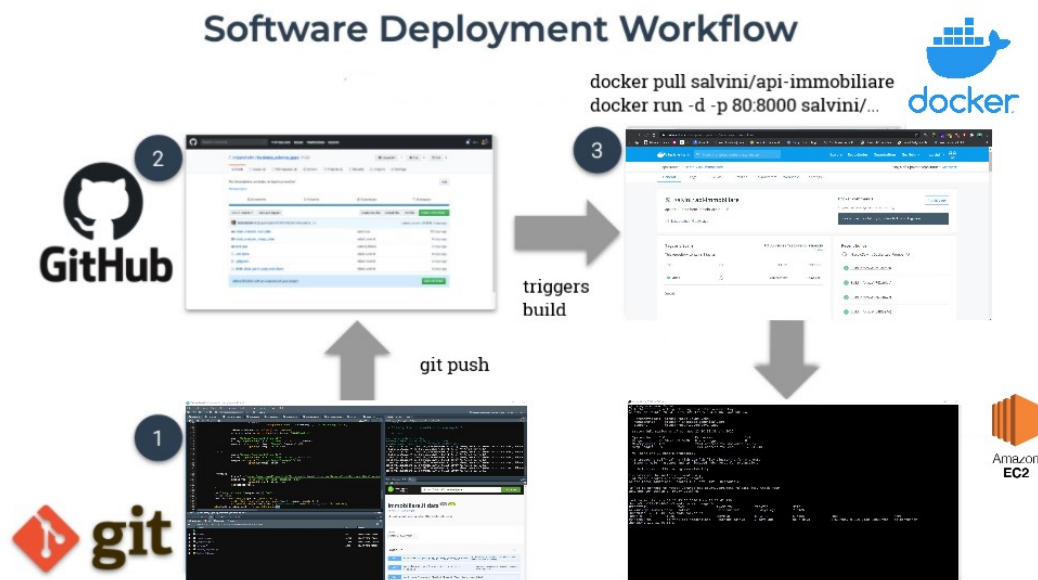


Figure 3.8: Software development CI/CD workflow, author's source

⁵<https://packagemanager.rstudio.com/client/#/>

3.8 Further SF Integrations

A more robust code can be obtained embedding recent R software development frameworks as Golem Colin Fay (2020) into the existing structure, anyway this will require a complete restyle of the existing code structure. The framework stimulates the usage of *modules* to enhance reusable codes. In addition for the way it is done it forces through automatic actions, articulated into a sequence of steps, to organize code and dependencies aimed at saving time to DevOps teams. It has also a convenient function to build custom dockerfiles based on the dependencies stated throughout the building framework. This is also truer according to the latest API literature which suggests (Shiny services as well) to wrap up code into R packages as in Santiago (2020), Which wraps around the aforementioned concepts to the specific API Plumber Trestle Technology, LLC (2018) framework. This is extensively treated in section 4.2 Colin Fay (2020) and in the comment⁶ by Dean Attali, as a matter of fact Golem is built upon the idea of package portability. Thanks to packages **TDD** (i.e. Test-Driven Development TDD (2004)) through the library Wickham (2011) can make software more reliable, and production grade. Moreover Loadtest ? can help figure out the traffic congestions visualizing sessions and enabling monitoring dashboards. A popular API development integration service and automate testing tool Postman⁷, which does its best when POST requests endpoints are served, since for the moment they are not required it is not used. Pins is an R packages this link⁸ software development framework and tools for testing this work⁹

⁶<https://deanattali.com/2015/04/21/r-package-shiny-app/>

⁷<https://www.postman.com/>

⁸https://rstudio.com/resources/rstudioconf-2020/deploying-end-to-end-data-science-with-shiny-plumber-and-pins/?mkt_tok=eyJpIjoiTmprNU1USXhPVEprWXpNMSIsInQiOiJtTUhKVzlvSjVIV2hKc0NRNVU1NTRQYSsrRGd5MWMY

⁹<https://github.com/isteves/plumbplumb>

Chapter 4

INLA

Bayesian estimation methods - by MCMC (Brooks et al., 2011) and MC simulation techniques - are usually much harder than Frequentist calculations (Wang et al., 2018). This unfortunately is also more critical for spatial and spatio-temporal model settings (Cameletti et al., 2012) where matrices dimensions and densities (in the sense of prevalence of values throughout the matrix) start becoming unfeasible. The computational aspect refers in particular to the ineffectiveness of linear algebra operations with large dense covariance matrices that in aforementioned settings scale to the order $\mathcal{O}(n^3)$. INLA (Rue et al., 2009, 2017) stands for Integrated Nested Laplace Approximation and constitutes a faster and accurate deterministic algorithm whose performance in time indeed scale to the order $\mathcal{O}(n)$. INLA is alternative and by no means substitute (de Rencontres Mathématiques, 2018) to traditional Bayesian Inference methods. INLA focuses on Latent Gaussian Models (LGMs)(2018), which are a rich class including many regressions models, as well as spatial or spatio-temporal models. INLA turns out to shorten model fitting time for essentially two reasons related to clever LGM model settings, such as: Gaussian Markov random field (GMRF) offering sparse matrices representation and Laplace approximation to approximate posterior marginals' integrals with proper search strategies. In the end of the chapter it is presented the R-INLA project and the package focusing on the essential aspects.

The chronological steps followed in the methodology presentation retraces the canonical one by the original paper by Rue et al. (2009), which seems to be also the default choice for all the related literature. The approach is more suitable and remains quite unchanged since it is top-down, which naturally fits the hierarchical framework imposed in the model. The GMRF introductory part heavily relies on Rue and Held (2005).

Notation is imported by Marta Blangiardo (2015) and integrated with Gómez Rubio (2020), whereas examples are drawn from Wang et al. (2018). Vectors and matrices are typeset in bold i.e. β , so each time they occur they have to be considered such as the *ensemble* of their values, whereas the notation β_{-i} denotes all elements in β but β_{-i} . $\pi(\cdot)$ is a generic notation for the density of its arguments and $\tilde{\pi}(\cdot)$ has to be intended as its Laplace approximation. Furthermore mathematical details, e.g. Laplace Approximations derivations and optimal strategy for integration, are overlooked with the aim to jump on the statistical intuition oriented to the practical usage of the algorithm.

4.1 The class of Latent Gaussian Models (LGM)

Bayesian theory is straightforward, but it is not always simple to measure posterior and other interest quantities (Wang et al., 2018). There are three ways to obtain a posterior estimate: by *Exact* estimation, i.e. operating on conjugate priors, but there are relatively few conjugate priors which are also employed in simple models. By *Sampling* through generating samples from the posterior distributions with MCMC methods (Hastings, 1970; Metropolis et al., 1953) and applied in Bayesian statistics by Gelfand and Smith (1990). MCMCs have improved over time due to inner algorithm optimization as well as both hardware and software progresses, nevertheless for certain model combinations and data they either fail or take an unacceptable amount of time

(2018). By *Approximation* through numerical integration and INLA can count on a strategy leveraging on three elements: *LGMs*, *Gaussian Markov Random Fields* (GMRF) and *Laplace Approximations* and this will articulates the steps according to which the arguments are treated. LGMs despite their anonymity are very flexible and they can host a wide range of models as regression, dynamic, spatial, spatio-temporal (Cameletti et al., 2012). LGMs necessitate further three interconnected elements: **Likelihood**, **Latent field** and **Hyperpriors**. To start it can be specified a generalization of a linear predictor η_i which takes into account both linear and non-linear effects on covariates:

$$\eta_i = \beta_0 + \sum_{m=1}^M \beta_m x_{mi} + \sum_{l=1}^L f_l(z_{li}) \quad (4.1)$$

where β_0 is the intercept, $\beta = \{\beta_1, \dots, \beta_M\}$ are the coefficients that quantifies the linear effects of covariates $x = (x_1, \dots, x_M)$ and $f_l(\cdot), \forall l \in 1 \dots L$ are a set of random effects defined in terms of a z set of covariates $z = (z_1, \dots, z_L)$ (e.g. Random Walks Rue and Held (2005), Gaussian Processes Besag and Kooperberg (1995)), such models are termed as General Additive Models i.e. GAM (Wang et al., 2018). For the response $\mathbf{y} = (y_1, \dots, y_n)$ it is specified an *exponential family* distribution function whose mean μ_i (computed as its expectation $E(\mathbf{y})$) is linked via a link function $g(\cdot)$ to η_i in eq. (4.1), i.e. $g(\mu_i) = \eta_i$. At this point is possible to group all the latent (in the sense of unobserved) inference components into a variable, said **latent field** and denoted as θ such that: $\theta = \{\beta_0, \beta, f\}$, where each single observation i is connected to a θ_i combination of parameters in θ . The latent parameters θ actually may depend on some hyper-parameters $\psi = \{\psi_1, \dots, \psi_K\}$. Then, given \mathbf{y} , the joint probability distribution function conditioned to both parameters and hyper-parameters, assuming *conditional independence*, is expressed by the **likelihood**:

$$\pi(\mathbf{y} \mid \theta, \psi) = \prod_{i=1}^I \pi(y_i \mid \theta_i, \psi) \quad (4.2)$$

The conditional independence assumption grants that for a general couple of conditionally independent θ_j and θ_i , where $i \neq j$, the joint conditional distribution is factorized by $\pi(\theta_i, \theta_j | \theta_{-i,j}) = \pi(\theta_i | \theta_{-i,j}) \pi(\theta_j | \theta_{-i,j})$ (Marta Blangiardo, 2015), i.e. the likelihood in eq:(4.2). The assumption constitutes a building block in INLA since as it will be shown later it will assure that there will be 0 patterns encoded inside matrices, implying computational benefits. Note also that the product index i ranges from 1 to \mathbf{I} , i.e. $\mathbf{I} = \{1 \dots n\}$. In the case when an observations are missing, i.e. $i \notin \mathbf{I}$, INLA automatically discards missing values from the model estimation (2020), this would be critical during missing values imputation sec. 6.4. At this point, as required by LGM, are needed to be imposed *Gaussian priors* on each linear effect and each model covariate that have either a univariate or *multivaried normal* density in order to make the additive η_i Gaussian (2018). An example might clear up the setting requirement: let assume to have a Normally distributed response and let set the goal to specify a Bayesian Generalized Linear Model (GLM). Then the linear predictor can have this appearance $\eta_i = \beta_0 + \beta_1 x_{i1}$, $i = 1, \dots, n$, where β_0 is the intercept and β_1 is the slope for a general covariate x_{i1} . While applying LGM are **needed** to be specified Gaussian priors on β_0 and β_1 , such that: $\beta_0 \sim N(\mu_0, \sigma_0^2)$ and $\beta_1 \sim N(\mu_1, \sigma_1^2)$, for which the latent linear predictor η_i is $\eta_i \sim N(\mu_0 + \mu_1 x_{i1}, \sigma_0^2 + \sigma_1^2 x_{i1}^2)$. It can be illustrated by some linear algebra (2018) that $\eta = (\eta_1, \dots, \eta_n)'$ is a Gaussian Process with mean structure μ and covariance matrix Q^{-1} . The hyperparameters σ_0^2 and σ_1^2 are to be either fixed or estimated by taking hyperpriors on them. In this context $\theta = \{\beta_0, \beta_1\}$ can group all the latent components and $\psi = \{\sigma_0^2, \sigma_1^2\}$ is the vector of **hyperpriors**. For what it can be noticed there is a clear hierarchical relationship for which three different levels are seen: a *higher* level represented by the exponential family distribution function on \mathbf{y} , given the latent parameter and the hyper parameters. The *medium* by latent Gaussian random field with density function given some other hyper parameters. The *lower* by the joint distribution or a product of several distributions for which priors can be specified So letting be $\mathbf{y} = (y_1, \dots, y_n)'$ at the *higher* level it is assumed an

exponential family distribution function given a first set of hyper-parameters ψ_1 , usually referred to measurement error precision Marta Blangiardo (2015)). Therefore as in (4.2),

$$\pi(\mathbf{y} \mid \theta, \psi_1) = \prod_{i=1}^{\mathbf{I}} \pi(y_i \mid \theta_i, \psi_1) \quad (4.3)$$

At the *medium* level it is specified on the latent field θ a latent Gaussian random field (LGRF), given ψ_2 i.e. the rest of the hyper-parameters,

$$\pi(\theta \mid \psi_2) = (2\pi)^{-n/2} |Q(\psi_2)|^{1/2} \exp \left(-\frac{1}{2} \theta' Q(\psi_2) \theta \right) \quad (4.4)$$

where $Q(\psi_2)$ denotes positive definite matrix and $|\cdot|$ its determinant. $'$ is the transpose operator. The matrix $Q(\psi_2)$ is called the *precision matrix* that outlines the underlying dependence structure of the data, and its inverse $Q(\cdot)^{-1}$ is the covariance matrix (Wang et al., 2018). In the spatial setting this would be critical since by specifying a multivariate Normal distribution of eq. (4.4) it will become a GMRF. Due to conditional independence GMRF precision matrices are sparse and through linear algebra and numerical method for sparse matrices model fitting time is saved (Rue and Held, 2005). In the *lower* level priors are collected together $\psi = \{\psi_1 \psi_2\}$ for which are specified either a single prior distribution or a joint prior distribution as the product of its independent priors. Since the end goal is to find the joint posterior for θ and ψ , then given priors ψ it possible to combine expression (4.3) with (4.4) obtaining:

$$\pi(\theta, \psi \mid \mathbf{y}) \propto \underbrace{\pi(\psi)}_{\text{priors}} \times \underbrace{\pi(\theta \mid \psi)}_{\text{LGRM}} \times \underbrace{\prod_{i=1}^{\mathbf{I}} \pi(\mathbf{y} \mid \theta, \psi)}_{\text{likelihood}} \quad (4.5)$$

Which can be further solved following (Marta Blangiardo, 2015) as:

$$\begin{aligned}
\pi(\theta, \psi \mid y) &\propto \pi(\psi) \times \pi(\theta \mid \psi) \times \pi(\mathbf{y} \mid \theta, \psi) \\
&\propto \pi(\psi) \times \pi(\theta \mid \psi) \times \prod_{i=1}^n \pi(y_i \mid \theta_i, \psi) \\
&\propto \pi(\psi) \times |Q(\psi)|^{1/2} \exp\left(-\frac{1}{2}\theta' Q(\psi)\theta\right) \times \prod_i^n \exp(\log(\pi(y_i \mid \theta_i, \psi)))
\end{aligned} \tag{4.6}$$

From final eq: (4.6) is derived Bayesian inference and INLA through Laplace can approximate posterior parameters distributions. Sadly, INLA cannot effectively suit all LGM's. In general INLA requires the following supplementary assumptions (2018):

- The hyper-parameter number ψ should be unpretentious, normally between 2 and 5, but not greater than 20.
- When the number of observation is considerably high (10^4 to 10^5), then the LGMR θ must be a Gaussian Markov random field (GMRF).

4.2 Gaussian Markov Random Field (GMRF)

In the order to make INLA working efficiently the latent field θ must not only be Gaussian but also Gaussian Markov Random Field (GMRF). A GMRF is a genuinely simple structure: It is just random vector following a multivariate normal (or Gaussian) distribution (Rue and Held, 2005). However It is more interesting to research a restricted set of GMRF for which are satisfied the conditional independence assumptions (section 4.1), from here the term “Markov”. Expanding the concept of conditional independence let assume to have a vector $\mathbf{x} = (x_1, x_2, x_3)^T$ where x_1 and x_2 are conditionally independent given x_3 , i.e. $x_1 \perp x_2 \mid x_3$. With that said if the objective is x_3 , then uncovering x_2 gives no information on x_1 . The joint density for \mathbf{x} is

$$\pi(\mathbf{x}) = \pi(x_1 \mid x_3) \pi(x_2 \mid x_3) \pi(x_3) \tag{4.7}$$

Now let assume a more general case of AR(1) exploiting the possibilities of defining $f_1(\cdot)$ function through the eq. (4.1). AR(1) is an *autoregressive model* of order 1 specified on the latent linear predictor η (use directly η instead of θ since latent components are few), with constant variance σ_η^2 and standard normal errors (2005; 2018). The model may have following expression:

$$\eta_t = \phi\eta_{t-1} + \epsilon_t, \quad \epsilon_t \stackrel{\text{iid}}{\sim} \mathcal{N}(0, 1), \quad |\phi| < 1$$

Where t pedix is the time index and ϕ is the correlation in time. The conditional form of the previous equation can be rewritten when $t = 2 \dots n$:

$$\eta_t \mid \eta_1, \dots, \eta_{t-1} \sim \mathcal{N}(\phi\eta_{t-1}, \sigma_\eta^2)$$

Then let also consider the marginal distribution for each η_i , it can be proven to be Gaussian with mean 0 and variance $\sigma_\eta^2 / (1 - \phi^2)$ (2018). Moreover the covariance between each general η_i and η_j is defined as $\sigma_\eta^2 \rho^{|i-j|} / (1 - \rho^2)$ which vanishes the more the distance $|i - j|$ increases. Therefore η is a Gaussian Process (whose definition is in ?? and whose basics are in the appendix 8.1) are with mean structure of θ s and covariance matrix Q^{-1} i.e. $\eta \sim N(\mathbf{0}, Q^{-1})$. Q^{-1} is an $n \times n$ dense matrix that complicates computations. But by a simple trick it is possible to recognize that AR(1) is a special type of GP with sparse precision matrix which is evident by showing the joint distribution for η

$$\pi(\eta) = \pi(\eta_1) \pi(\eta_2 \mid \eta_1) \pi(\eta_3 \mid \eta_1, \eta_2) \cdots \pi(\eta_n \mid \eta_{n-1}, \dots, \eta_1)$$

whose precision matrix compared to its covariance matrix is:

$$Q = \begin{pmatrix} 1 & -\phi & & & & & \\ -\phi & 1+\phi^2 & -\phi & & & & \\ & & \ddots & \ddots & \ddots & & \\ & & & -\phi & 1+\phi^2 & -\phi & \\ & & & & -\phi & 1 & \end{pmatrix} \quad Q^{-1} = \frac{1}{1-\phi^2} \begin{pmatrix} 1 & \phi & \phi^2 & \phi^3 & \phi^4 & \phi^5 & \phi^6 \\ \phi & 1 & \phi & \phi^2 & \phi^3 & \phi^4 & \phi^5 \\ \phi^2 & \phi & 1 & \phi & \phi^2 & \phi^3 & \phi^4 \\ \phi^3 & \phi^2 & \phi & 1 & \phi & \phi^2 & \phi^3 \\ \phi^4 & \phi^3 & \phi^2 & \phi & 1 & \phi & \phi^2 \\ \phi^5 & \phi^4 & \phi^3 & \phi^2 & \phi & 1 & \phi \\ \phi^6 & \phi^5 & \phi^4 & \phi^3 & \phi^2 & \phi & 1 \end{pmatrix}$$

with zero entries outside the diagonal (right panel fig. ??) and first off-diagonals

(?). The conditional independence assumption makes the precision matrix tridiagonal since for general η_i and η_j are conditionally independent for $|i - j| > 1$, given all the rest. In other words Q is sparse since given all the latent predictors in η , then η_t depends only on the preceding η_{t-1} . For example in (4.8), let assume to have η_2 and η_4 , then:

$$\begin{aligned}\pi(\eta_2, \eta_4 \mid \eta_1, \eta_3) &= \pi(\eta_2 \mid \eta_1) \pi(\eta_4 \mid \eta_1, \eta_2, \eta_3) \\ &= \pi(\eta_2 \mid \eta_1) \pi(\eta_4 \mid \eta_3)\end{aligned}\tag{4.8}$$

For which the conditional density of η_2 does only depend on its preceding term i.e. η_1 . The same inner reasoning can be done for η_4 , which strictly depends on η_3 and vice versa. Therefore ultimately it is possible to produce a rather formal definition of a GMRF:

Definition 4.1 (GMRF). A latent gaussian random field (LGRM) e.g. η is said a GMRF if it has a multivariate Normal density with additional conditional independence (also called the “Markov property”) (Wang et al., 2018).

4.3 INLA Laplace Approximations

The goals of the Bayesian inference are the marginal posterior distributions for each of the elements of the latent field. INLA is not going to try to approximate the whole joint posterior marginal distribution from expression (4.6) i.e. $\pi(\theta \mid \psi, \mathbf{y})$, in fact if it would (two-dimensional approx) it will cause a high biased approximations since it fail to capture both location and skewness in the marginals. Instead INLA algorithm will try to estimate the posterior marginal distribution for each θ_i in the latent parameter θ , for each hyper-parameter prior $\psi_k \in \psi$ (back to the θ latent field notation). The mathematical intuition behind Laplace approximation is contained in the appendix sec. ...

Therefore the key focus of INLA is to approximate with Laplace only densities that are near-Gaussian (2018) or replacing very nested dependencies with their

more comfortable conditional distribution which ultimately are “more Gaussian” than the thier joint distribution. Into the LGM framework let assume to observe n counts, i.e. $\mathbf{y} = y_i = 1, 2, \dots, n$ drawn from Poisson distribution whose mean is $\lambda_i, \forall i \in \mathbf{I}$. Then a the link function $g(\cdot)$ is the $\log(\cdot)$ and relates λ_i with the linear predictor and so the latent filed θ , i.e. $\log(\lambda_i) = \theta_i$. The hyper-parameters are $\psi = (\tau, \rho)$ with their covariance matrix structure.

$$Q_\psi = \tau \begin{bmatrix} 1 & -\rho & -\rho^2 & -\rho^3 & \dots & -\rho^n \\ -\rho & 1 & -\rho & -\rho^2 & -\rho^3 & -\rho^{n-1} \\ -\rho^2 & -\rho & 1 & -\rho & -\rho^2 & -\rho^{n-2} \\ -\rho^3 & -\rho^2 & -\rho & 1 & -\rho & -\rho^{n-3} \\ -\dots & -\rho^3 & -\rho^2 & -\rho & 1 & -\rho \\ -\rho^n & -\rho^{n-1} & -\rho^{n-2} & -\rho^{n-3} & -\rho & 1 \end{bmatrix}$$

Let also to assume once again to model θ with an AR(1). Then fitting the model into the LGM, at first requires to specify an exponential family distribution function, i.e. Poisson on the response \mathbf{y} . then the *higher* level (recall last part sec. 4.1) results in:

$$\pi(\mathbf{y} \mid \theta, \psi) \propto \prod_{i=1}^{\mathbf{I}} \frac{\exp(\theta_i y_i - e^{\theta_i})}{y_i!}$$

Then the *medium* level is for the latent Gaussian Random Field a multivariate gaussian distribution $\psi_i \sim \text{MVN}_2(\mathbf{0}, \Omega)$:

$$\pi(\theta \mid \psi) \propto |Q_\psi|^{1/2} \exp\left(-\frac{1}{2}\theta' Q_\psi \theta\right)$$

and the *lower*, where it is specified a joint prior distribution for $\psi = (\tau, \rho)$, which is $\pi(\psi)$. Following eq.(4.5) then:

$$\pi(\theta, \psi \mid \mathbf{y}) \propto \underbrace{\pi(\psi)}_{\text{priors}} \times \underbrace{\pi(\theta \mid \rho)}_{\text{LGRM}} \times \underbrace{\prod_{i=1}^{\mathbf{I}} \pi(\mathbf{y} \mid \theta, \tau)}_{\text{likelihood}} \quad (4.9)$$

Then recalling the goal for Bayesian Inference, i.e. approximate posterior marginals for $\pi(\theta_i | \mathbf{y})$ and $\pi(\tau | \mathbf{y})$ and $\pi(\rho | \mathbf{y})$. First difficulties regard the fact that Laplace approximations on this model implies the product of a Gaussian distribution and a non-gaussian one. As the INLA key point suggest, the algorithm starts by rearranging the problem so that the “most Gaussian” are computed at first. Ideally the method can be generally subdivided into three tasks. At first INLA attempts to approximate $\tilde{\pi}(\psi | \mathbf{y})$ as the joint posterior of $\pi(\psi | \mathbf{y})$. Then subsequently will try to approximate $\tilde{\pi}(\theta_i | \psi, \mathbf{y})$ to their conditional marginal distribution fro θ_i . In the end explores $\tilde{\pi}(\psi | \mathbf{y})$ with numerical methods for integration. The corresponding integrals to be approximated are:

- for task 1: $\pi(\psi_k | \mathbf{y}) = \int \pi(\psi | \mathbf{y}) d\psi_{-k}$
- for task 2: $\pi(\theta_i | \mathbf{y}) = \int \pi(\theta_i, \psi | \mathbf{y}) d\psi = \int \pi(\theta_i | \psi, \mathbf{y}) \pi(\psi | \mathbf{y}) d\psi$

As a result the approximations for the marginal posteriors are at first:

$$\tilde{\pi}(\theta_j | \mathbf{y}) = \int \tilde{\pi}(\theta | \mathbf{y}) d\theta_{-j} \quad (4.10)$$

and then,

$$\tilde{\pi}(\theta_i | \mathbf{y}) \approx \sum_j \tilde{\pi}(\theta_i | \psi^{(j)}, \mathbf{y}) \tilde{\pi}(\psi^{(j)} | \mathbf{y}) \Delta_j \quad (4.11)$$

Where in the integral in (4.11) $\{\psi^{(j)}\}$ are some relevant integration points and $\{\Delta_j\}$ are weights associated to the set of hyper-parameters in a grid. (Marta Blangiardo, 2015). In other words the bigger the Δ_j weight the more relevant are the integration points. Details on how INLA finds those points is beyond the scope, an indeep resource if offered by Wang et al. (2018) in sec. 2.3.

4.4 R-INLA package

INLA library and algorithm is developed by the R-INLA project whose package is available on their website at their source repository¹. Users can also enjoy on INLA website (recently restyled) a dedicated forum where discussion groups are opened and an active community is keen to answer. Moreover It also contains a number of reference books, among which some of them are fully open sourced. INLA is available for any operating system and it is built on top of other libraries still not on CRAN. The core function of the package is `inla()` and it works as many other regression functions like `glm()`, `lm()` or `gam()`. `Inla` function takes as argument the *model formula* i.e. the linear predictor for which it can be specified a number of linear and non-linear effects on covariates as seen in eq. (4.1), the whole set of available effects are obtained with the command `names(inla.models())$latent`. Furthermore it requires to specify the dataset and its respective likelihood family, equivalently `names(inla.models())$likelihood`. Many other methods in the function can be added through lists, such as `control.family` and `control.fixed` which let the analyst specifying parameter and hyper-parameters priors family distributions and control hyper parameters. They come in the of nested lists when parameters and hyper parameters are more than 2, when nothing is specified the default option is non-informativeness. Inla output objects are `inla.dataframe` summary-lists-type containing the results from model fitting for which a table is given in figure 4.1.

SPDEtoy dataset \mathbf{y} are two random variables that simulates points location in two coordinates s_1 and s_2 .

Imposing an LGM model requires at first to select as a *higher* hierarchy level a likelihood model for \mathbf{y} i.e. Gaussian (by default), and a model formula (eq. (4.1)), i.e. $\eta_i = \beta_0 + \beta_1 s_{1i} + \beta_2 s_{2i}$, which link function \mathbf{g} is identity. There are not Non-linear effects effect on covariates in $\$ \$$ nevertheless they can be easily added with `f()` function. Note that this will allow to integrate random

¹<https://www.r-inla.org/download-install>

Function	Description
<code>summary.fixed</code>	Summary of fixed effects.
<code>marginals.fixed</code>	List of marginals of fixed effects.
<code>summary.random</code>	Summary of random effects.
<code>marginals.random</code>	List of marginals of random effects.
<code>summary.hyperpar</code>	Summary of hyperparameters.
<code>marginals.hyperpar</code>	List of marginals of the hyperparameters.
<code>mlik</code>	Marginal log-likelihood.
<code>summary.linear.predictor</code>	Summary of linear predictors.
<code>marginals.linear.predictor</code>	List of marginals of linear predictors.
<code>summary.fitted.values</code>	Summary of fitted values.
<code>marginals.fitted.values</code>	List of marginals of fitted values.

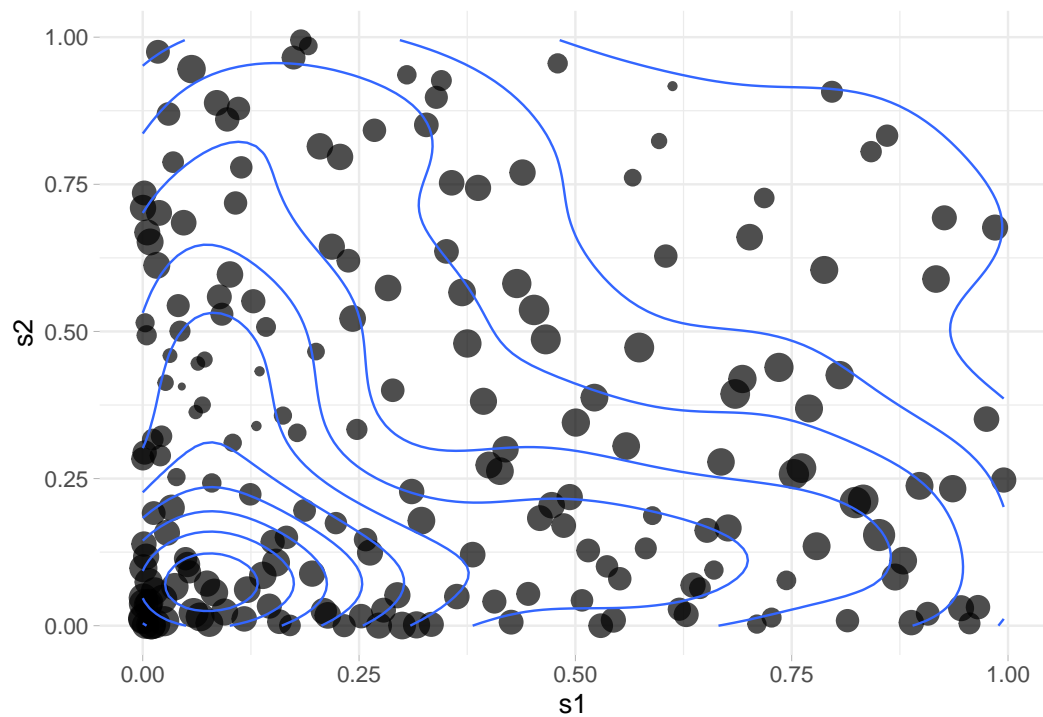
Figure 4.1: outputs for a `inla()` call, source: Krainski (2019)

Figure 4.2: SPDEtoy bubble plot, author's source

effects i.e. spatial effects inside the model. Secondly in the *medium* step a LGRF on the latent parameters θ . In the *lower* end some priors distributions ψ which are Uniform for the intercept indeed Gaussian vagues (default) priors i.e. centered in 0 with very low standard deviation. Furthermore the precision hyper parameter τ which accounts for the variance of the latent GRF, is set as Gamma distributed with parameters $\alpha = 1$ and $\beta = 0.00005$ (default). Note that models are sensitive to prior choices (sec. 5.6), as a consequence if necessary later are revised. A summary of the model specifications are set below:

$$\begin{aligned}
 y_i &\sim N(\mu_i, \tau^{-1}), i = 1, \dots, 200 \\
 \mu_i &= \beta_0 + \beta_1 s_{1i} + \beta_2 s_{2i} \\
 \beta_0 &\sim \text{Uniform} \\
 \beta_j &\sim N(0, 0.001^{-1}), j = 1, 2 \\
 \tau &\sim Ga(1, 0.00005)
 \end{aligned} \tag{4.12}$$

Then the model is fitted within `inla()` call.

```
formula = y ~ s1 + s2
m0 = inla(formula, data = SPDEtoy)
```

The table below offers summary of the posterior marginal values for intercept and covariates' coefficients, as well as precision. Marginals distributions both for parameters and hyper-parameters can be conveniently plotted as in figure ???. From the table it can also be seen that the mean for s_2 is negative, so the Norther the y-coordinate, the less is response. That is factual looking at the SPDEtoy contour plot in figure4.2 where bigger bubbles are concentrated throughout the origin.

	mean	sd	0.025quant	0.5quant	0.975quant	mode	
(Intercept)	10.1321487	0.2422118	9.6561033	10.1321422	10.6077866	10.1321497	7
s1	0.7624296	0.4293757	-0.0814701	0.7624179	1.6056053	0.7624315	7
s2	-1.5836768	0.4293757	-2.4275704	-1.5836906	-0.7404955	-1.5836811	7

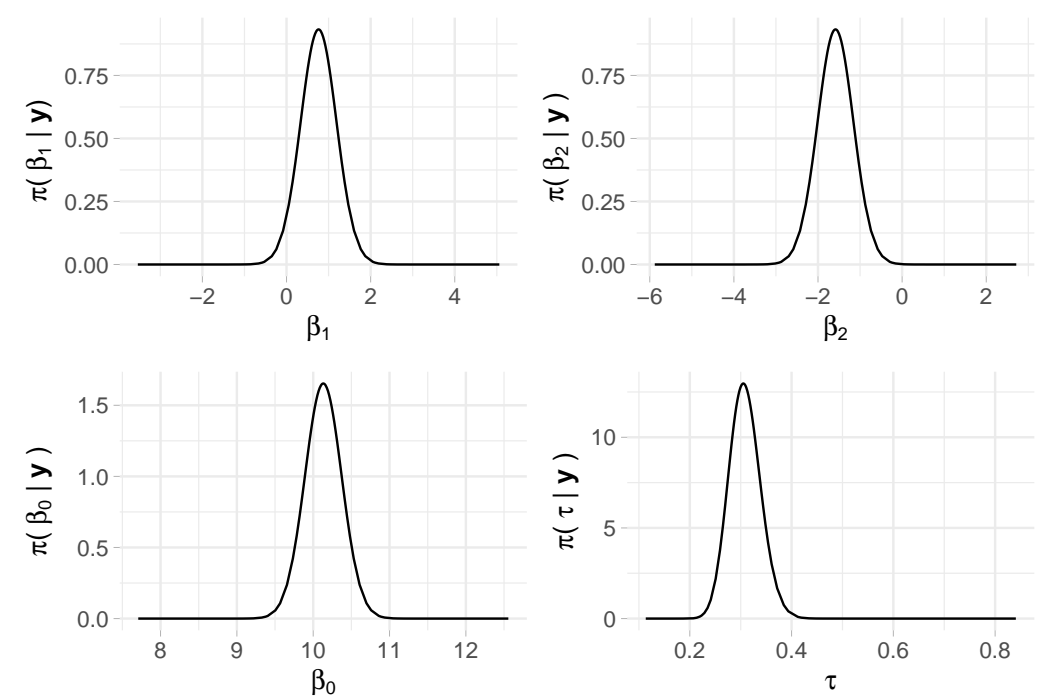


Figure 4.3: Linear predictor marginals, plot recoded in ggplot2, author’s source

In the end R-INLA enables also `r-base` style function to compute statistics on marginal posterior distributions for the density, distribution as well as the quantile function respectively with `inla.dmarginal`, `inla.pmarginal` and `inla.qmarginal`. One option which, packed into a dedicated function, computes the higher posterior density credibility interval `inla.hpdmarginal` for a given covariate’s coefficient, such that $\int_{q_1}^{q_2} \tilde{\pi}(\beta_2 | y) d\beta_2 = 0.90$ (90% credibility), whose result is in table `@ref(tab:higer_posterior)`.

	low	high
level:0.9	-2.291268	-0.879445

Note that the interpretation is more convoluted (2018) than the traditional

frequentist approach: in Bayesian statistics β_j comes from probability distribution, while frequentists considers β_j as fixed unknown quantity whose estimator (random variable conditioned to data) is used to infer the value (2015).

Chapter 5

Point Referenced Data Modeling

Geostatistical data are a collection of samples of geo type data indexed by coordinate Reference Systems (CRS), projected (e.g. Eastings and Northings) or unprojected (e.g. Latitude and Longitude), that originates from a spatially continuous phenomenon (Moraga, 2019). Data as such can monitor a vast range of phenomena, e.g. accidental fisheries bycatch for endangered species (Cosandey-Godin et al., 2015), COVID19 severity and case fatality rates in Spain (Moraga et al., 2020), PM10 pollution concentration in a North-Italian region Piemonte (Cameletti et al., 2012). Moreover a large geostatistical application takes place on Real Estate where Boston house prices lattice data from MASS Venables and Ripley (2002) package Bivand et al. (2015) are developed according to several spatial models, where apartment transaction prices in Corsica (France) are modeled in time and space (Ling, 2019). All the Examples taken before and might document a spatial nature of data according to which closer observations can display similar values, this phenomenon is named spatial autocorrelation. Spatial autocorrelation conceptually stems from geographer Waldo Tobler whose famous quote, known as first law of geography, inspires geostatisticians:

“Everything is related to everything else, but near things are more

related than distant things”

— Waldo R. Tobler

Spatial data can be partitioned into three spatial data type whose modeling tools are specific to their respective category.

- Areal Data
- **Point Referenced Data**
- Point Pattern Data

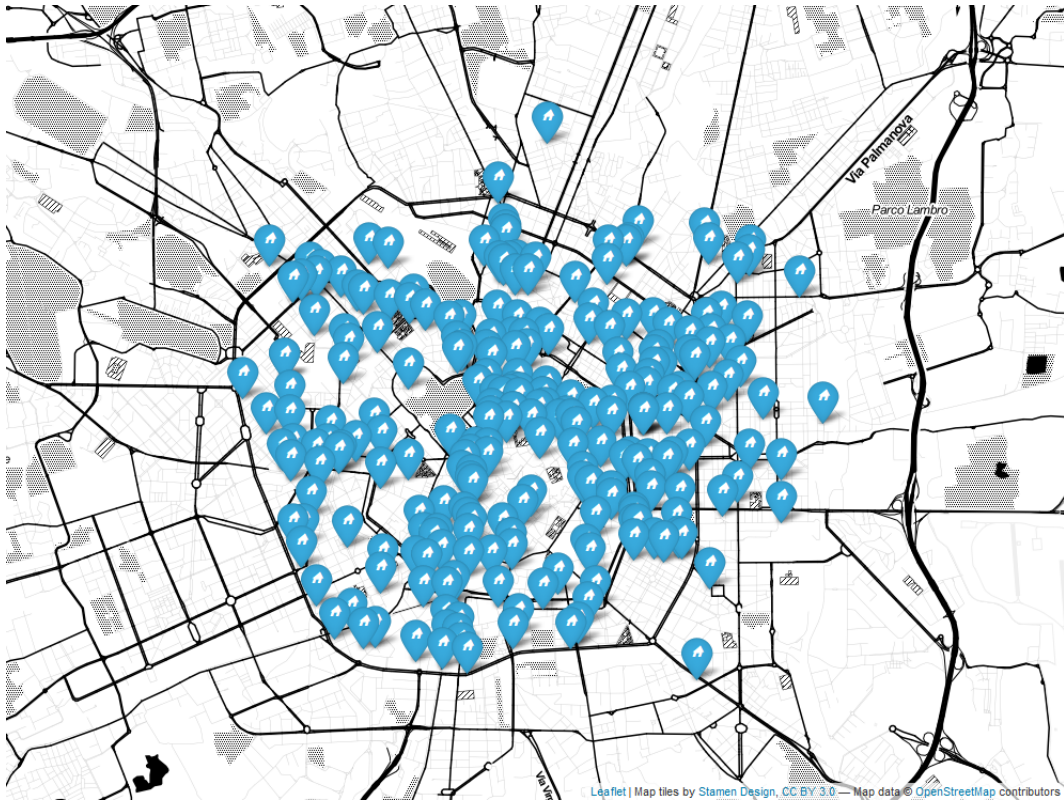


Figure 5.1: Point Referenced Data map plot (Leaflet Cheng et al. (2019)) of a RESTful API call on Milan Rental Real Estate 20-11-2019, Author’s Source

RESTful scraping API in 3 allows to grab point referenced data (and covariates in tab. 6) by simply specifying the city or the sub-entity wanted. Moreover it allows also to specify the number of observation, this may result helpful in some context when complex models can not ingest large amounts of data or when the analyst’s interest resides in only certain type of house characteristics.

RESTful scraping API designed in chapter 3 extracts geostatistical components in the form of Latitude and Longitude nested in a hidden source code JSON object. Resulting observations can be represented through a map as in fig. 5.1. API allows gather data

Large areas with no housing within the polygons have been removed (e.g. parks, the University of Zaragoza campus, hospital areas, etc.). What is retained is, essentially, a full census of apartment sale transactions in and around the city center

Modeling methodologies described in this analysis will exclusively take into account point referenced techniques within the INLA algorithm. Geostatistical data can be considered as a stochastic process indexed on a continuous plane (Arbia, 2012) i.e Gaussian Process. This information is essential to interpolate points and build a Gaussian Process over the y-studied variable domain in order to predict the phenomenon at locations not yet observed. GPs ,at first, have to be introduced and constrained to the properties of Stationarity and Isotropy and then they are considered with a convenient covariance function, i.e. Matérn. The reason why Matérn is selected as candidate for covariance function relies, besides its inner flexibility, on the fact that GP whose covariance function is Matérn are able to determine a GMRF 4.2 through the Stochastic Partial Differential Equations (SPDE) approach (?). The main benefit proceeding from a GP to a GMRF arises from the good computational properties that the latter appreciate enabling to wrap up modeling around INLA and consequently benefiting from it. Hedonic Price Models brings to the present analysis the theoretical foundation according to which covariates are added to the model. Spatial kriging is essential to predict the process at new locations given the continuous spatial surface. In the end models have to be checked and verified with resampling schemes which are once again specific to the data type and the scope of the analysis.

5.1 Gaussian Process (GP)

Point referenced data are defined as realizations of a stochastic process indexed by space.

$$Y(s) \equiv \{y(s), s \in \mathcal{D}\}$$

where \mathcal{D} is a (fixed) subset of \mathbb{R}^d (in the present work *Latitude* and *Longitude*, i.e. $d = 2$). The actual data can be then represented by a collection of observations $\mathbf{y} = \{y(s_1), \dots, y(s_n)\}$ (recall notation from previous chapter 4.1) where the set (s_1, \dots, s_n) points to the spatial location where data has been observed. For example, following Cameletti et al. (2012), assume to have collection of samples from air pollutant measurements obtained by observing a set of monitoring stations. Then The stochastic process $Y(s)$ is monitored in a fixed set of spatial indexes corresponding to the station locations (upward arrows left in figure 5.2). This information is essential to interpolate points and build a spatially continuous surface (right panel in figure 5.2) over the y-studied variable domain in order to predict the phenomenon at locations not yet observed. (Paci, 2020).

The first step in defining a spatial model within INLA is to impose a LGM which requires at first to identify a probability distribution function for the observed data \mathbf{y} . The most common choice is to draw distributions from the *Exponential family*, indexed by a set of parameters θ as in 4.1, accounting for the spatial correlation. From now on it will be used index for the generic spatial point or area with the subscript i , rather than the indicator s_i . In the case of geostatistical data, the model parameters θ , following notation imposed in chapter 4 are defined as a latent Gaussian Process (GP). The GP theoretical foundations and the spatial intuition are offered as a companion in the appendix 8.1.

Definition 5.1 (GP definition). A collection of n random variables, such as $Y(s_1), Y(s_2), \dots, Y(s_n)$ that are *valid* and *finite* stochastic processes are said

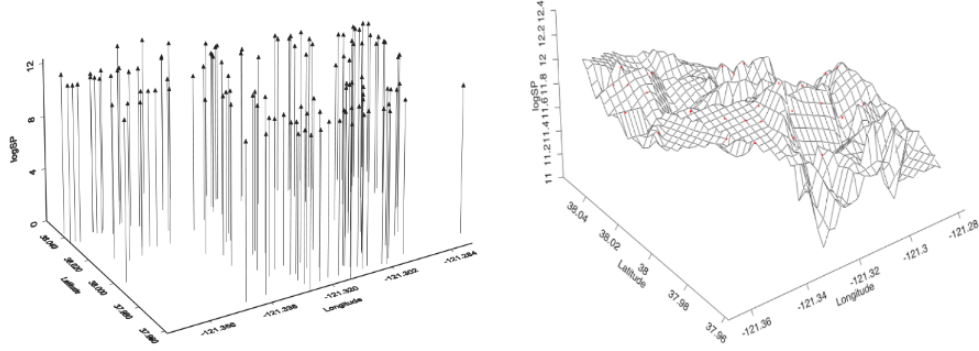


Figure 5.2: Stockton data, Left: Spatial Lat and Long points projected into the 3^{rd} dim $\log(\text{Price})$, Right: spatial interpolation of points, source Marta Blangiardo (2015)

to be a **GP** if for any set of spatial index n and for each set of corresponding locations $\{y(s_1), \dots, y(s_n)\}$ follows a *Multivariate Gaussian* distribution with mean $\mu = \{\mu(s_1), \dots, \mu(s_n)\}$ and covariance matrix $\mathbf{Q}_{i,j}^{-1}, \forall i \neq j$ defined then by a covariance function \cdot, \cdot

The latent GP are in function of some hyper-parameters ψ and their respective prior $\pi(\psi)$. Moreover a GP is completely characterized by a mean $\mu = (\mu_1, \dots, \mu_n)'$ and a spatially structured covariance matrix \mathbf{Q}^{-1} , whose generic element is $\mathbf{Q}^{-1}_{ij} = \text{Cov}(\theta_i, \theta_j) = \sigma_c^2 \mathcal{C}(\Delta_{ij})$, where σ_c^2 is the variance component and for $i, j = 1, \dots, n$. $\mathcal{C}(\cdot, \cdot)$ function generally ensures that all the values that are close together in input space will produce output values that are close together, by inheriting the *validity* and *positive definiteness* characteristics from the GP. The spatial stochastic process commonly is assumed to fulfill two important properties: **stationary**, **Isotropy** (both of the two can be relaxed and the cost of using differten). A process is said **stationary** i.e. weak stationary, if process values at any two locations can be summarized by a covariance function $\mathcal{C}(\Delta_{ij})$ depending only on the distance. In other words it is invariant

under *translation* (Krainski, 2019). A process is said **Isotropic** if the covariance function depends only on the between-points distance $\Delta_{ij} = \|s_i - s_j\|$ (in this context *Euclidean*), so it is invariant under *rotation* (2019). A further way of seeing this property is that Isotropy implies concentric decaying contours (Paci, 2020), green in 5.3, that implies the vanishing of spatial dependence (Marta Blangiardo, 2015), and so for covariance values.

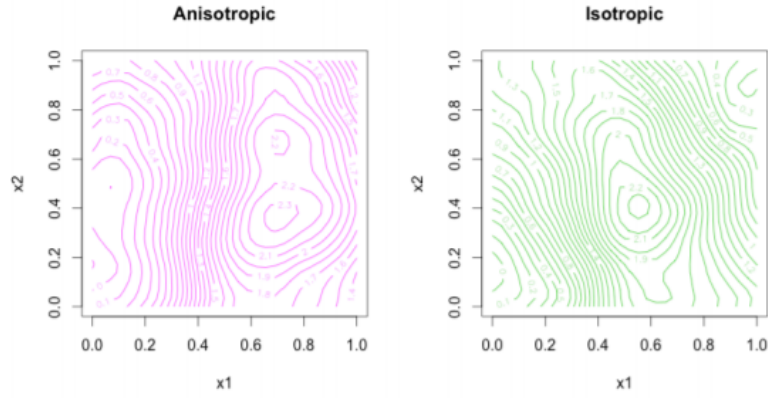


Figure 5.3: Left: isotropy concentric decaying contours, Right: anisotropy concentric decaying contours, source Blanchet-Scalliet et al. (2019)

In spatial statistics the assumption of isotropy is very frequent despite being restrictive for describing the rich variety of interactions that can characterize spatial processes. Anyway assuming the property it offers a wide range of underlying functions that can model spatial dependence for which three are the most common ones (Krainski et al., 2018), where all the parameters below are special quantities derived from the empirical covariance function, where ϕ^2 , τ^2 and σ^2 are respectively the range, the distance at which correlation vanishes, the nugget, i.e. the non spatial variance and the partial sill, i.e. the spatial effect variance (Paci, 2020).

$$\begin{aligned}
\text{Exponential} \quad \mathcal{C}(\mathbf{ij}) &= \begin{cases} \tau_{\mathcal{C}}^2 + \sigma_{\mathcal{C}}^2 & \text{if } \Delta_{ij} = 0 \\ \sigma_{\mathcal{C}}^2 \exp(-\phi_{\mathcal{C}} \Delta_{ij}) & \text{if } \Delta_{ij} > 0 \end{cases} \\
\text{Gaussian} \quad \mathcal{C}(\mathbf{ij}) &= \begin{cases} \tau_{\mathcal{C}}^2 + \sigma_{\mathcal{C}}^2 & \text{if } \Delta_{ij} = 0 \\ \sigma_{\mathcal{C}}^2 \exp(-\phi_{\mathcal{C}}^2 \Delta_{ij}^2) & \text{if } \Delta_{ij} > 0 \end{cases} \\
\text{Matérn} \quad \mathcal{C}(\mathbf{ij}) &= \begin{cases} \tau_{\mathcal{C}}^2 + \sigma_{\mathcal{C}}^2 & \text{if } \Delta_{ij} = 0 \\ \frac{\sigma_{\mathcal{C}}^2}{2^{\nu-1} \Gamma(\nu)} (\phi_{\mathcal{C}} \Delta_{ij})^{\nu} K_{\nu}(\phi_{\mathcal{C}} \Delta_{ij}) & \text{if } \Delta_{ij} > 0 \end{cases}
\end{aligned}$$

In particular the focus is on the *Matérn* – as it is required by the SPDE approach in section 5.2 – and this should not be intended as a restriction. In fact, as longly described in Gneiting et al. (2006), the Matérn family is a very flexible class. Matérn is tuned mainly by two hyper-parameters, a scaling one $\kappa > 0$, usually set equal to the range $\sigma_{\mathcal{C}}^2$ i.e. the distance at which the spatial dependence becomes negligible, by the relation $\sigma_{\mathcal{C}}^2 = \frac{\sqrt{8\lambda}}{\kappa}$, and a smoothing one $\nu > 0$. A *isotropic* Matérn covariance expression is obtained by isolating the $\sigma_{\mathcal{C}}^2$, the variance component (Cressie, 2015):

$$\mathcal{C}(\Delta_{ij}) = \frac{1}{\Gamma(\lambda) 2^{\lambda-1}} (\kappa \Delta_{ij})^{\lambda} K_{\lambda}(\kappa \Delta_{ij})$$

$\Gamma(\nu)$ is a Gamma function depending on ν values, $K_{\nu}(\cdot)$ is a modified Bessel function of second kind. The smoothness parameter ν in figure 5.4 takes 4 different values showing the flexibility of Matérn to relate different distances according to varying parameters. When $\nu = 1$... When $\nu = 1/2$ it becomes the exponential covariance function, When $\nu = 3/2$ it uncovers a convenient closed form (Paci, 2020), when $\nu \approx \infty$, e.g. for graphical constraints $\nu = 80$, it becomes Gaussian covariance function. In the the case shown in section 5.2 $\sigma_{\mathcal{C}}^2$ range is set equal to the distance at which dependence vanishes below .1, for any λ .

<!-- <!-- <!-- <!--

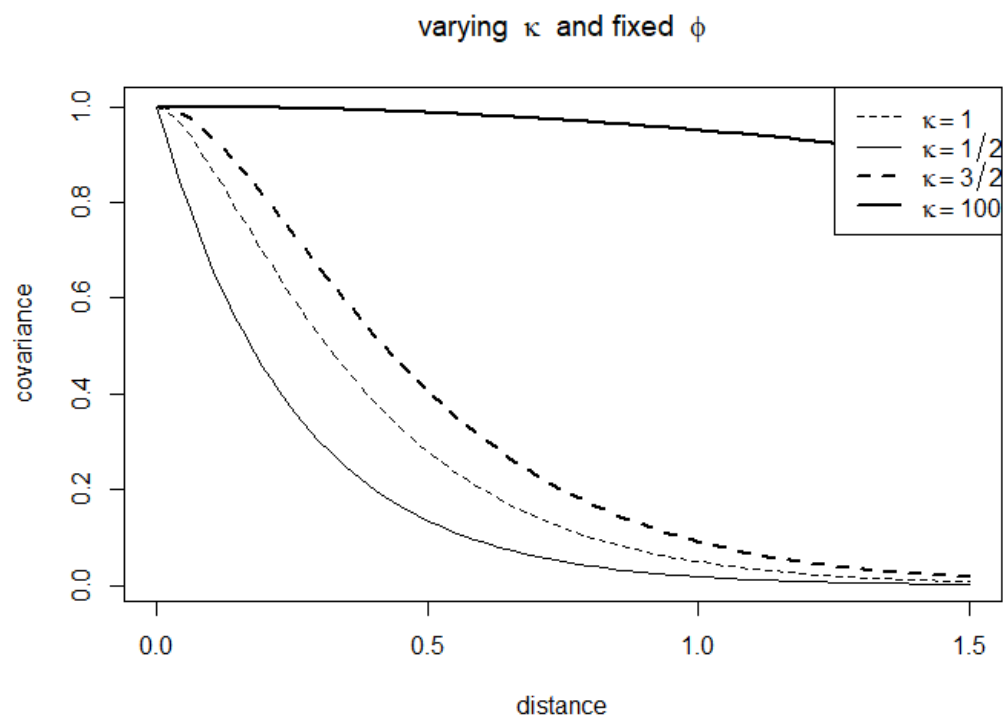


Figure 5.4: Matérn function with 4 different values of ν (upper right legend), kept ϕ fixed, author's source

5.2 The Stochastic Partial Differential Equation (SPDE) approach

Locations in the spatial setting are considered as realizations of a stationary, isotropic unobserved GP to be estimated (5.1). Before approaching the problem with SPDE, GPs were treated as multivariate Gaussian densities and Cholesky factorizations were applied on the covariance matrices and then fitted with likelihood (Paci, 2020). Covariance matrices in the context of spatial and spatio-temporal models (Paci et al., 2017; Cameletti et al., 2012) are $n \times n$ dimension matrices defined by the number of observations at each single point location (at each time stamp in spatio-temporal) (Blangiardo et al., 2013). Covariance matrix as such are very dense and they were scaling with the order of $\mathcal{O}(n^3)$ (Banerjee et al., 2014). Problem were linked to the computational costs needed for linear algebra operations for model fitting and spatial interpolation as well as prediction (Cameletti et al., 2012), having led to obvious *big-n* problem. The breakthrough came with Lindgren et al. (2011) that proves that a stationary, isotropic (can be both relaxed at the cost of different settings) GP with Matérn covariance can be represented as a GMRF using SPDE solutions by Finite Element Method (Krainski, 2019). In other words given a GP whose covariance matrix is Q^{-1} , SPDE can provide a method to approximate Q^{-1} without the previous computational constraints. As a matter of fact SPDE are equations whose solutions are GPs with a chosen covariance function focused on satisfying the relationship SPDE specifies (2019). Benefits are many but the most important is that the representation of the GP through a GMRF provides a sparse representation of the spatial effect through a sparse precision matrix Q . Sparse matrices enable convenient inner computation properties of GMRF 4.3 which are exploited by INLA algorithm 4 leading to a more feasible big-O $\mathcal{O}(n^{3/2})$. Mathematical details and deep understanding of the equations in SPDE are beyond the scope of the analysis. Luckily enough R-INLA has a set of functions that makes clear to the practitioner the minimal requirements to pass from discrete locations to their continuously indexed surface alter-ego.

In few words SPDE approach uses a finite element (FEM method) representation to shape the Matérn field as a linear combination of basis functions defined on a triangulation of the domain \mathcal{D} (2012), also named *mesh*. What it internally does is splitting the domain \mathcal{D} into a number of non-intersecting triangles which converge in a common edge or corner. Then the initial vertices of the triangles are set at $s_1 \dots s_d$. In order to get a proper triangulation, useful for spatial prediction, additional vertices are then added. The more vertices are added the more the triangulation is accurate since many more triangles can better interpolate the surface reaching more complex shapes. Secondly SPDE projects the values of the triangularization to the discretized spatial surface with weighted sum of areas of the underlying triangles. A less superficial intuition is offered in the appendix in section 8.2 on how SPDE computes triangularized values and how it projects the triangulation to the GRMF.

To illustrate the concept of triangulation Cameletti et al. (2012) provide a simple example for Piemonte PM10 concentration observed at 24 monitoring stations left in figure 5.5 and using 123 vertices and a Piemonte borders, right in figure 5.5.

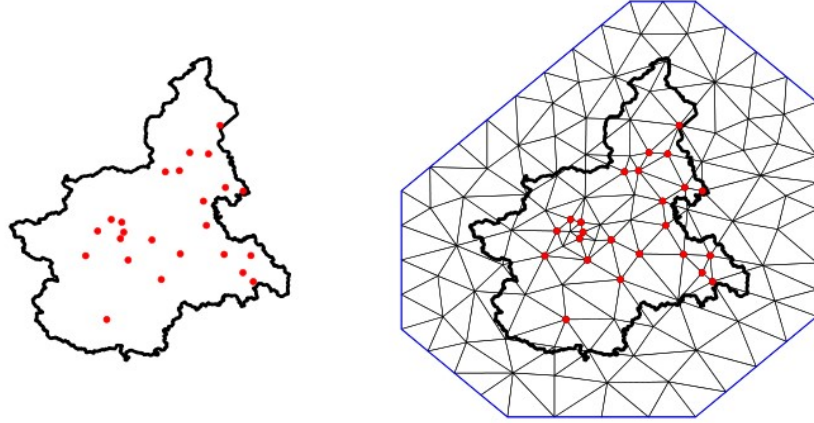


Figure 5.5: Left: monitoring stations in Piemonte region for PM10 pollution levels. Right: its triangulation using 123 vertices. Cameletti et al. (2012) source

Any triangle height (the size of the spatial field at each vertex triangle) is calculated by weighted sum, with linear interpolation deciding the values within

the triangle. Figure 5.6 shows a continuously indexed random spatial field (left side of figure 5.6) with the corresponding SPDE on the basis of a triangulation (right panel 5.6).

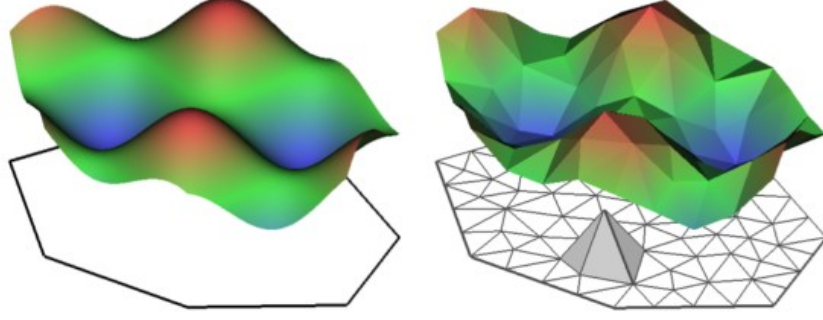


Figure 5.6: Left: example of a spatial random field where $X(s) = \cos(s_1) + \sin(s_2)$, Right: $X(s)$ SPDE representation given a triangulation, Cameletti et al. (2012) source

5.3 Hedonic (rental) Price Models

The theoretical foundation of the Hedonic Price Models (from now on HPM) resides in the consumer utility theory of Lancaster (1966) together with Rosen (1974) market equilibrium. According to Lancaster the utility of a commodity does not exist by itself, instead it exists as the sum of the utilities associated to its separable characteristics. Integrating Lancaster, Rosen introduces HPM and suggests that each separate commodity characteristics are priced by the markets on the basis of supply and demand equilibria. Applying HPM to Real Estate in a market context, from the buy side house prices (indeed also rents) are set as the unit cost of each household attributes, conversely from the selling side the expenditures associated to build of each them. Formalizing the results, Hedonic Price P in Real Estate is expressed as a general f functional form that takes as input the house characteristics vector $\mathbf{C} = \{c_1, c_2, c_3, \dots, c_n\}$.

$$P = f(c_1, c_2, c_3, \dots, c_n)$$

Vector \mathbf{C} since now might contain a unidentified and presumably vast number of ungrouped characteristics. In this setting Malpezzi (2008) tried to organize house features by decomposing \mathbf{C} into mutually exclusive and exhaustive subgroups. The vector components involves the house price P , which is in a f relation with: S , the structural characteristics of the house, N , the neighborhood characteristics, L , the locational characteristics, C , the contract conditions and T time dimension (not included in the model). β is the vector of the parameters to be estimated. Therefore:

$$P = f(S, N, L, C, T, \beta)$$

However the critical part of studying house characteristics in geostatistics is the *estimation* and a recent (and not recent) number of emerging trends are observed (Sheppard, 1999). Trends, other than the methods presented in this analysis suggests semi-parametric or non-parametric methods and applications of spatial econometrics Ling (2019). Researchers would also contend with problems ranging from variable selection to model specification (2019). For semi-paramametric models a local polynomial regression is developed by Clapp (2003). The model provides a nonlinear term for the measurement of housing position values dependent on latitudes and longitudes. Proper geoaddivitive models family was originally proposed by Kammann and Wand (2003), which offers a combination of additive modeling (Buja et al., 1989) and a geostatistical component. As Ling (2019) points out the candidates for the spatial component are many, e.g. kriging component (Dey et al., 2017) (which will be then subsituted with a GP 5.1) or a smooth spatial trend component based on a tensor product of longitude and latitude for which Basile et al. (2013) have investigated European industrial agglomeration externalities. The model outshines the other parameteric model performances by better managing spatial unobserved patterns. Furthermore they made available a third study dimension which is time (2019). Spatial econometrics' evolution trends are seen in Shi and Lee (2017) and lately in Anselin (2010) where point referenced data

are modeled with endogenous time varying spatial weights matrices and unobserved common factors and ultimately are fitted with traditional bayesian estimation methods as MCMC (2010). Then two further interesting modeling approach does not fall perfectly in the categories, but are highly considered in literature within the Hedonic Price models. Dubé and Legros (2013) recognize that the modeling tools available analyzing point referenced data were not sufficient to take into account all the dimensions according to which they want to evaluate the phenomenon. They acknowledge that *Moran's I* index and his statistics test relies mainly on an exogenous specification of a spatial weights matrix (2013). As a result they assemble a spatio-temporal weights matrix to evaluate spatial dependence through Moran's I index whose application is on real estate data (selling) for Québec City from 1986 to 1996. The second approach was addressed in Baltagi et al. (2015) whose object is price estimation based on flats sold in the city of Paris over the period 1990–2003. This is a rich and unbalanced pseudo panel data which are modeled with spatial lag. Results displayed a nested structure of the Paris housing data, which have been tested with likelihood ratio. A similar approach was followed by Nardelli and Arbia (Arbia and Nardelli, 2020) which collected crowdsourced as well as webscraped (as in section 2) data and lately applied Spatial Lag Model (SLM) on a “post-sampled” (Arbia et al., 2020) version of the same. As a result bias in the model is diminished, indeed variance of the estimators is increased. A further aspect of the problem is posed by scholars not considering rents to be representative for the actual value of the real estate due to heavier legislation on rent and indebtedness (for selling). As a consequence predictors choice and functional relationship should be different from the selling. Nevertheless in many empirical analysis rent values are considered as a proxy for real estate pricing when considered in long-run (Herath and Maier, 2011). A further argument to endorse this hypothesis is brought by Manganelli et al. (2013) considering housing a commodity, then the selling or the rental option should be interchangeable economic actions with respect to same inner need to be satisfied. This assumption is also stronger in this context since Manganelli,

Morano, and Tajani have centered their analysis on italian Real Estate data. Moreover Capozza and Seguin (1996) discussed on how much rent-price ratio predicts future changes both in rents and prices. Among all the other points raised they brought the decomposition of rent-price ratio into two parts: the predictable part and the unexplained residuals part. The predictable part was discovered to be negatively correlated with price changes, in other words cities in which prices are relatively high with respect to rents are associated with higher capital gains that might justify that misalignment. This is also true for the opposite, that is cities in which prices are lower with respect to the rents, and this effect can not be associated to any local condition, realize lower capital gains. A further argument is offered by Clark (Clark, 1995) which went after the Capozza and Seguin work. Rent-price ratio is negatively correlated with following future changes in rents. In other words prices are still higher when areas in which they are observed documents an increase in rent prices.

5.4 Spatial Kriging{#kriging} 6.8

The most important aspect in geostatistics regards the possibility to predict response where the phenomenon is not yet observed as well as predicting on latent parameters also named kriging (Gelfand et al., 2010). The name Kriging dates back to a South African mining engineer who actually was the the inventor of the methodology. In general Bayesian settings

At first it may be convenient to look at general bayesian prediction

- general bayesian prediction (wang + balngiaro)
- spartial prediction by Gelfand
- integrating with paci
- code from blangiaro

In Geostatistics the main interest resides in the spatial prediction of the spatial latent field pr the response variable at location not yet observed. Assumed the

model in the previous section, suppose that y^* is not a observed occurrence of the response variable at location s_0 (not in the data) of the GP w_i spatial surface estimated through observed refereced points in y . As a consequence of exchangeability (first step previous section ??) then $y^\otimes = \{y, y^*\}$. Then considering INLA notation it is obtained:

$$\begin{aligned}
 \pi(y^* | y) &= \frac{\pi(y, y^*)}{\pi(y)} \text{ from the conditional probability} \\
 &= \frac{\int \pi(y^* | \theta) \pi(y | \theta) \pi(\theta) d\theta}{\pi(y)} \text{ by exchangeability} \\
 &= \frac{\int \pi(y^* | \theta) \pi(\theta | y) \pi(y) d\theta}{\pi(y)} \text{ applying Bayes' theorem} \\
 &= \int \pi(y^* | \theta) \pi(\theta | y) d\theta
 \end{aligned}$$

A DAG representation might offer the intuition behind Prediction in spatial models:

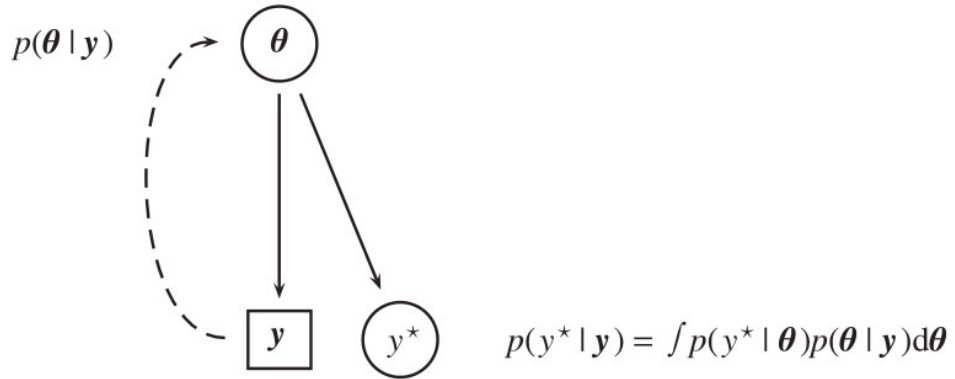


Figure 5.7: Spatial prediction representation through DAG, source Marta Blangiardo (2015)

where $\pi(y^* | y)$ is said predictive distribution and it is meaningful only in the Bayesian framework since the posterior distribution is treated as a random variable, which is totally not true in frequentist statistics.

5.5 Model Criticism

Since INLA can fit a wide range of model then the flexibility should be reflected by a mouldable tool to check model suitability. Once the model is set up and fitted a resampling scheme has to be chosen in order to evaluate the model performance. One of the most used method to assess beyasian model quality is LOOCV cross validation and default choice fo R-INLA package. From data is left out one single observation and so that the Validation set is $y_v = y_{-i}$ and the Assesement set is a $y_a = y_i$ the rest of the observations. Two KPI are assumed to be representative:

- CPO conditional predictive ordinate (pettit, 1990): $CPO_i = \pi(y^* | y_v)$
- PIT probability integral tranform (dawid, 1984): $PIT_i = \pi(y^* < y_i | y_v)$

These quantities are used by default by setting control options in the `inla(control.compute = list())` list object by setting them equal o TRUE. Inla also provides an inner method to authomatically handlee failing in computing those two quantities, leadind to values of 1 when predictions are not reliable and the ipposite for 0. Moreover the empirical distribution of the PIT can be used to asses predictive performance: if it is Uniform, so there are not values that strongly differ from the others then the model is correctly checked. Otherwise if the dostribtuon almost approxiamtes any of the other possibles then the Cross validation assesement prediction has led incorrectly predict the “out of the bag” validation sample.

Posterior checking method exploits a full cross validation where $y_a = y_v$ and it is called predictive checks. Th assesement set now is equal to the validation set, a s a consequence all the observation are evaluated twice. 4 quantities are driver to model estimate quality:

- the *posterior predictive distribution*: $\pi(y^* | y) = \int \pi(y^* | \theta_i) \pi(\theta_i | y) d\theta_i$ which is the likelihood of a replicate observation. When values are small that indicates that are those values are coming from tails, since the

area under the curve (i.e. probability) is less. If this happens for many observation then outliers are driving the model leading to poor estimates

- the *posterior predictive p-value* whose math expression is: $\pi(y^* \leq y_i | y)$ for which values near to 0 and 1 indicates poor performances.
- *Root Mean Square Predictive Error RMSE*: $\sqrt{\frac{1}{n} \sum_{i=1}^n (y_i - y_i^*)^2}$
- R^2

R-INLA has already anticipated in chapter 4 section ?? have designed function to compute statistics on posterior distribution as `inla.pmarginal()` returning the cumulative density distribution.

5.6 Prior Specification

The priors choice is the most central part of a Bayesian analysis and at the same time the weakest since any selection might be criticized. Priors expression involves a considerably high amount of subjectivity and domain experience which may be imported from other comparable literature works or results. However according to purists Bayesian priors should be decided *a-priori*, without either looking at the data, nor the posterior results. This can be tedious since many models are sensitive to priors, as evidenced in the example in sec. 4.4. Priors may negatively impact posteriors when are wrong and they usually require a later revision. The choice in this context is also more difficult since it is also constrained to LGM requirements for which the latent field demands them to be jointly Gaussian. Simpson et al. (2017) provide a solid backbone knowledge on priors specification in Hierarchical models by setting up 4 guidelines principles on top of which it is built a new prior class called Penalized Complexity (PC) priors. Before jumping into the principles it is needed an abstract concept that goes by the name of “base model”. For a general density $\pi(\mathbf{y} | \xi)$ which is controlled by a flexibility parameter ξ the base model is the most uncomplicated one in the class. Following the notation this would be the model corresponding to $\xi = 0$. The base model ideally grabs the parameter

choice with the lowest possible complexity given the model and set it as a ground benchmark. The following example regards base model for a Gaussian Random effect and it considers a multivariate gaussian distributed with mean $\mathbf{0}$ and precision matrix τQ , i.e. $\mathbf{y} \mid \xi \sim \text{MVN}(\mathbf{0}, \tau Q)$, where $\tau = \xi^{-1}$. The base model tries to put the mass (2017) on $\xi = 0$ since the base model in this case is a model without the random effect. At this point it is possible to present the building blocks, first principle is *Occam's razor* according to which priors should be weighted down in function of the distance between the added complexity and the base model i.e. simpler models are preferred. The second principle regards how it is measured complexity whose solution is found in KLD (Kullback–Leibler divergence), calculating distance d from base model. KLD in this context along with principle 1 affirms that the prior shall have high mass in areas where replacing the base model with the flexible model will not cause any information loss. Principle 3 is constant rate penalization as names suggest relates the distance d to a constant rate penalization. In the end principle 4 regards a scale parameter which actually ends up not being very sharp in posterior results (2017). A prior satisfying all the requirements is said Penalized in Complexity. Priors of this class should be then derived with respect to the specific content they are needed. In this context PC priors are seen for Gaussian Random effect, i.e. the GP process 5.1 modeling spatial dependence for which a precision hyper parameter is demanded. Then the latent field has mean 0 and covariance matrix Q^{-1} , i.e. $\mathbf{x} \sim \mathcal{N}(\mathbf{0}, \tau^{-1}Q^{-1})$. The base model considers the absence of the random effect which implies $\tau \rightarrow \infty$. Then the derived (Simpson et al., 2017) PC prior does not depend on the matrix Q and takes the form of an exponential distribution i.e. “type-2 Gumbel distribution” on the standard deviation (in contrast to the exponential on the precision seen in the default). The distribution depends on a scale parameter λ that regulates the penalty deviating from the base model.

```
x = rnorm(20, mean = 40, sd = 2)
sdres = sd(x)
pc.prior = function(tau, alpha, u = 3*sdres) {
```

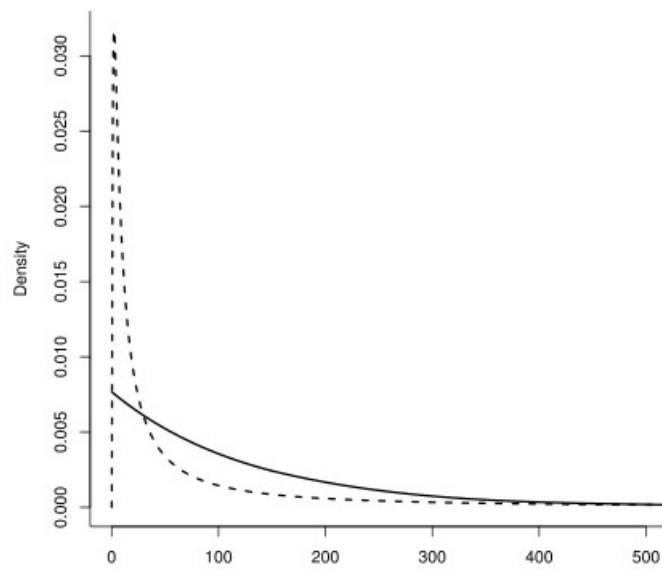


Figure 5.8: New prior (dashed) with parameters ($U = 0.968, \alpha = 0.01$), and the $\Gamma(shape = 1, rate = b)$ prior (solid).

```

lambda = -log(alpha)/u
res = lambda/2*tau^(-3/2)*exp(-lambda*tau^(-1/2))
return(res)
}

```

```

curve(pc.prior(x, alpha = 0.1))

```

Chapter 6

Exploratory Analysis

Data emerging from the RESTful API body response is not in its tidiest form regardless of the query arguments sent. Yet data undergoes to a series of pre-processing step during scraping, which still requires to clear up some unnecessary character and to separate columns containing more than one covariate. To the analysis extent data should be reproducible in the sense that it should be constrained to the same geographic area otherwise the analysis would be not comparable and reproducible. As a result REST API parameters calls are kept permanent (e.g. Milan rental real estate within “circonvallazione” approximated geo-borders) by passing to the `.thesis` parameter, section 3.1.5. In other words the argument (required) option secures to specify to the API an already composed query url to be passed to the scraping endpoint, which corresponds to the zones imposed while searching for advertisements on Immobiliare.it, in this context the *Municipality of Milan*. From a more practical point of view the operation is the equivalent to refresh each time the same immobiliare.it url for which query parameters have already been specified. A further parameter specified is `npages = 120`, leading to 3000 data points. [disclaimer sul fatto che i dati sono chiamati una volta e poi messi in un file]

A summary table of the columns involved in the analysis is presented with the goal to familiarize with incoming covariates. Data already comes semi-processed but due to API fluency it still needs some processing, treated

in 6.1, to be ready to be modeled. Data gathered from the second /complete-scraper endpoint contains geo-statistical components and consequently a map representation of Real Estate rental market at that time is given. A further plot points out that geographic coordinates are non-linearly related to the y-response monthly price variable so dedicated techniques are required. Exploration starts with factor counts evidencing a “Bilocale” prevalence which is then compared to other cities. This suggests some critical Milan real estate market demand information and consequently reflections on the offer. Heating and cooling systems, two of the covariates extracted, are grouped and then arranged by descending order prevalence. They both do not display any significant price’s spin but they bring to the surface an important environmental concern. The same is done by highlighting ridges distribution for other two newly engineered covariates. Data displays bimodality in prices distribution for different n-roomed accommodations and the model should take account of the behavior. Then a piece-wise linear regression is fitted for each n-roomed accommodation sub-group whose single predictor is the square meter footage. The analysis emphasizes some valuable economic consequences both for investors interested in property expansions and for tenants that are planning to partition single properties into rentable sub-units. The previous analysis brings along a major question which addresses the most valuable properties per single square meter surface and an answer based on data is given. Then a log-linear model is fitted on some presumably important covariates to evaluate each single house characteristic contribution to the price. A Tie Fighter plot displays for which coefficient, associated to each dummified predictor, data suggests surprisingly high monthly prices compared to the effect of the square meter footage expansion. A partial conclusion is that disposing of 2 or 3 bathrooms truly pays back an extra monthly return, also due to the number of tenants the accommodations could host. Text mining techniques are applied on real estate operator reviews and a network graph can help to distinguish topics. Then Missing assessment and imputation takes place. At first is made a brief revision on randomness in missing by Little and Rubin (2014)

which may help to figure out if data is missing due to API or for other reasons. Theory is applied by visualizing missing in combination with heat-map and co-occurrence plot. Combined missing observation test is able to detect whether data is missing because of inner scraping failiures or simple rarity in data appereance. Then for the observations that passed the test imputation is made through INLA posterior expectation. That is the case of data lost in predictors so the missing covariates (*condominium*) are brought into a model as response variable whose this time predictors are explanatory ones. Through a method specified within the INLA function the posterior statistics are computed and then finally imputed in the place of missing ones.

prova a farla in latex*

| name | ref |
|------------|---|
| ID | ID of the apartamentos |
| LAT | latitude coordinate |
| LONG | longitude coordinate |
| LOCATION | the complete address: street name and number |
| CONDOM | the condominium monthly expenses |
| BUILDAGE | the age in which the building was contructed |
| FLOOR | the property floor |
| INDIVSAPT | indipendent property type versus appartement type |
| LOCALI | specification of the type and number of rooms |
| TPPROP | property type residential or not |
| STATUS | the actual status of the house, ristrutturato, nuovo, |
| HEATING | the heating system Cen_Rad_Gas (centralizzato a |
| AC | air conditioning hot and cold, Autonomo, freddo/ca |
| PUB_DATE | the date of publication of the advertisement |
| CATASTINFO | land registry information |
| APTCHAR | appartement main characteristics |
| PHOTOSNUM | number of photos displayed in the advertisement |

| | |
|---------------------------|--|
| AGE | real estate agency name |
| LOWRDPRIce_ORIGINAL_PRICE | If the price is lowered it flags the starting price |
| LOWRDPRIce_CURRENT_PRICE | If the price is lowered it flags the current price |
| LOWRDPRIce_PASSED_DAYS | If the price is lowered indicates the days passed since |
| LOWRDPRIce_DATE | If the price is lowered indicates the date the price has |
| ENCLASS | the energy class according to the land registers |
| CONTR | the type of contract |
| DISP | if it is still available or already rented |
| TOTPIANI | the total number of the building floors |
| PAUTO | number of parking box or garages available in the property |
| REVIEW | estate agency review, long chr string |
| HASMULTI | it if has multimedia option, such as 3D house virtual tour |
| PRICE | the monthly price <- response |
| SQFEET | square meters footage |
| NROOM | the number of rooms in the house, and their types |
| TITLE | title of published advertisement |

6.1 Data preparation

Data needs to undergo to many previous cleaning preprocess steps, this is a forced stage since API data comes in human readable format JSON, which is not prepared to be modeled. Cleaning steps mainly regards:

- encoding from UTF-8 to Latin due to Italian characters incorrectly parsed.
- *floors* covariate needs to be separated by its *ascensore* and *accdisabili* components, adding 2 more bivariate covariates.
- *locali* needs to be separated too. 5 category levels drain out: *totlocali*, *camereletto*, *altro*, *bagno*, *cucina*. *nroom* is a duplicate for *totlocali*, so it is discarded.

- *aptchar* is a character string column that contains a various number of different features per house. The preprocess steps include cleaning the string from unnecessary characters, then finding the whole set of unique elements across the character column by splitting on a regex pattern, in the end recoding newly created bivariate columns “yes” or “no” according to a matching pattern whether the feature appears in the string not. A slice from the API output APTCHAR is:

fibra ottica videocitofono impianto di allarme porta blindata reception balcone portiere intera giornata impianto tv centralizzato parzialmente arredato esposizione doppia

6.1.1 Maps and Geo-Visualisations

Geographic coordinates can be represented on a map in order to reveal first symptoms of spatial autocorrelation. Observations are spread almost equally throughout the surface even though the response var *price* indicates unsurprisingly that higher prices are nearer to the city center. The map in figure @ref(fig:leaflet_visuals) is a leaflet object, which needs to be overlapped with layers indicating different maps projections. This is interactive in the .html version, and static is proposed in the .pdf output version. The map object takes a input the latitude and longitude coordinates coming from THE API, and they do not need any CRS (Coordinate Reference System) projection since leaflet can accept the data type.

Predictors, in this case latitude and longitude appear to have nonlinear relationships with the outcome price. The relationship appears to be Gaussian whose mean points to the city center, red dashed line represent latitude and longitude coordinates for the Dome of Milan. Non linearities can be treated with regression splines

ggplot2 visualzitaion matt dancho inspiration::

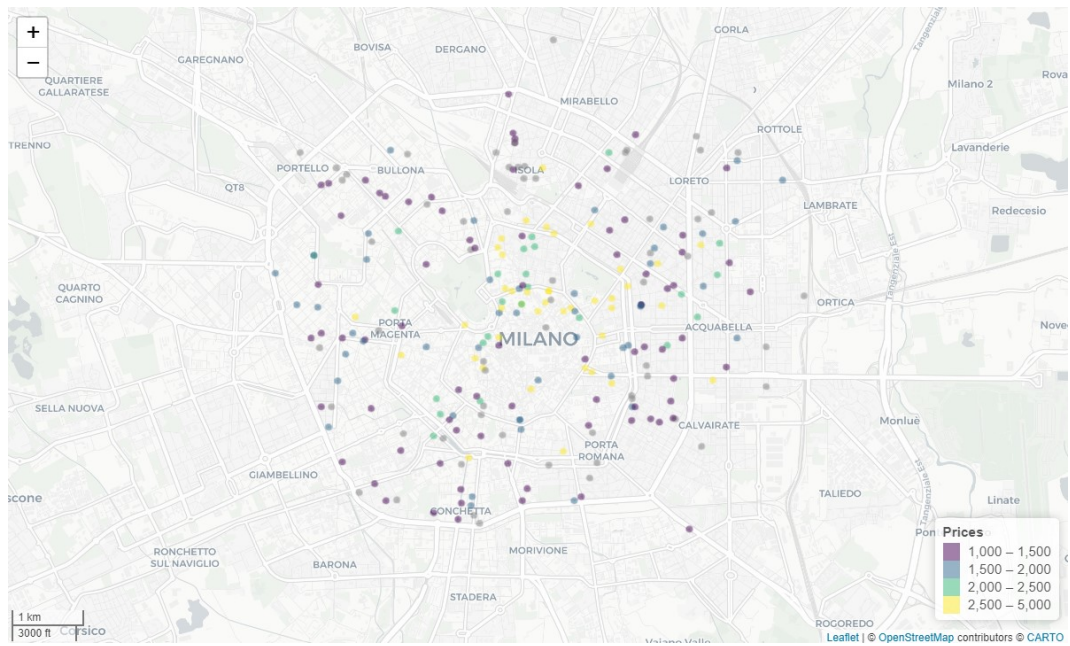


Figure 6.1: Leaflet Map

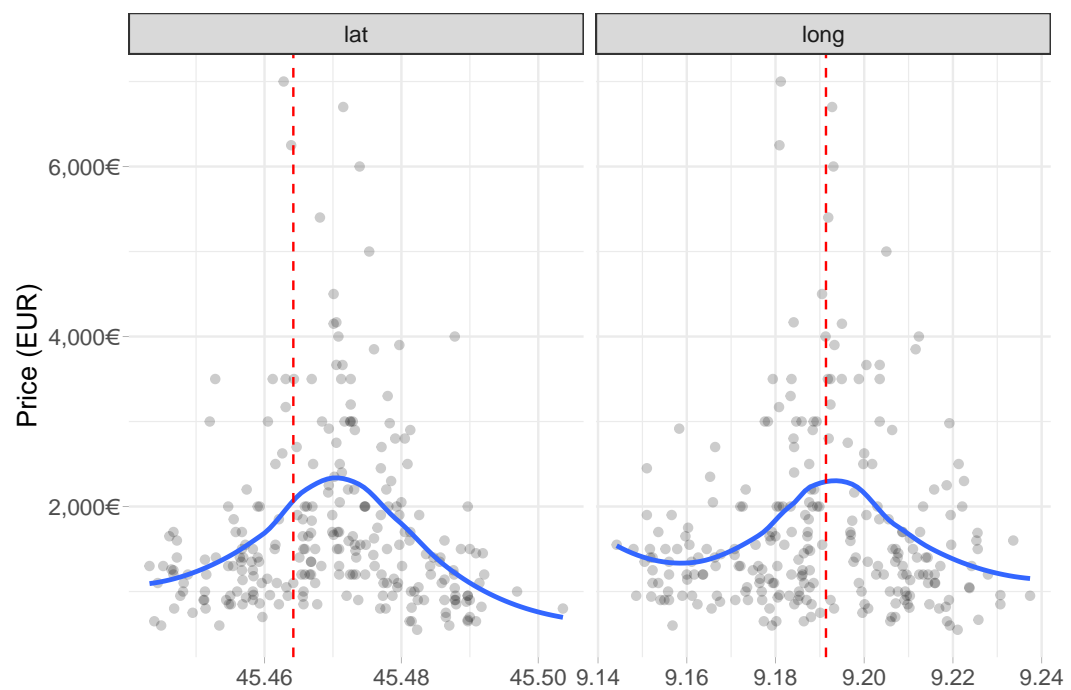


Figure 6.2: Non Linear Spatial Relationship disclosed

6.2 Counts and First Orientations

Arranged Counts for categorical columns can give a sense of the distribution of categories across the dataset suggesting also which predictor to include in the model. The visualization in figure 6.3 offers the rearranged factor *TOT-LOCALI*. Bilocali are the most common option for rent, then trilocali comes after. The intuition behind suggests that Milan rental market is oriented to “lighter” accommodations in terms of space and squarefootage. This should come natural since Milan is both a vivid study and working area, so short stayings are warmly welcomed.

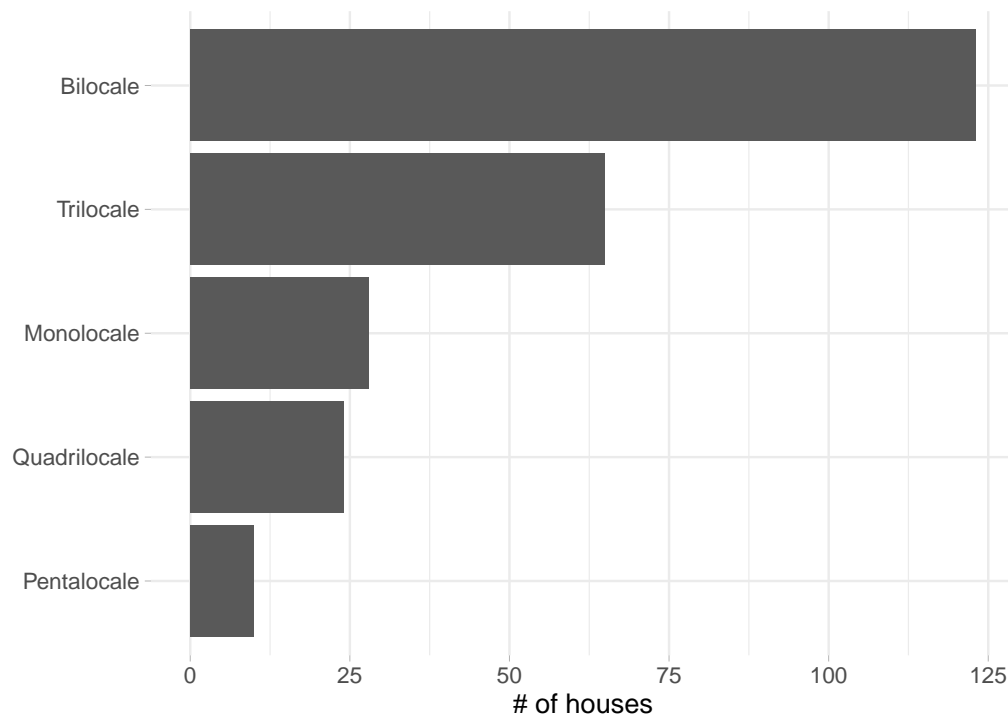


Figure 6.3: Count plot for each housedolds category

Two of the most requested features for comfort and livability in rents are the heating/cooling systems installed. Moreover rental market demand, regardless of the rent duration, strives for a ready-to-accomodate offer to meet clients needs. In this sense accomodation coming with the newest and most techonological systems are naturally preferred with respect the contrary. x-axis in figure 6.4 represents \log_{10} price for both of the two plots. Logarithmic scale

is needed to smooth distributions and the resulting price interpretation have to be considered into relative percent changes. Furthermore factors are reordered with respect to decreasing price.

y-axis are the different level for the categorical variables recoded from the original data due to simplify labels and to hold plot dimension. Moreover counts per level are expressed between brackets close to their respective factor. The top plot displays the most prevalent heating systems categories, among which the most prevalent is “Cen_Rad_Met” by far. This fact is extremely important since metano is a green energy source and if the adoption is wide spread and pipelines are well organized than it brings enormous benefit to the city. As a consequence one major concern regards that for many years policies have been oriented to reduce vehicles emission (euro1 euro2...) instead of focusing on house emissions. This was also a consequence of the lack of house data especially in rural areas. According to data there are still a 15% portion of houses powered by oil fired. Then in bottom plot Jittering is then applied to point out the number of outliers outside the IQR (Inter Quantile Range) .25 and their impact on the distribution. A first conclusion is that outliers are mainly located in autonomous systems, which leads of course to believe that the most expensive houses are heated by autonomous heating systems. Indeed in any case this fact that does not affect monthly price. The overlapping IQR signifies that the covariates levels do not impact the response variable.

this visualization intersects allows to discover bimodality in the response variable. Log scales was needed since they are all very skewed and log scale then is needed also in the model.

(qui ci puoi mettere a confronto per variabile bianria, così vedi cosa includere nel modello esempio sotto dove commentato,)

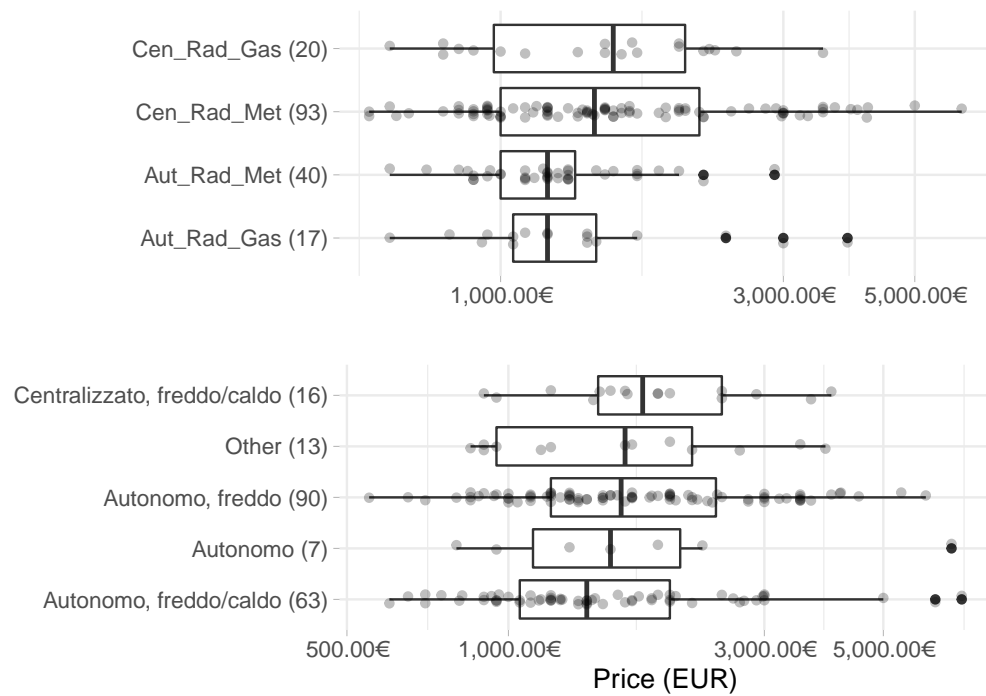
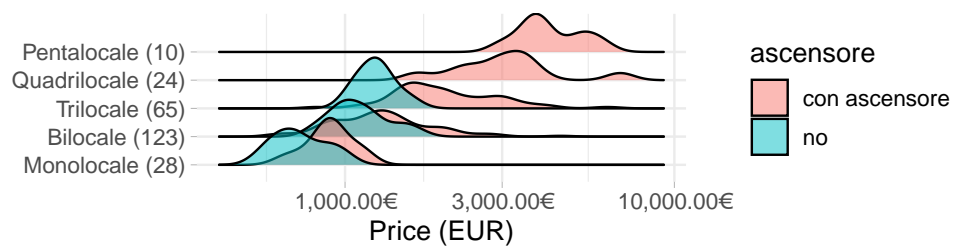
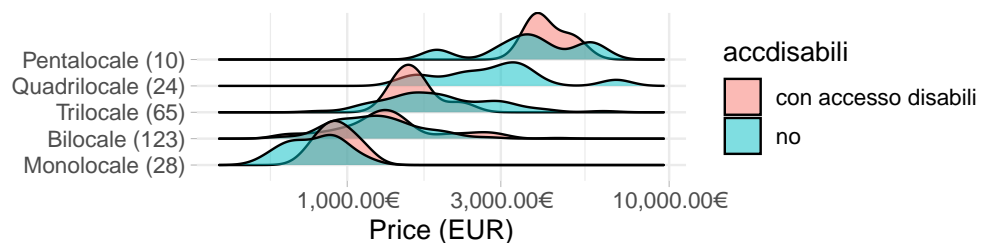


Figure 6.4: Log Monthly Prices box-plots for the most common factor levels in Heating systems and Air Conditionings

How much do Cost items in each category cost?



How much do Cost items in each category cost?



What it might be really relevant to research is how monthly prices change with

respect to house square footage for each house configuration. The idea is to asses how much adding a further square meter affetes the monthly price for each n-roomed flat. One implication is how the property should be developed in order to request a greater amount of money per month. As an example in a situation in which the household has to lot its property into different sub units he can be helped to decide the most proficient choice in economic terms by setting ex ante the square footage extensions for each of the sub-properties. A further implication can regard economic convenience to enlarge new property acquisitions under the expectation to broadened the square footage (construction firms). Some of the potential enlargements are economically justified, some of the other are not. The plot 6.5 has two continuous variables for x (price) and y (sqfeet) axis, the latter is log 10 scaled due to smoothness reasons. Coloration discretizes points for the each j household rooms totlocali. A sort of overlapping piece-wise linear regression (log-linear due to transformation) is fitted on each totlocali group, whose response variable is price and whose only predictor is the square footage surface (i.e. $\log_{10}(\mathbf{price}_j) \sim +\beta_{0,j} + \beta_{1,j}\mathbf{sqfeet}_j$). Five different regression models are proposed in the top left. The interesting part regards the models slopes $\hat{\beta}_{1,j}$. The highest corresponds to “Monolocale” for which the enlargement of a 10 square meters in surface enriches the apartment of a 0.1819524% monthly price addition. Almost the same is witnessed in “Bilocale” for which a 10 square meters extension gains a 0.1194379% value. One more major thing to notice is the “ensamble” regression line obtained as the interpolation of the 5 plotted ones. The line suggests a clear slope descending pattern (logarithmic trend) from Pentalocale and beyond whose assumption is strengthened by looking at the decreasing trend in the $\hat{\beta}_1$ predictor slopes coefficients. Furthermore investing into an extension for “Quadrilocale” and “Trilocale” is *coeteris paribus* an interchangeable economic choice.

In table (...) resides the answer to the question “which are the most profitable properties per month in terms of the price per square meter footage ratio”. The covariate floor together with the totpiani are not part of the model, indeed they can explain the importance and the height of the building justifying

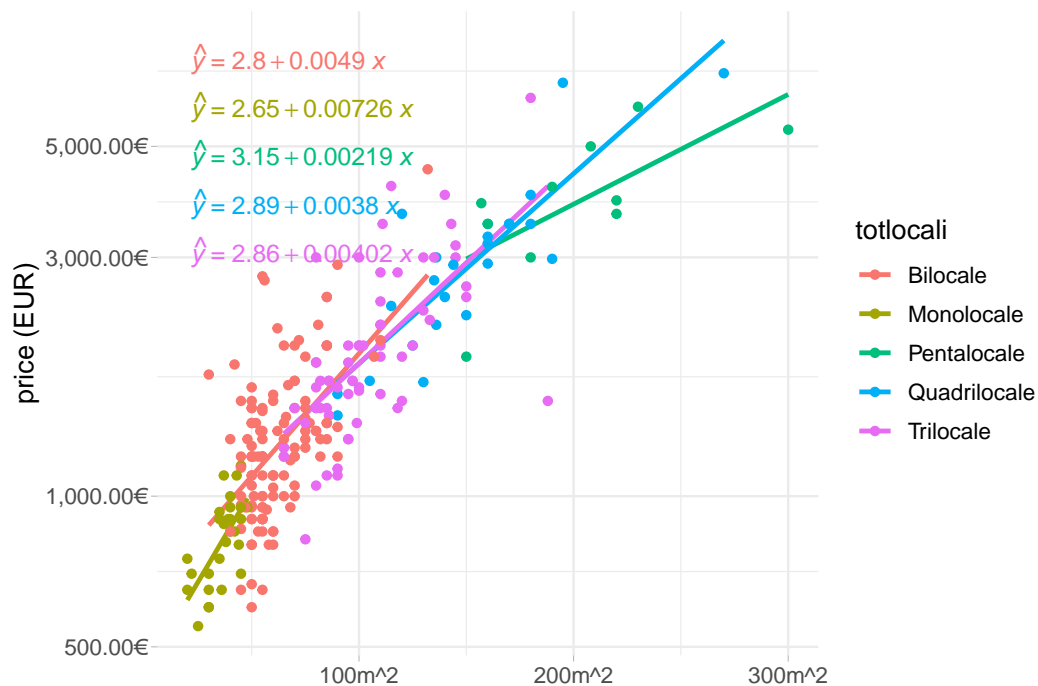


Figure 6.5: Monthly Prices change wrt square meters footage in different n-roomed apt

extraordinary prices. The first 4 observations are unsurprisingly “Bilocale”, the spatial column location, not a regressor, can lend a hand to acknowledge that the street addresses point to very central and popular zones. The zones are, first City Life, second Brera and third Moscova, proving that in modeling real estate rents the spatial component is fundamental , even more in Milan.

| location | totlocali | price | sqfeet | floor | totpiani | abs_pri |
|--------------------------------|------------|-------|--------|-------------|----------|---------|
| viale cassiodoro 28 | Bilocale | 1750 | 30 | 9 piano | 10 piani | 58.333 |
| via della spiga 23 | Bilocale | 2750 | 55 | 2 piano | 4 piani | 50.000 |
| corso giuseppe garibaldi 95 | Bilocale | 2700 | 56 | 2 piano | 5 piani | 48.214 |
| piazza san babila C.A. | Bilocale | 1833 | 42 | 4 piano | 4 piani | 43.642 |
| ottimo stato piano terra, C.A. | Trilocale | 3000 | 80 | Piano terra | 3 piani | 37.500 |
| via federico confalonieri 5 | Monolocale | 750 | 20 | 1 piano | 3 piani | 37.500 |

Then as a further point it might be important to investigate a linear model whose response is price and whose covariates are the newly created abs_price

and some other presumably important ones e.g. floor, bagno, totpiani. The model fitted is $\log_2(\text{price}) \sim \log_2(\text{abs_price}) + \text{bagno} + \text{floor} + \text{totpiani}$. The plot in figure 6.6 has the purpose to demonstrate how monthly price is affected by covariates conditioned to their respective square meter footage. The interpretation of the plot starts by fixing a focus point on 0, which is the null effect highlighted by the red dashed line. Then the second focus is on house surface effect (i.e. House Surface (doubling) in the plot, the term $\log_2(\text{abs_price})$ has been converted to more familiar House Surface (doubling)), which contributes to increase the price of an estimated coefficient of $\approx .6$ for each doubling of the square meter footage. Then what it can be noticed with respect to the two focus points are the unusual effects provoked by the other predictors to the right of the house surface effect and to the far left below 0. “2 and 3 bagni” are unusually expensive with respect to the square meter footage increment, on the other hand “al piano rialzato” and “al piano terra” are undervalued with respect to their surface. The fact that 2 and 3 bathrooms can guarantee a monthly extra check is probably caused to a minimum rent plateau requested for each occupant. the number of bathrooms are a proxy to both house extension since normally for each sleeping room there also exist at least 1 bathroom as well as prestigious houses dispose of more than 1 toilette services. So the more are the occupants regardless of the square meter footage dedicated to them, the more the house monthly returns, it can be noticed is that ultimo piano, together with 2 abagni ad 3 bagni are unusually expensive with respect to their proper square meter footage. On the other hand the piano rialzato and piano terra are unusually undervalued given their surface.

In other words to help with the interpretation. The fact that 2 and 3 bathrooms can guarantee a monthly extra check is probably caused to a minimum rent plateau requested for each occupant. So the more are the occupants regardless of the square meter footage dedicated to them, the more the house returns. The conclusion

Tie fighter coefficient plot for the linear model: $\log_2(\text{price}) \sim \log_2(\text{abs_price}) + \text{condominium} + \text{other_colors}$

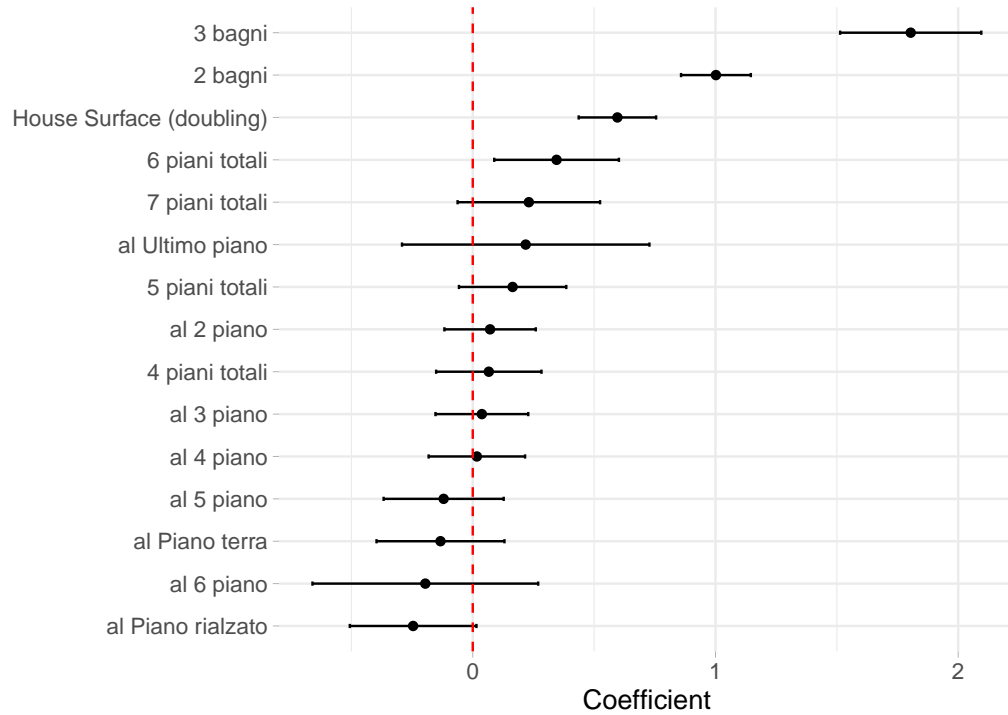


Figure 6.6: Tie fighter coefficient plot for a log-linear model

6.3 Text Mining in estate Review

The word network in figure ??fig:WordNetworkgraph) tries to summarize relevant information from real estate agency review into each advertisement. `avg_totprice` expresses the sum of the price per month plus the condominium in order to fully integrate inner property characteristics together with building exclusivity. Tokenized words are then filtered with “stopwords-iso” italian dictionary. Nodes associated with hotter colours are also associated to more expensive in and out-house characteristics. The size of nodes keeps track of the number of reviews in which the specific word appears. A table of the most common words can help highlight both the real estate jargon as well as words that brings up house values.

| word | count | reviews | avg_totprice |
|---------------|-------|---------|--------------|
| bagno | 249 | 192 | 1888.622 |
| cucina | 247 | 190 | 2088.814 |
| ingresso | 194 | 173 | 1964.062 |
| soggiorno | 182 | 159 | 1872.500 |
| camera | 200 | 158 | 1936.945 |
| piano | 197 | 157 | 1982.234 |
| arredato | 184 | 152 | 1744.614 |
| composto | 158 | 146 | 1758.911 |
| riscaldamento | 171 | 144 | 1877.404 |
| zona | 282 | 139 | 1930.213 |

Furthermore it is possible to grossly divide the plot in figure ??fig:WordNetworkgraph) into 3 sub-groups of nodes, each of which addresses a specific part of the house comprehensive evaluation. In the far right side of the plot are considered the external appliances like neighbor stores, subway stations and services and are associated to mean prices. The correspondent number of reviews are not justifying by any type of price increasing effect. Whereas slightly moving the view to the left, the area centered in portineria evidences a sub-groups of nodes associated to relatively higher avg-totprice. Some of them are servizio signorile palazzo. The previous set of nodes indicates services that are proper to the building can lead to some sort of extra payment. Then still moving Possiamo immaginare di dividere il network in 3 raggruppamenti di nodi, ognuno dei quali parla di un specifico tema. nella parte alta sinistra ci si parla delle circostanze esterne dell'appartamento, i negozi i mezzi servizi la metri, i prezzi evidenziati dal colore nei nodi sono neutri, indicando che non impattano il prezzo in maniera significativa. poco più sotto è possibile vedere un altro centroide verso il quale puntano una serie di edges peritenti che riguardano i servizi interni al building come la portineria, l'ingresso, il palazzo. in questo caso i colori sono più caldi e i servizi sembrano essere pagati di più. successivamente spostandoci verso il centro del network si

Based on 250 rental reviews and their respective price

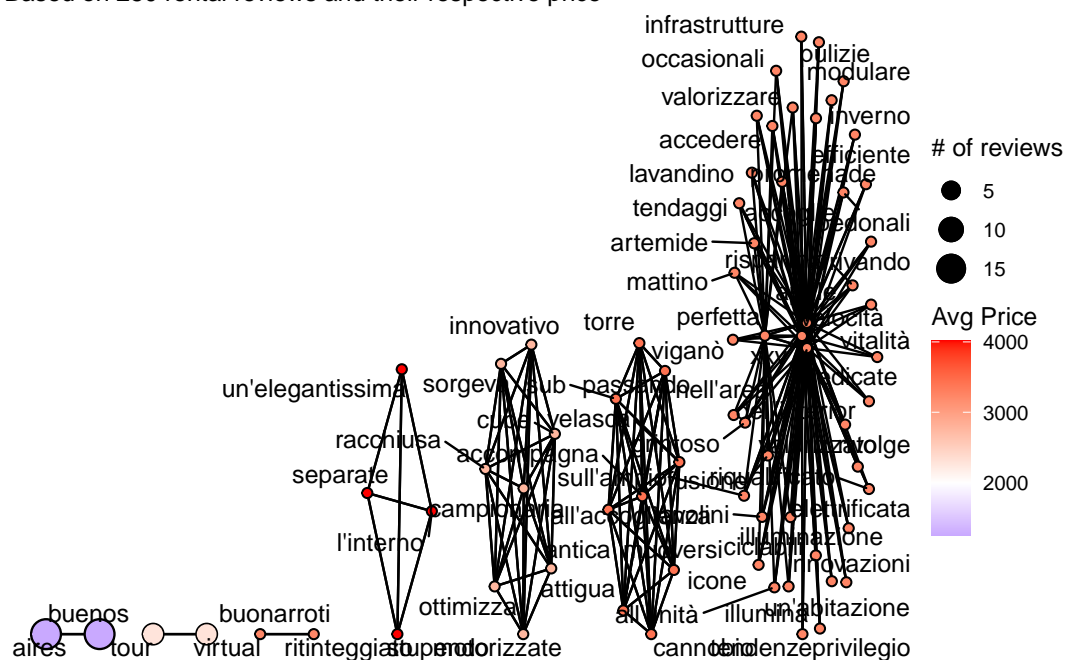


Figure 6.7: Word Network Graph for 250 Estate Agencies Review

6.4 Missing Assessment and Imputation

As already pointed out some data might be lost since immobiliare provides the information that in turn are pre filled by estate agencies or privates through standard document formats. Some of the missing can be reverse engineered by other information in the web pages e.g. given the street address it is possible to trace back the lat and long coordinates. Some other information can be encountered in .json files hidden inside each of the single web pages. The approach followed in this part is to prune redundant data and rare predictors trying to limit the dimensionality of the dataset.

6.4.1 Missing assesement

The first problem to assess is why information are missing. As already pointed out in the preliminary part as well as in section ?? many of the presumably important covariates (i.e. price lat, long, title ,id ...) undergo to a sequence of forced step inside scraping functions with the aim to avoid to be lost. If at the end of the sequence covariates are still missing, the correspondent observation is not considered and it is left out of the resulting scraped dataset. The choice originates from empirical missing patterns suggesting that when important information are missing then the rest of the covariates are more likely to be missing to, as a consequence the observation should be discarded. The missing profile is crucial since it can also raise suspicion on the scraping failures. By Taking advantage of the missing pattern in observations the maintainer can directly identify the problem and derivatives and immediately debug the error. In order to identify if the nature of the pattern a revision of missing and randomness is introduced by Little and Rubin (2014). Missing can be devided into 3 categories:

- *MCAR* (missing completely at random) likelihood of missing is equal for all the information, in other words missing data are one idependetn for the other.

- *MAR* (missing at random) likelihood of missing is not equal.
- *NMAR* (not missing at random) data that is missing due to a specific cause, scarping can be the cause.

MNAR is often the case of daily monitoring clinical studies (Kuhn and Johnson, 2019), where patient might drop out the experiment because of death and so all the relating data starting from the death time +1 are lost. To identify the pattern a *heat map* plot 6.8 clarifies the idea:

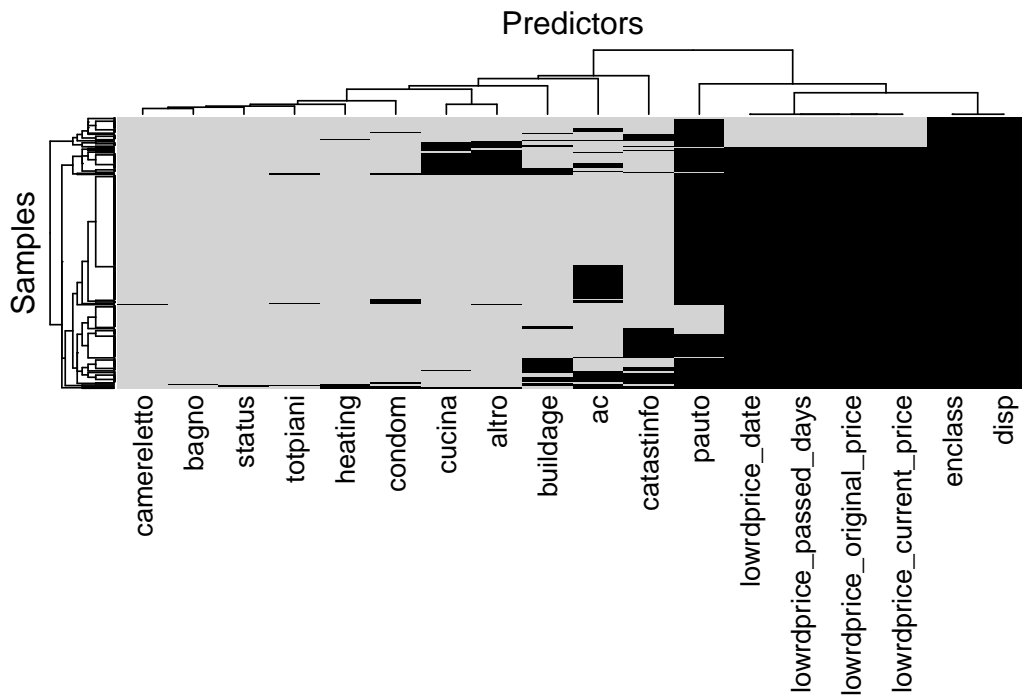


Figure 6.8: Missingness Heatmap plot

Looking at the top of the heat map plot, right under the “Predictor” label, the first tree split divides predictors into two sub-groups. The left branch considers from *TOTPIANI* to *CATASTINFO* and there are no evident patterns. Then missingness can be traced back to *MAR*. Imputation needs to be applied up to *CONDOM* included, the others are discarded due to rarity: i.e. *BUILDAGE*: 14% missing, *CATASTINFO*: 21% and *AC*: 24%. Moreover *CUCINA* and *ALTRO* are generated as “childred” of the original *LOCALI* variable, so it should not surprise that their missing behavior is similar ,whose prevalence is

respectively 13% and 14%, for that reason are discarded. In the far right hand side *ENCLASS* and *DISP* data are completely missing and a pattern seems to be found. The most obvious reason is a scraping fail in capturing data. Further inspection of the API scraping functions focused on the two covariates is strongly advised. From *LOWRDPRICE*. covariates group class it seems to be witnessing a missing underlining pattern NMAR which is clearer by looking at the *co_occurrence* plot in figure 6.9. Co-occurrence analysis might suggest frequency of missing predictor in combination and *LOWRDPRICE*. class covariates are displaying this type of behavior. *PAUTO* is missing in the place where *LOWRDPRICE*. class covariates are missing, but this is not happening for the opposite, leading to the conclusion that *PAUTO* should be treated as a rare covariate MAR, therefore *PAUTO* is dropped. After some further investigation on *LOWRDPRICE*., the group class flags when the *PRICE* covariate is effectively decreased and this is unusual. That is solved by grouping the covariate's information and to encode it as a two levels categorical covariate if lowered or not. Further methods to feature engineer the *LOWRDPRICE*. class covariates can be with techniques typical of profile data, further references are on Kuhn and Johnson (2019).

6.4.2 Covariates Imputation

A relatively simple approach to front missingness is to build a regression model to explain the covariates that have some missing and plug-back-in the respective estimates (e.g. posterior means) from their predictive distributions Little and Rubin (2014). This approach is fast and easy to implement in most of the cases, but it ignores the uncertainty behind the imputed values (Gómez Rubio, 2020). However it has the benefit to be a more than a reasonable choice with respect to the number of computation required, especially with INLA and in a spatial setting. That makes it the first choice method to follow since imputation regards also a small portion of data and predictors. At first it is considered the predictor *condominium* for which some observation are missing.

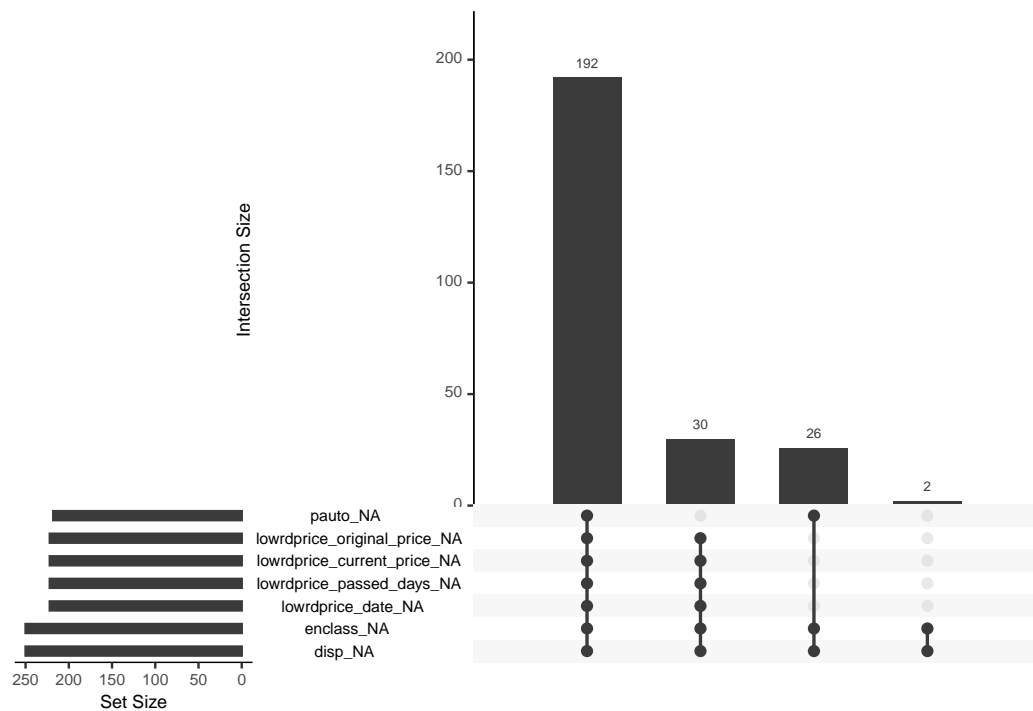


Figure 6.9: Missingness co-occurrence plot

Indices are:

```
## [1] 19 74 77 90 99 113 116 120 179 249
```

A model is fitted based on missing data for which the response var is condominium and predictors are other important explanatory ones, i.e. $\text{condom} \sim 1 + \text{sqfeet} + \text{totlocali} + \text{floor} + \text{heating} + \text{ascensore}$. In addition to the formula in the `inla` function a further specification has to be provided with the command `compute = TRUE` in the argument `control.predictor`. The command `compute` estimates the posterior means of the predictive distribution in the response variable for the missing points. The estimated posterior mean quantities are then imputed and are in table `@red(tab:CondomImputation)`

| | mean | sd |
|----------------------|-----------|----------|
| fitted.Predictor.019 | 198.11095 | 19.67085 |
| fitted.Predictor.074 | 162.96544 | 13.29456 |
| fitted.Predictor.077 | 99.38197 | 32.34108 |
| fitted.Predictor.090 | 331.73519 | 33.05035 |
| fitted.Predictor.099 | 170.54068 | 12.30267 |
| fitted.Predictor.113 | 196.61593 | 15.86545 |
| fitted.Predictor.116 | 108.40482 | 20.79689 |
| fitted.Predictor.120 | 162.86977 | 25.61622 |
| fitted.Predictor.179 | 165.03632 | 20.53485 |
| fitted.Predictor.249 | 117.24234 | 30.80290 |

A further method for imputation has been designed by *Gómez-Rubio, Cameletti, and Blangiardo 2019*) *miss lit* by adding a sub-model for the imputations to the final model through the `inla` function. This is directly handled inside the predictor formula adding a parameter in the latent field. However the approach makes the model more complex with a further layer of uncertainty to handle. At first the additive regression model with all the covariates is called including the covariates with missing values. The response variable *PRICE* displays no missing values and the model fitted is:

Arguments can tune triangularization through `inla.mesh.2d()` :

- `loc`: location coordinates that are used as initial mesh vertices
- `boundary`: object describing the boundary of the domain,
- `offset`: argument is a numeric value (or a length two vector) and it is used to set the automatic extension distance. If positive, it is the extension distance in the same scale units. If negative, it is interpreted as a factor relative to the approximate data diameter; i.e., a value of -0.10 (the default) will add a 10% of the data diameter as outer extension.
- `cutoff`: points at a closer distance than the supplied value are replaced by a single vertex. Hence, it avoids small triangles

- `max.edge`: A good mesh needs to have triangles as regular as possible in size and shape.
- `min.angleargument` (which can be scalar or length two vector) can be used to specify the minimum internal angles of the triangles in the inner domain and the outer extension

A convex hull is a polygon of triangles out of the domain area, in other words the extension made to avoid the boundary effect. All meshes in Figure 2.12 have been made to have a convex hull boundary. If borders are available are generally preferred, so non convex hull meshes are avoided.

6.4.3 Shinyapp for mesh assessment

INLA includes a Shiny (Chang et al., 2018) application that can be used to tune the mesh params interactively

The mesh builder has a number of options to define the mesh on the left side. These include options to be passed to functions `inla.nonconvex.hull()` and `inla.mesh.2d()` and the resulting mesh displayed on the right part.

Chapter 7

Model Selection & Fitting

- metti Ling (2019) che ha messo i priors come defaults nella inla call

ref.¹

```
library(readr)
data = read_csv("data/data2021.csv")
mesh2 <- inla.mesh.2d(confini, max.edge = c(0.2, 0.2),
  cutoff = 3)
ggplot(data) + gg(mesh2) + geom_sf() +
  ggtitle(paste("Vertices:", mesh2$n)) + coord_sf(datum
    = st_crs(5880))
```

mega ref²

mega mega ref³

```
library(inlabru)
formula = price ~ condom + totlocali + sqfeet

ggplot(data)+
  geom_point(aes(lat, long), size = 2) +
```

¹https://inbo.github.io/tutorials/tutorials/r_inla/spatial.pdf

²<https://inlabru-org.github.io/inlabru/>

³<https://besjournals.onlinelibrary.wiley.com/doi/full/10.1111/2041-210X.13168>

```
coord_fixed(ratio = 1) +  
scale_color_gradient(low = "blue", high = "orange") +  
geom_sf(data = confini) +  
theme_bw()
```

Chapter 8

Conclusions

Appendix

8.1 Gaussian Process

Let assume to have cloud of points represented by two variables X_1 and X_2 , figure ???. The cloud of points are observation taken from a realization of two variables e.g. height and weight, What it might be observed is:

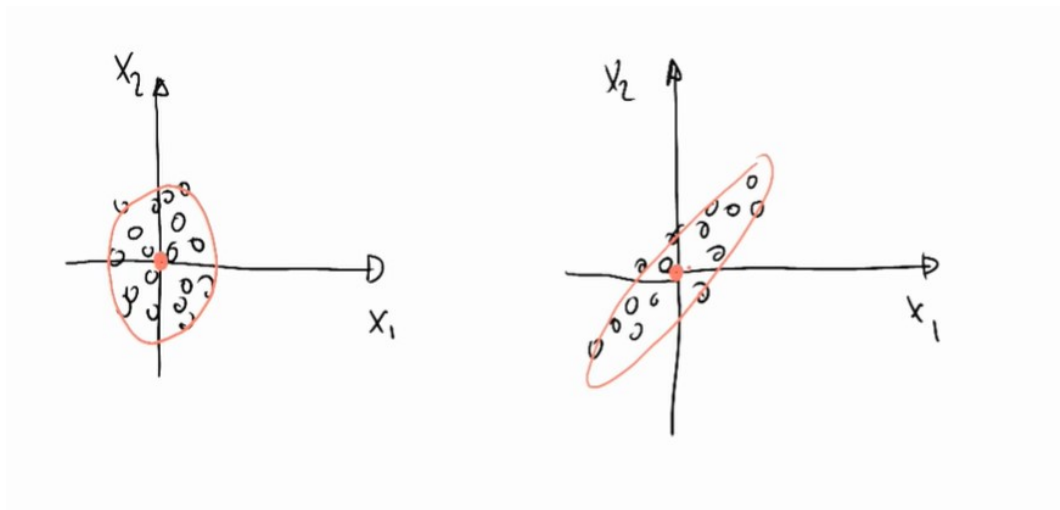


Figure 8.1: Left panel: GP cloud of points fitted with a *circle*, Right panel: GP cloud of points fitted with a *ellipse*, source de Freitas (2013)

Each circle in both panels figure 8.1 represents a measurements of the observed phenomenon. Let assume to fit a multivariate gaussian distribution to the left panel data. The process of learning is to fit a Gaussian to data, the ultimate goal is to describe the data, the most perfectly evident Gaussian is the one interpolating the points and centering in $(0, 0)$, a circle might be a good guess. Instead for the right one in 8.1, a smart guess could be still centering the mean

in, indeed now it is an ellipse describing the variability. At this point it might be interesting to vectorized what has been measured, the centers are then compressed into a vector μ_i , i.e. it has two components X_1 and X_2 whose corresponding mean is 0.

$$\mu = \begin{bmatrix} \mu_{x_1} \\ \mu_{x_2} \end{bmatrix}$$

This is true for all the observations which have two coordinates too x_1 and x_2 . for each of the points, e.g. for point 1:

$$\mathbf{x}_1 = \begin{bmatrix} x_1 \\ x_2 \end{bmatrix}$$

they can be negative positive, the Real numbers, usually we have \mathbb{R}^2 extending from - infinity to + infinity, to the power of two because we have 2 dimensions, a Real plane. any point is gaussian distributed when with mean .. an variance. how we explain covariance, through *correlation*. we do it by correlation with its normal forms. the covariance is the term that goes inside the matrices in the upper right of the matrix we have the expectation of x_1 times x_2 , like $\mathbb{E}(x_1 \cdot x_2)$, where the expectation in the gaussian case is the mean which is 0, so the corresponding value is 0. the covariance essentially is the dot product ref dot product¹ of x_1 and x_2 variable, so what happens when you take the dot product of vectors, if for example you take a vector that looks like 1 and 0 and you take the dot product of one other vector 1 and 0, so that:

$$\begin{bmatrix} 1 \\ 0 \end{bmatrix} \begin{bmatrix} 1 & 0 \end{bmatrix} = 1$$

You will end up with 1, recall dot product first element first vector times first element second vector and second element first vector times second element second vector. So identical vector will get a high dot product value leading to a

¹https://mathinsight.org/dot_product_matrix_notation

high similarity measure. Dot product can be indeded as a similarity measure.
 ... But if you take two different vector as 1 0 and 0 1 then:

$$\begin{bmatrix} 1 \\ 0 \end{bmatrix} \begin{bmatrix} 0 & 1 \end{bmatrix} = 0$$

This time the multiplication leads to 0 value, as a matter of fact they are different. They are no similar. IF two points are closed the dot product will be high in 2D. What the covariance should be? if variances are assumed to be 1 then in this case i qould expect to be 0, i.e. covariance matrix is:

$$\begin{bmatrix} 1 & 0 \\ 0 & 1 \end{bmatrix} = \mathbf{cov}_{\mathbf{plot1}}(x_1, x_2)$$

because I can picka poin tin two pointa in this cloud. Suppose i increase x1 then my chance of getting a x2 point that is positive or negative is the samee, knowing somthin about x1 give nothign about x2. no information is proivede. On the other hand i the second plot knowing a positive value of 1 can suggest with a certain probability that x2 will be positive (great proability. So some information is provided), e.g.

$$\begin{bmatrix} 1 & 0.5 \\ 0.5 & 1 \end{bmatrix} = \mathbf{cov}_{\mathbf{plot2}}(x_1, x_2)$$

Some positive number idicates that i expect a positive inc rease iwhen boht of the two are increasing singularly. thsi is what the correlation, the basis to do linear regresssion and non linear- thei is a bivariate gaussian. If the entri3es are means that they are uncoorellated, if they are non-zero then they are correlated, theby can be both positive or negative (correlatiob)

now lets generate a gassiiian distrivution so x_1 and x_2 in 2D and then a third dimension hwere we express probability, this is said joint distribution. So i am going to cu this gaussian at certain point for x_1 and cut a plain

right though this gaussian imagine to have a cake and then take a knife and cut it. (see the image)

from the main perspective you are going to see a gaussian distribution, you will be looking at x_1 and you will be seeing a gaussian plot in green. this is the probability of x_1 given x_2 . also said “conditioned” probability. This gaussian has a mean like the one already seen and this is the center of the gaussian, we can rewrite the mean and variance of the multivariate gaussian describing the cloud of points. sigma are the covariance matrix sigma.

... sigma 1 and sigma 2 if you have 1 d variable the width has to be positive, for multivariate gaussian equal so here positive definiteness: covariance matrix symmetric.

... any arbitrary variable transposed x times the covariance matrix needs to be positive. what is the mean of this gaussian i might want to know what is the width of this gaussian would it be great if there is a formula that given the cloud of point and likelihood estimation. we could obtain the red bell in figure. Compute the green curve how it is done? this requires some work and it is said matrix *inversion lemma*, this is fundamental for machine learning. let's assume it. The theorem says that the mean of the gaussian is the mean of x_1 and then some other operation with sigma, see below from pac (miss ref)

■ $E[X_1 | X_2] = \mu_{1|2} = \mu_1 + \Sigma_{12}\Sigma_{22}^{-1}\Sigma_{21}(X_2 - \mu_2)$ is the **conditional mean**

■ $\text{Var}[X_1 | X_2] = \Sigma_{1|2} = \Sigma_{11} - \Sigma_{12}\Sigma_{22}^{-1}\Sigma_{21}$ is the **conditional variance**

the theorem says to consider a multivariate gaussian a vector 1 and a vector 2 each vector component has a mean and a covariance matrix, this by lemma gives us the expression and the math behind is not tremendous, but it is long. What is important is to understand to go from a joint to a conditional distribution in our case. that's the value of the theorem.

One background further thing: assume that we have a gaussian variable distribution that we want to sample from, we had now we are going to do

the opposite, before we had points and we tried to figure out the curve, now we have the curve and we are going to try to reproduce data. I need to be able to draw sample from a gaussian distribution. I will assume that I have a mechanism that produces a uniform samples, so you have a random number generator with equal probability from 0 to 1, I assume also the cumulative of a gaussian.

the cumulative of a gaussian is what you get if you start summing the area under the curve of the gaussian as you move from the left. value after value you can plot the cumulative ahead (see figure) the point where there is a flex point is the mean because the gaussian is symmetric. The asymptote is 1 because the area under the curve sums to 1. If I can draw a random number from Uniform and then project it to the cumulative and then finally project it back to the gaussian distribution. Inverse cumulative mapping. If you do this multiple times you are going to have many samples placed next to the mean and as sparse as the variance. In this process of sampling try to sample a point from a gaussian that has mean 0 and variance 1, now let's try to draw a point from a gaussian with mean μ and variance σ

In the multivariate case suppose that we have a vector with two variables how do I draw a vector from a multivariate gaussian with 0 means and plot 1 covariance matrix. the theorem also says that the marginal distribution can be seen by covariance matrix, first take the mean_1 and take upper left element from the covariance matrix obtaining the marginal probability for x_1 , i.e.

Then for simplicity we can simplify by grouping vector into: (vector expression multivariate)

I need a way to take square root of matrices, if x come from a MVG

35:01–

8.2 SPDE and Triangularization (YT speech: Moraga (2020))

In order to fit LGM type of models with a spatial component INLA uses SPDE (Stochastic Partial Differential Equations) approach. Suppose that is it given have a continuous Gaussian random process (a general continuous surface), what SPDE does is to approximate the continuous process by a discrete Gaussian process using a triangulation of the region of the study. Let assume to have a set of points defined by a CRS system (Latitude and Longitude, Eastings and Northings), and let assume that the object of the analysis is to estimate a spatially continuous process. Instead of exploiting this property as a whole, it is estimated the process only at the vertices of this triangulation. This requires to put a triangularization of the region of the study on top the the process and the software will predict the value of the process at its vertices, then it interpolates the rest of the points obtaining a “scattered” surface.

Imagine to have a point a location X laying inside a triangle whose vertices are S_1, S_2 and S_3 . SPDE operates by setting the values of the process at location x equal to the value of the process at their vertices with some weights, and the weights are given by the *Baricentric coordinates (BC)*. BC are proportional to the area at the point and the vertices. Let assume to have a piece of triangularization A and let assume that the goal is to compute the value at location X . X , as in formula above A , would be equal to S_1 , multiplied by the area A_1 dived by the whole triangle area (A) + S_2 multiplied by the area A_2 divided by A + S_3 , multiplied by the area A_3 dived by (A . This would be the value of the process at location X given the triangulations (numeber of vertices). SPDE is actually apprximatring the value of hte process using a weighted average of the value of the process at the triangle vertices which ir proportional to the area of the below triangle. In order to do this within INLA 4 it is needed also a *Projection Matrix* , figure 8.3. The Projection matrix maps the continuous GRMF (when it is assumed a GP) from the observation

Projection matrix

$S(\mathbf{x})$ weighted average of the values of the GMRF in the vertices of the triangle containing the location of the observation.

Weights = barycentric coordinates

$$S(\mathbf{x}) \approx \frac{A_1}{A} S_1 + \frac{A_2}{A} S_2 + \frac{A_3}{A} S_3$$

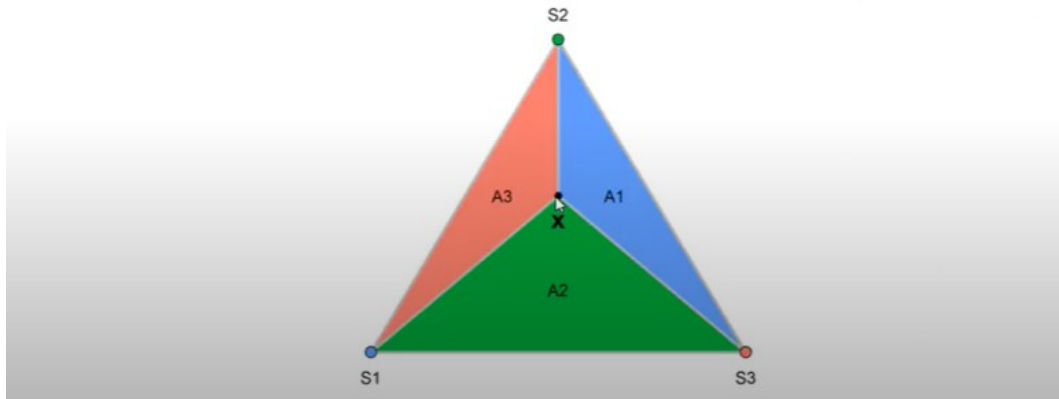


Figure 8.2: Triangulation weights and associated process value, Moraga (2020) source

to the triangulation. It essentially assigns the height of the triangle for each vertex of the triangularization to the process. Matrix \mathcal{A} , whose dimensions are \mathcal{A}_{ng} . It has n rows and g columns, where n is the number of observations and g is the number of vertices of the triangulation. Each row has possibly three non-0 values, right matrix in figure 8.3, and the columns represent the vertices of the triangles that contains the point. Assume to have an observation that coincides with a vertex S_1 of the triangle in 8.2, since the point is on top of the vertex (not inside), there are no weights ($A_1 = \mathcal{A}$) and 1 would be the value at $A_{(1,1)}$ and 0 would be the rest of the values in the row. Now let assume to have an observation coinciding with S_3 (vertex in position 3), then the result for $A_{(2,3)}$ would be 1 and the rest 0. Indeed when the value is X that lies within one of the triangles all the elements of the rows will be 0, but three elements in the row corresponding of the position of the vertices $1 = .2, 2 = .2$ and $g = .6$, as a result X will be weighted down for the areas.

Projection matrix

$$S(\mathbf{x}_i) \approx \sum_{g=1}^G A_{ig} S_g$$

where A is a projection matrix that maps the GMRF from the observations to the triangulation nodes

Row i in A corresponding to observation i has possibly three non-zero values at columns that represent the vertices of the triangle containing the point (non-zero values are equal to the barycentric coordinates)

$$A = \begin{pmatrix} A_{11} & A_{12} & A_{13} & \dots & A_{1G} \\ A_{21} & A_{22} & A_{23} & \dots & A_{2G} \\ \vdots & \vdots & \vdots & \ddots & \vdots \\ A_{n1} & A_{n2} & A_{n3} & \dots & A_{nG} \end{pmatrix} = \begin{pmatrix} \underline{1} & 0 & 0 & \dots & 0 \\ 0 & 0 & \underline{1} & \dots & 0 \\ \vdots & \vdots & \vdots & \ddots & \vdots \\ \underline{.2} & \underline{.2} & 0 & \dots & \underline{.6} \end{pmatrix}$$

Figure 8.3: Projection Matrix to map values from triangulation back to the GP, Moraga (2020) source

8.3 Laplace Approximation

Marta Blangiardo (2015) offers an INLA focused intuition on how the Laplace approximation works for integrals. Let assume that the interest is to compute the following integral, assuming the notation followed throughout the analysis:

$$\int \pi(x)dx = \int \exp(\log f(x))dx$$

Where X is a random variable for which it is specified a distribution function π . Then by the Taylor series expansions (Fosso-Tande, 2008) it is possible to represent the $\log \pi(x)$ evaluated in an exact point $x = x_0$, so that:

$$\log \pi(x) \approx \log \pi(x_0) + (x - x_0) \left. \frac{\partial \log \pi(x)}{\partial x} \right|_{x=x_0} + \frac{(x - x_0)^2}{2} \left. \frac{\partial^2 \log \pi(x)}{\partial x^2} \right|_{x=x_0} \quad (8.1)$$

Then if it is assumed that x_0 is set equal to the mode x_* of the distribution (the highest point), for which $x_* = \operatorname{argmax}_x \log \pi(x)$, then the first order derivative with respect to x is 0, i.e. $\left. \frac{\partial \log f(x)}{\partial x} \right|_{x=x_*} = 0$. That comes natural since once the function reaches its peak, i.e. the max then the derivative in that point is 0. Then by leaving out the first derivative element in eq. (8.1) it is obtained:

$$\log \pi(x) \approx \log \pi(x_*) + \frac{(x - x_*)^2}{2} \left. \frac{\partial^2 \log \pi(x)}{\partial x^2} \right|_{x=x_*}$$

Then by integrating what remained, exponentiating and taking out non integrable terms,

$$\int \pi(x)dx \approx \exp(\log \pi(x_*)) \int \exp \left(\frac{(x - x_*)^2}{2} \left. \frac{\partial^2 \log \pi(x)}{\partial x^2} \right|_{x=x_*} \right) dx \quad (8.2)$$

At this point it might be already intuited the expression (8.2) is actually the

density of a Normal. As a matter of fact, by imposing $\sigma_*^2 = -1 / \left. \frac{\partial^2 \log f(x)}{\partial x^2} \right|_{x=x_*}$, then expression (8.2) can be rewritten as:

$$\int \pi(x) dx \approx \exp(\log \pi(x_*)) \int \exp\left(-\frac{(x-x_*)^2}{2\sigma_*^2}\right) dx \quad (8.3)$$

Furthermore the integrand is the *Kernel* of the Normal distribution having mean equal to the mode x_* and variance specified as σ_*^2 . By computing the finite integral of (8.3) on the closed neighbor $[\alpha, \beta]$ the approximation becomes:

$$\int_{\alpha}^{\beta} f(x) dx \approx \pi(x_*) \sqrt{2\pi\sigma_*^2} (\Phi(\beta) - \Phi(\alpha))$$

where $\Phi(\cdot)$ is the cumulative distribution function corresponding value of the Normal distribution in eq. (8.3).

For example consider the Chi-squared χ^2 density function (since it is easily differentiable and Gamma Γ term in denominator is constant). The following quantities of interest are the $\log \pi(x)$, then the $\frac{\partial \log \pi(x)}{\partial x}$, which has to be set equal to 0 to find the integrating point, and finally $\log \pi(x) \frac{\partial^2 \log \pi(x)}{\partial x^2}$. The χ^2 pdf, whose support is $x \in \mathbb{R}^+$ and whose degrees of freedom are k :

$$\chi^2(x, k) = \frac{x^{(k/2-1)} e^{-x/2}}{2^{k/2} \Gamma\left(\frac{k}{2}\right)}, x \geq 0$$

for which are computed:

$$\log f(x) = (k/2 - 1) \log x - x/2$$

This single variable *Score Function* and the $x_* = \operatorname{argmax}_x \log \pi(x)$,

$$\begin{aligned} \frac{\partial \log \pi(x)}{\partial x} &= \frac{(k/2 - 1)}{x} - \frac{1}{2} = 0 \quad \text{solving for 0} \\ (k/2 - 1) &= x/2 \quad \text{moving addends} \\ x_* &= (k - 2) \end{aligned} \quad (8.4)$$

And the *Fisher Information* in the x_* (for which it is known $\sigma_*^2 = -1/f''(x)$)

$$\begin{aligned}
 \frac{\partial^2 \log \pi(x)}{\partial x^2} &= -\frac{(k/2 - 1)}{x^2} \quad \text{substituting } x_* \\
 &= -\frac{(k/2 - 1)}{(k - 2)^2} = -\frac{2(k/2 - 1)}{2(k - 2)^2} \quad \text{multiply by 2} \\
 &= -\frac{(k - 2)}{2(k - 2)^2} = 2(k - 2) = \sigma_*^2 \quad \text{change of sign and inverse}
 \end{aligned} \tag{8.5}$$

finally,

$$\chi^2 \stackrel{LA}{\sim} N(x_* = k - 2, \sigma_*^2 = 2(k - 2))$$

Assuming $k = 8, 16$ degrees of freedom χ^2 densities against their Laplace approximation, the figure 8.4 displays how the approximations fits the real density. Integrals are computed in the case of $k = 8$ in the interval $(5, 7)$, leading to a very good Normal approximation that slightly differ from the original CHisquared. The same has been done for the $k = 16$ case, whose interval is $(12, 17)$ showing other very good approximations. Note that intervals are very close to the mode of distributions, if they were evaluated farther results would be inaccurate.

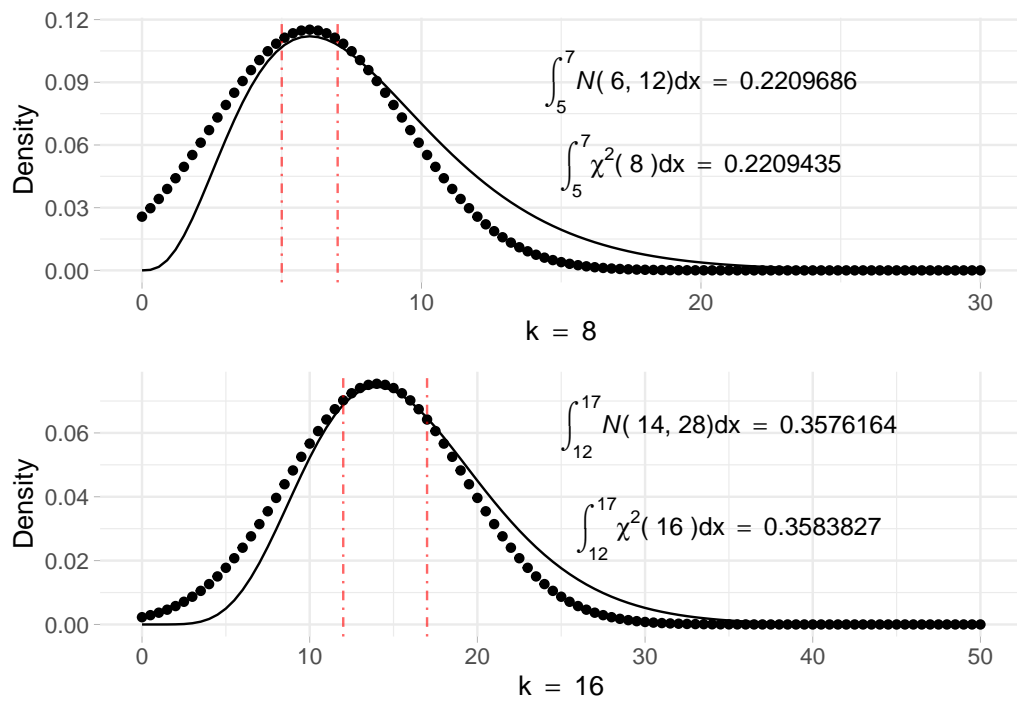


Figure 8.4: Chisquared density function with parameter $k = 8$ (top) and $k = 16$ (down) solid line. The point line refers to the corresponding Normal approximation obtained using the Laplace method

Bibliography

- (2004). Test driven development.
- (2014). *Scraping the Web*, chapter 9, pages 219–294. John Wiley & Sons Ltd.
- (2018).
- (2020). Css.
- (2020). Html.
- (2020). What is parallel computing.
- Allaire, J., Xie, Y., McPherson, J., Luraschi, J., Ushey, K., Atkins, A., Wickham, H., Cheng, J., Chang, W., and Iannone, R. (2020). *rmarkdown: Dynamic Documents for R*. R package version 2.3.
- Anselin, L. (2010). Thirty years of spatial econometrics. *Papers in Regional Science*, 89(1):3–25.
- Arbia, G. (2012). *Spatial data configuration in statistical analysis of regional economic and related problems*, volume 14. Springer Science & Business Media.
- Arbia, G. and Nardelli, V. (2020). On spatial lag models estimated using crowdsourcing, web-scraping or other unconventionally collected data.
- Arbia, G., Solano-Hermosilla, G., Micale, F., Nardelli, V., and Genovese, G. (2020). Post-sampling crowdsourced data to allow reliable statistical inference: the case of food price indices in nigeria.

- Baker, H. C. and Hewitt, C. (1977). The incremental garbage collection of processes. *SIGPLAN Not.*, 12(8):55–59.
- Baltagi, B. H., Bresson, G., and Etienne, J.-M. (2015). Hedonic housing prices in paris: An unbalanced spatial lag pseudo-panel model with nested random effects. *Journal of Applied Econometrics*, 30(3):509–528.
- Banerjee, S., Carlin, B. P., and Gelfand, A. E. (2014). *Hierarchical Modeling and Analysis for Spatial Data*. Chapman and Hall/CRC.
- Barney, B. (2020). Introduction to parallel computing.
- Basile, R., Benfratello, L., and Castellani, D. (2013). Geoaddivitive models for regional count data: An application to industrial location. *Geographical Analysis*, 45(1):28–48.
- Bengtsson, H. (2020a). *future.batchtools: A Future API for Parallel and Distributed Processing using 'batchtools'*. R package version 0.9.0.
- Bengtsson, H. (2020b). A unifying framework for parallel and distributed processing in r using futures.
- Bengtsson, H. (2020c). A unifying framework for parallel and distributed processing in r using futures.
- Bengtsson, H. (2020d). A unifying framework for parallel and distributed processing in r using futures.
- Besag, J. and Kooperberg, C. (1995). On conditional and intrinsic autoregressions. *Biometrika*, 82(4):733–746.
- Bivand, R., Gómez Rubio, V., and Rue, H. (2015). Spatial data analysis with r-inla with some extensions. *Journal of statistical software*, 63:1–31.
- Blanchet-Scalliet, C., Helbert, C., Ribaud, M., and Vial, C. (2019). Four algorithms to construct a sparse kriging kernel for dimensionality reduction. *Computational Statistics*, pages 1–21.

- Blangiardo, M., Cameletti, M., Baio, G., and Rue, H. (2013). Spatial and spatio-temporal models with r-inla. *Spatial and Spatio-temporal Epidemiology*, 7:39 – 55.
- Brooks, S., Gelman, A., Jones, G., and Meng, X.-L. (2011). *Handbook of Markov Chain Monte Carlo*.
- Buja, A., Hastie, T., and Tibshirani, R. (1989). Linear smoothers and additive models. *Ann. Statist.*, 17(2):453–510.
- Cameletti, M., Lindgren, F., Simpson, D., and Rue, H. (2012). Spatio-temporal modeling of particulate matter concentration through the SPDE approach. *AStA Advances in Statistical Analysis*, 97(2):109–131.
- Cantino, A. and Maxwell, K. (2013). Selectorgadget: point and click css selectors. (Accessed on 12/16/2020).
- Capozza, D. and Seguin, P. (1996). Expectations, efficiency, and euphoria in the housing market. *Regional Science and Urban Economics*, 26:369–386.
- Chang, W., Cheng, J., Allaire, J., Xie, Y., and McPherson, J. (2020). *shiny: Web Application Framework for R*. R package version 1.4.0.2.
- Cheng, J., Karambelkar, B., and Xie, Y. (2019). *leaflet: Create Interactive Web Maps with the JavaScript 'Leaflet' Library*. R package version 2.0.3.
- Cisco, W. P. (2020). Cisco annual internet report - cisco annual internet report (2018–2023). (Accessed on 12/28/2020).
- Clapp, J. M. (2003). A Semiparametric Method for Valuing Residential Locations: Application to Automated Valuation. *The Journal of Real Estate Finance and Economics*, 27(3):303–320.
- Clark, T. E. (1995). Rents and prices of housing across areas of the United States. A cross-section examination of the present value model. *Regional Science and Urban Economics*, 25(2):237–247.

Colin Fay, S. R. (2020).

Contributors (2004). Beautiful soup: We called him tortoise because he taught us. (Accessed on 01/02/2021).

contributors, W. (2020a). Clean url — Wikipedia, the free encyclopedia. Online; accessed 14-December-2020.

contributors, W. (2020b). Denial-of-service attack — Wikipedia, the free encyclopedia. Online; accessed 4-December-2020.

contributors, W. (2020c). Fork (system call) — Wikipedia, the free encyclopedia. Online; accessed 5-December-2020.

contributors, W. (2020d). Hiq labs v. linkedin — Wikipedia, the free encyclopedia. [Online; accessed 2-January-2021].

contributors, W. (2020e). Http client hints — Wikipedia, the free encyclopedia. Online; accessed 4-December-2020.

contributors, W. (2020f). Javascript — Wikipedia, the free encyclopedia. [Online; accessed 28-December-2020].

contributors, W. (2020g). Json — Wikipedia, the free encyclopedia. [Online; accessed 28-December-2020].

contributors, W. (2020h). Url — Wikipedia, the free encyclopedia. Online; accessed 14-December-2020.

contributors, W. (2020i). User agent — Wikipedia, the free encyclopedia. Online; accessed 4-December-2020.

contributors, W. (2020j). Xml — Wikipedia, the free encyclopedia. [Online; accessed 28-December-2020].

Corporation, L. (2017). Letter from linkedin to hiq labs. (Accessed on 01/02/2021).

- Corporation, M. and Weston, S. (2020). *doParallel: Foreach Parallel Adaptor for the 'parallel' Package*. R package version 1.0.16.
- Cosandey-Godin, A., Krainski, E. T., Worm, B., and Flemming, J. M. (2015). Applying bayesian spatiotemporal models to fisheries bycatch in the canadian arctic. *Canadian Journal of Fisheries and Aquatic Sciences*, 72(2):186–197.
- Cressie, N. (2015). *Statistics for Spatial Data*. Probability and Mathematical Statistics. Wiley-Interscience, revised edition edition.
- de Freitas, N. (2013). Machine learning - introduction to gaussian processes - youtube. (Accessed on 01/13/2021).
- de Rencontres Mathématiques, C. I. (2018). Håvard rue: Bayesian computation with inla. (Accessed on 12/28/2020), speech originally.
- Densmore, J. (2019). Ethics in web scraping.
- Dey, S., Mukhopadhyay, T., and Adhikari, S. (2017). Metamodel based high-fidelity stochastic analysis of composite laminates: A concise review with critical comparative assessment. *Composite Structures*, 171:227–250.
- Doepud (2010). Anatomy of a url. Accessed on 12/14/2020.
- Dogucu, M. and Cetinkaya, M. (2020). Web scraping in the statistics and data science curriculum: Challenges and opportunities. *Journal of Statistics Education*, pages 1–24.
- Dubé, J. and Legros, D. (2013). A spatio-temporal measure of spatial dependence: An example using real estate data*. *Papers in Regional Science*, 92(1):19–30.
- Eddelbuettel, D. (2020). Parallel computing with r: A brief review.
- Edward G. Black, P. J. R. (2017). hiq labs, inc. v. linkedin corp.: A federal court weighs in on web scraping, free speech rights, and the computer fraud and abuse act | casetext. (Accessed on 01/02/2021).

- Fosso-Tande, J. (2008). Applications of taylor series.
- Gelfand, A. E., Diggle, P., Guttorp, P., and Fuentes, M. (2010). *Handbook of spatial statistics*. CRC press.
- Gelfand, A. E. and Smith, A. F. (1990). Sampling-based approaches to calculating marginal densities. *Journal of the American statistical association*, 85(410):398–409.
- Gneiting, T., Genton, M. G., and Guttorp, P. (2006). Geostatistical space-time models, stationarity, separability, and full symmetry. *Monographs On Statistics and Applied Probability*, 107:151.
- Google (2020). Presentazione dei file robots.txt - guida di search console.
- Gómez Rubio, V. (2020). *Bayesian Inference with INLA*. Chapman and Hall/CRC.
- Hadley Wickham, G. G. (2017). *R for Data Science: Import, Tidy, Transform, Visualize, and Model Data*. O'Reilly Media, 1 edition.
- Hastings, W. K. (1970). Monte Carlo sampling methods using Markov chains and their applications. *Biometrika*, 57(1):97–109.
- Herath, S. and Maier, G. (2011). Hedonic house prices in the presence of spatial and temporal dynamics. *Territorio Italia - Land Administration Cadastre, Real Estate*, 1:39–49.
- immobiliare.it (2020). Condizioni generali - immobiliare.it. (Accessed on 01/02/2021).
- Inc., D. (2020a). Get docker.
- Inc., D. (2020b). Use volumes | docker documentation. (Accessed on 01/03/2021).
- Kamman, E. E. and Wand, M. P. (2003). Geoaddivitive models. *Journal of the Royal Statistical Society: Series C (Applied Statistics)*, 52(1):1–18.

- Khalil, S. (2018). *Rcrawler: Web Crawler and Scraper*. R package version 0.1.9-1.
- Krainski, E., Gómez-Rubio, V., Bakka, H., Lenzi, A., Castro-Camilo, D., Simpson, D., Lindgren, F., and Rue, H. (2018). *Advanced Spatial Modeling with Stochastic Partial Differential Equations Using R and INLA*. Chapman and Hall/CRC.
- Krainski, E. T. (2019). *Advanced spatial modeling with stochastic partial differential equations using R and INLA*. Chapman and Hall/CRC.
- Krotov, V. and Silva, L. (2018). Legality and ethics of web scraping.
- Krotov, V. and Tennyson, M. (2018). Tutorial: Web scraping in the r language.
- Kuhn, M. and Johnson, K. (2019). *Feature Engineering and Selection*. Chapman and Hall/CRC.
- LaFrance, A. (2017). The internet is mostly bots - the atlantic. <https://www.theatlantic.com/technology/archive/2017/01/bots-bots-bots/515043/>. (Accessed on 12/29/2020).
- Lancaster, K. J. (1966). A new approach to consumer theory. *Journal of Political Economy*, 74(2):132–157.
- Lindgren, F., Rue, H., and Lindström, J. (2011). An explicit link between gaussian fields and gaussian markov random fields: the stochastic partial differential equation approach. *Journal of the Royal Statistical Society: Series B (Statistical Methodology)*, 73(4):423–498.
- Ling, Y. (2019). Time, space and hedonic prediction accuracy evidence from the corsican apartment market. *The Annals of Regional Science*, page 28.
- Lionel Henry RStudio, H. W. R. (2020a). Capture side effects. — safely • purrr. Accessed on 12/05/2020.
- Lionel Henry RStudio, H. W. R. (2020b). Create delaying rate settings - rate-helpers. Accessed on 11/05/2020.

- Little, R. and Rubin, D. (2014). *Statistical Analysis with Missing Data, Second Edition*, pages 200–220.
- Maheedharan, V. (2016). A detailed overview of web crawlers. (Accessed on 12/29/2020).
- Malpezzi, S. (2008). *Hedonic Pricing Models: A Selective and Applied Review*, pages 67–89.
- Manganelli, B., Morano, P., and Tajani, F. (2013). Economic relationships between selling and rental prices in the italian housing market.
- Marta Blangiardo, M. C. (2015). *Spatial and Spatio-temporal Bayesian Models with R-INLA*. Wiley.
- Media, A. (2017). What courts have said about the legality of data scraping. (Accessed on 12/29/2020).
- Meissner, P. (2020).
- Meissner, P. and Ren, K. (2020). *robotstxt: A 'robots.txt' Parser and 'Web-bot'/'Spider'/'Crawler' Permissions Checker*. R package version 0.7.7.
- Merkel, D. (2014). Docker: lightweight linux containers for consistent development and deployment. *Linux journal*, 2014(239):2.
- MERRIAM-WEBSTER (2018). Kitchen-sink | definition of kitchen-sink by merriam-webster. (Accessed on 12/29/2020).
- Metropolis, N., Rosenbluth, A. W., Rosenbluth, M. N., Teller, A. H., and Teller, E. (1953). Equation of State Calculations by Fast Computing Machines. 21(6):1087–1092.
- Microsoft (2018). Gateway api - azure architecture center | microsoft docs. (Accessed on 12/23/2020).
- Microsoft and Weston, S. (2020). *foreach: Provides Foreach Looping Construct*. R package version 1.5.0.

- Moraga, P. (2019). *Geospatial Health Data*. Chapman and Hall/CRC.
- Moraga, P. (2020). Spatial modeling and interactive visualization with the r-inla package.
- Moraga, P., Ketcheson, D. I., Ombao, H. C., and Duarte, C. M. (2020). Assessing the age- and gender-dependence of the severity and case fatality rates of COVID-19 disease in Spain. *Wellcome Open Research*, 5:117.
- NGINX (2014). What is a reverse proxy server? | nginx. (Accessed on 12/22/2020).
- Nolis, J. (2020). R docker faster. suddenly r docker images build much... | medium. (Accessed on 12/24/2020).
- Paci, L. (2020). Statistical models for high dimensional and spatio-temporal data.
- Paci, L., Beamonte, M. A., Gelfand, A. E., Gargallo, P., and Salvador, M. (2017). Analysis of residential property sales using space-time point patterns. *Spatial Statistics*, 21:149 – 165.
- Perepolkin, D. (2019). *polite: Be Nice on the Web*. R package version 0.1.1.
- Peterson, R. A. and Merino, M. C. (2003). Consumer information search behavior and the internet. *Psychology & Marketing*, 20(2):99–121.
- Rosen, S. (1974). Hedonic prices and implicit markets: Product differentiation in pure competition. *Journal of Political Economy*, 82(1):34–55.
- Rue, H. and Held, L. (2005). *Gaussian Markov Random Fields*. Chapman and Hall/CRC.
- Rue, H., Martino, S., and Chopin, N. (2009). Approximate bayesian inference for latent gaussian models by using integrated nested laplace approximations. *Journal of the Royal Statistical Society: Series B (Statistical Methodology)*, 71(2):319–392.

- Rue, H., Riebler, A., Sørbye, S. H., Illian, J. B., Simpson, D. P., and Lindgren, F. K. (2017). Bayesian computing with inla: A review. *Annual Review of Statistics and Its Application*, 4(1):395–421.
- Santiago, J. (2020). *plungr: Opinionated Framework for Developing Plumber APIs*. <https://ocean12.github.io/plungr>.
- Shah, T. (2018). *ratelimitr: Rate Limiting for R*. R package version 0.4.1.
- Sheppard, S. (1999). Chapter 41 hedonic analysis of housing markets. In *Applied Urban Economics*, volume 3 of *Handbook of Regional and Urban Economics*, pages 1595 – 1635. Elsevier.
- Shi, W. and Lee, L.-f. (2017). A spatial panel data model with time varying endogenous weights matrices and common factors. *Regional Science and Urban Economics*, 72.
- Simpson, D., Rue, H., Riebler, A., Martins, T. G., and Sørbye, S. H. (2017). Penalising model component complexity: A principled, practical approach to constructing priors. *Statist. Sci.*, 32(1):1–28.
- SMARTBEAR (2019). Rest api documentation tool | swagger ui. (Accessed on 12/27/2020).
- Trestle Technology, LLC (2018). *plumber: An API Generator for R*. R package version 0.4.6.
- UserAgentString.com (1999). Useragentstring.com - chrome version 81.0.4044.110. (Accessed on 12/21/2020).
- User:Jallan (2011). Definition of user agent - wai ua wiki. Accessed on 12/04/2020.
- Vaughan, D. and Dancho, M. (2018). *furrr: Apply Mapping Functions in Parallel using Futures*. R package version 0.1.0.
- Venables, W. N. and Ripley, B. D. (2002). *Modern Applied Statistics with S*. Springer, New York, fourth edition. ISBN 0-387-95457-0.

- Wang, X., Yue, Y. R., and Faraway, J. J. (2018). *Bayesian regression modeling with INLA*. CRC Press.
- WhoIsHostingThis.com (2020). User agent: Learn your web browsers user agent now.
- Wickham, H. (2011). testthat: Get started with testing. *The R Journal*, 3:5–10.
- Wickham, H. (2019). *rvest: Easily Harvest (Scrape) Web Pages*. R package version 0.3.5.
- Wickham, H., Averick, M., Bryan, J., Chang, W., McGowan, L. D., François, R., Grolemund, G., Hayes, A., Henry, L., Hester, J., Kuhn, M., Pedersen, T. L., Miller, E., Bache, S. M., Müller, K., Ooms, J., Robinson, D., Seidel, D. P., Spinu, V., Takahashi, K., Vaughan, D., Wilke, C., Woo, K., and Yutani, H. (2019). Welcome to the tidyverse. *Journal of Open Source Software*, 4(43):1686.
- Wickham, H., Hester, J., Müller, K., and Cook, D. (2017). *memoise: Memoisation of Functions*. R package version 1.1.0.
- Xie, Y. (2016). *bookdown: Authoring Books and Technical Documents with R Markdown*. Chapman and Hall/CRC, Boca Raton, Florida. ISBN 978-1138700109.